LA VOÛTE DE MAÇONNERIE

JACQUES HEYMAN, M.A., Ph.D., F.I.C.E., F.S.A.
Professeur d'ingénierie, Université de Cambridge

ELLIS HORWOOD LIMITED
Editeurs - Chichester

Halsted Press: division de JOHN WILEY & SONS
New York - Brisbane - Chichester - Toronto

LA VOÛTE DE MAÇONNERIE

JACQUES HEYMAN, Professeur d'ingénierie, Université de Cambridge

Ce livre rassemble les vastes connaissances de l'auteur et son expérience des constructions en maçonnerie, accumulées et consolidées au fil des années, et offre une contribution utile à la construction civile. Il développe de nouvelles méthodes d'analyse et de dessin des voûtes maçonnées en présentant l'approche complètement nouvelle d'un ingénieur largement reconnu faisant autorité.

Le texte est rédigé dans un style élégant et fluide avec une lucidité qui s'adresse tout autant aux ingénieurs académiques qu'aux ingénieurs en exercice. Les technologies éprouvées d'analyse des voûtes de maçonnerie sont passées en revue vis à vis des données théoriques issus des puissants théorèmes de la plasticité ; l'étude qui en résulte va placer un nouvel outil dans les mains des designers et pourrait entraîner une augmentation accentuée des débats concernant des voûtes de maçonnerie dans les programmes de construction contemporains.

L'auteur propose ici une étude particulièrement intéressante du développement historique du sujet ; l'accent est mis sur des considérations statiques et cinématiques qui sont indépendantes de la constitution précise du matériau constituant la voûte. C'est une approche plus large des théorèmes limites jusqu'à présent presque exclusivement associés aux matériaux plastiques. Parmi les questions posées par le Professeur Heyman : quelle est la meilleure forme pour une voûte devant supporter des charges données ? de quelle épaisseur devrait être l'arch ring ? quelle charge peut supporter un pont médiéval donné ? L'auteur répond à ces questions et insiste tout au long sur le concept utile du facteur géométrique du sûreté. Des planches techniques illustrent le texte ainsi que de nombreuses illustrations.

Lectorat : ce livre s'adresse aux dessinateurs et ingénieurs civil et mécanique en exercice, de même qu'aux autorités locales ; avec une attention particulière aux professeurs et étudiants en troisième cycle d'études.

Table des matières

Préface

La partie la plus inattendue de ce livre est probablement son dernier chapitre qui tente d'utiliser la théorie des voûtes de maçonnerie pour comprendre les arcs de fonte ou de fer forgé (made of cast or wrought iron). Comment appliquer des techniques destinées aux constructions en pierre à celles faites de fer ? Cela, je l'espère, deviendra clair au fur et à mesure du développement de la théorie.

Cette théorie est introduite dans le premier chapitre qui rappelle des idées bien connues à propos de la ligne de poussée (axiale) line of thrust ; l'équilibre est traité de façon conventionnelle en se référant à la règle du tiers médian. Dans le second chapitre, la théorie est examinée par rapport à un arrière-plan d'idées issues des théorèmes de la plasticité, et un certaine quantité de rigueur académique est apportée au travail. Cette étude, même superficielle, de l'histoire de l'analyse technique des ponts apporte une compréhension plus profonde du comportement des voûtes ; en tout cas, le troisième chapitre en donne un court résumé. Les histoires de Fuller peuvent être trouvées par ailleurs, et ma discussion des *Mémoires sur la statique* de Coulomb fournit de plus amples informations.

Cette façon de présenter le matériau pourrait être celle d'un historien whig. La vision pour ainsi dire 'correcte' est exposée en premier et le témoignage historique est ensuite interprété à la lumière de cette vision correcte. Les ingénieurs qui s'acharnent sur le problème des voûtes de maçonnerie se débattent laborieusement vers un but connu ; certains l'atteignent, d'autres semblent éviter obstinément le bon chemin. Si l'on m'accuse de donner une vision déformée de l'évidence, je répondrais simplement que toutes les perles de l'histoires doivent être enfilées sur un lacet de sorte que le collier obtenu soit à la fois résistant et beau. Mon fil est celui de la théorie plastique.

Dans le quatrième chapitre, les méthodes plastiques sont confrontées aux méthodes élastiques d'analyse des voûtes de maçonnerie et des techniques sont développées pour évaluer les voûtes maçonnées existantes qui seront, je l'espère, utile aux personnes en charge de la maintenance et de la réhabilitation de telles constructions. Les exemples donnés dans le cinquième chapitre décrivent comment de telles techniques peuvent être utilisées. Ces deux chapitres concluent réellement cette monographie.

Cependant, le très court sixième n'a pas fonction de rembourrage. Il tente de montrer que les idées développées pour la maçonnerie des voûtes peuvent être utilisées plus largement, et qu'en fait les techniques fondées sur les principes de plasticité tendent à être universellement valables. La question est technique. La règle du tiers médian, remplacée ici par le concept équivalant et plus large du facteur géométrique de sûreté, fournit des solutions pour les voûtes en dépit du fait que l'une des trois équations majeures de l'analyse structurelle a été laissée de côté. Celle qui n'est pas nécessaire est l'équation exprimant la géométrie de la déformation. Les équations d'équilibre sont suffisantes pour déterminer la sûreté des arcs et l'ingénieur est ainsi ramené à sa première tâche, à savoir à construire un état d'équilibre plausible et satisfaisant sur lequel baser son dessin.

L'ingénieur a parfois besoin qu'on lui rappelle cela. Sa façon de penser peut être tellement conditionnée par les concepts de la théorie élastique conventionnelle qu'il n'est pas toujours conscient des limites de ses calculs. En effet, la théorie élastique ne fournit pas un état d'équilibre possible pour une structure, mais elle en donne seulement un parmi un nombre infini pour n'importe quelle structure qui est statiquement indéterminée. Caché au cœur de la théorie élastique et sous les capots des ordinateurs ou de l'analyse des éléments finis basés sur la théorie élastique, se trouvent des idées de compatibilité de la déformation. L'ingénieur est obligé de fournir des informations, par exemple à propos des conditions au niveau des sommiers (at the abutments of an arch), avant qu'une analyse élastique ne puisse être mise en œuvre.

En outre, comme précisé au Chapitre 2, l'ingénieur ne connaît ni les conditions aux sommiers (at the abutments) ni même si la structure a été forcée was forced together au moment de sa construction, de sorte qu'elle subit des contraintes même en l'absence de charges. Il devra prendre pour principe, afin de faire fonctionner son programme d'ordinateur, que la structure est initialement non-contrainte et que (les piedroits) the abutments sont rigides (or qu'ils ont une certaine réponse élastique) ; mais ce sont des postulats dont la validité est inconnue et qui peuvent tout de même avoir un effet important sur les résultats produits par l'ordinateur.

L'analyse des arcs par la théorie plastique montre que leur sûreté ne dépend ni des conditions précises at the abutments, ni du fait que les arcs étaient ou non construits à l'origine pour correspondre parfaitement à those abutments. Le dessinateur n'a pas besoin d'informations à propos de ces imperfections géométriques ; il a une méthode alternative d'analyse qui est toujours sûre, grâce aux théorèmes de la plasticité. Et cette méthode peut être appliquée aussi bien eu fer qu'à des voûtes de maçonnerie.

1

La règle du tiers-médian (The middle-third rule)

En 1746, William Edwards, un maçon, s'engagea à construire pour £500 un pont sur le Taff à Pontypridd. Ces tentatives pour mener à bien ce contrat illustrent quelques unes des difficultés que rencontre le dessinateur de voûtes de maçonnerie.

Le premier pont comptait trois ou quatre travées et résista deux ans et deux mois. L'un (au moins) des piliers était dans la rivière et une inondation fit tomber le pont, probablement à la suite de l'érosion de ses fondations. William Edwards qui devait, selon son contrat, fournir un pont qui durerait sept années décida alors d'enjamber la rivière avec une seule travée (mesurant plus de 42 m). Quand cette arche fut quasiment terminée, le cintrage (centering) en bois s'effondra, soit à cause du trop grand poids de la maçonnerie, soit parce qu'une inondation fut encore la cause d'une surcharge imprévue.

Le troisième pont, de 1754, était fait d'une maçonnerie plus légère basée sur un coffrage plus solide. L'arche (arch ring) fut terminée en septembre et le coffrage fut enlevé ; le travail se poursuivit par la maçonnerie des murs-allège (the spandrel walls) et la pose des épaules (filling the haunches) terminant la chaussée. Alors que ce travail était en cours, au mois de novembre, l'arche s'effondra, la clé subissant des contraintes ascendantes. Il n'y avait pas d'erreur dans les arcs-boutants (abutments of the arch) ou de contrainte trop forte de la maçonnerie ; l'arche n'avait apparemment pas la bonne forme pour soutenir son propre poids.

William Edwards tira évidemment des enseignements de cet effondrement, et il put modifier le dessin de son quatrième et dernier pont, lequel est toujours debout. La charge au sommet fut augmentée et celle aux épaules (at the haunches) diminuée par le percement de larges ouvertures cyclindriques, (Fig. 1.1). L'arche résultante est très élancée avec une épaisseur d'environ 760 mm seulement au sommet, et un petit peu moins aux épaules (at the haunches), où le remblai (fill) est retouché pour permettre les ouvertures cylindriques. (Les murs du parapet font paraître la hauteur du pont sur la Fig. 1.1 plus importante qu'elle n'est en réalité.) On peut concevoir que la marge de sécurité de cette structure élancée est faible et il n'est pas étonnant que la troisième arche se soit effondrée durant sa construction.

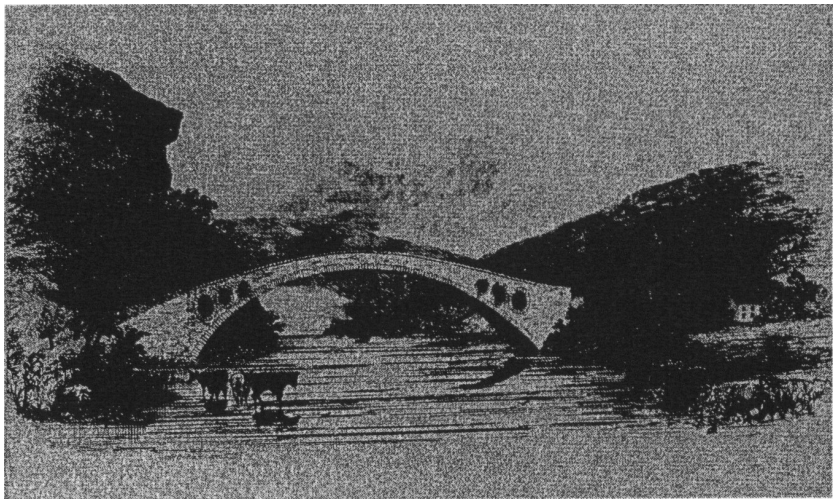

Fig. 1. 1 Le quatrième pont de William Edwards à Pontypridd.

Le terme ‘marge de sécurité’ est assez vague ; le sens de la phrase précédente est probablement clair, mais aucune précision quant au poids n’est associée à ce terme. Si le troisième pont s’est effectivement effondré, comme il est décrit, après une dislocation majeure et sans aucune surcharge préalable (overstressing) du matériau, il semblerait alors que l’estimation de la ‘sûreté’ du pont ne dépende pas (du moins pas de manière significative) de la résistance du matériau. En revanche, la sûreté d’une arche pourrait sans doute être reliée à sa forme ; c’est alors une question de géométrie, et non pas ‘de contraintes et de déformations’ d’une théorie moderne de construction.

Comme nous allons le voir, une approche géométrique de l’étude des voûtes comprend des antécédents historiques respectables. Le propos de ce livre est de construire sur ces antécédents, en utilisant si nécessaire des techniques récents d’analyse, et de tenter d’établir une théorie à propos des voûtes de maçonnerie reposant en grande partie sur la géométrie. Les hypothèses nécessaires à l’analyse seront établies en temps voulu. En clair, les voûtes étudiées sont d’une taille modeste de sorte qu’il n’y a pas de problème d’écrasement du matériau ; une voûte en pierre (an arch of any reasonable stone), assemblée avec ou sans mortier, peut supporter sans encombre les charges qui lui sont imposées. De plus, il n’y aura pas de débat sur le dessin des arcs-boutants (abutments of the arch) ; il sera admis qu’ils sont suffisamment solides pour résister, sans nécessairement être absolument rigides, à une quelconque poussée appliquée.

L’étude s’intéresse aussi à la voûte elle-même : quelle est la meilleure forme pour une voûte devant supporter des charges données ? de quelle épaisseur devrait être l'arch ring ? quelle charge peut supporter un pont médiéval donné ?

DEFINITIONS

Une voûte de maçonnerie est construite sur un étaiement provisoire, ou un cintrage. Ce cintrage est traditionnellement une poutre et il faut prévoir au moyen de coins ou de dispositifs similaires de retirer les étais une fois la voûte terminée.

The arch ring lui-même qui est la pièce de base pour la construction du pont est composé de voussoirs en forme de coins (Fig. 1.2). Les voussoirs doivent être taillés avec beaucoup de soin pour une voûte à large travée et assemblés avec un minimum de mortier ; pour des voûtes plus petites, on pourra utiliser des pierres taillées plus grossièrement avec des joints de mortier plus épais pour combler les irrégularités de la construction. Dans le cas de Pontypridd, les voussoirs sont très fins (Fig. 1.3), et ils doivent absolument être en forme de coins pour permettre la faible courbure du arch ring.

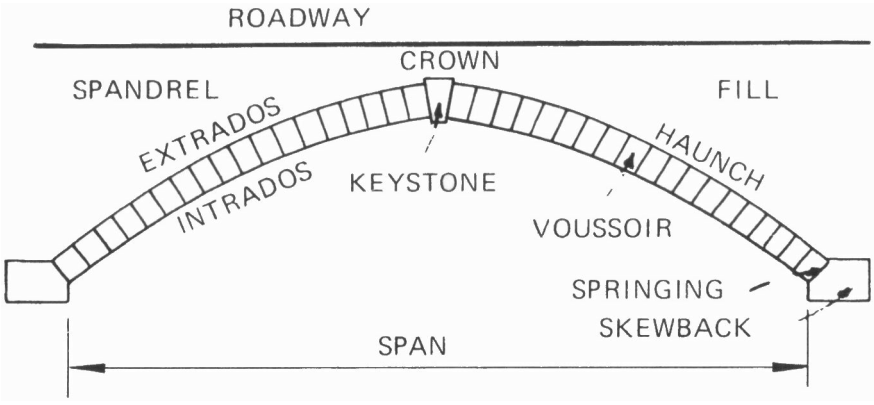

Fig. 1.2 Les différentes parties d’un pont maçonné.

En revanche, le pont voûté à voussoirs classique a une section (ring) formée de pierres relativement épaisses ; la Fig. 1.4 montre le Clare College Bridge, dessiné en 1638. La clé de voûte a une signification particulière dans la construction ; c’est la dernière pierre posée et, lorsque la voûte est complète on peut alors la décoffrer. La clé de voûte est souvent, mais pas toujours, mise en valeur visuellement par le dessinateur en raison de sa fonction dans la construction. En fait son rôle dans la structure est le même que celui de chacun des voussoirs, comme un maillon d’une chaîne n’est pas

différent des autres maillons. Les maillons de la chaîne transmettent la tension le long de la chaîne ; les voussoirs dans une voûte transmettent la compression au cœur de la voûte. Cette analogie naïve entre voûte et chaîne peut sembler tout à fait triviale mais a en fait une importance capitale.

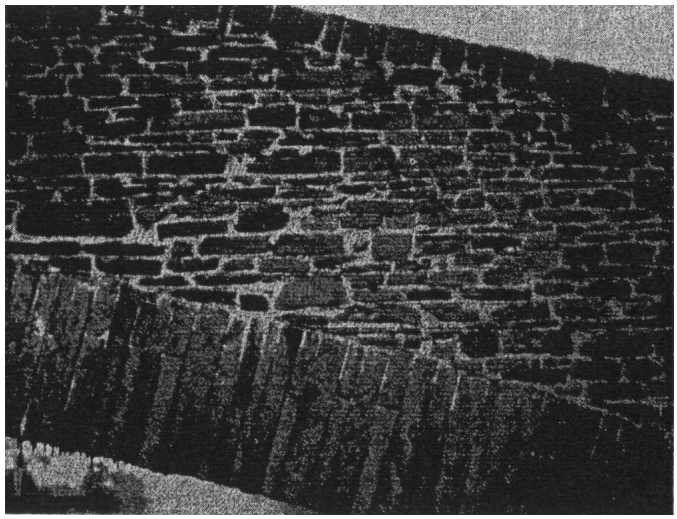

Fig. 1.3 Voussoirs et parapet à Pontypridd (photographié par Ted Ruddock, reproduit avec l'autorisation de l'University Cambridge Press).

Une fois que le voûte est terminée on peut commencer à retirer le coffrage. Au moins un partie du remblai (some of the fill) doit être placée au-dessus des extrados de la voûte au niveau des abutments (et des piliers intérieurs) afin de stabiliser the arch ring. Cependant, la plus grande partie du poids total de la voûte de maçonnerie réside dans ce remblai non-structurant (non-structural fill) et il est très important de décoffrer la voûte avant que le poids imposé aux étais (the falsework) ne rende ceci difficile. L'équilibre de la voûte peut alors devenir précaire et il faut prendre soin à conserver la symétrie et à équilibrer les charges tout au long des travées. Le troisième pont de Pontypridd était trop chargé aux épaules (at the haunches) et trop peu au sommet (at the crown). Le pont de Clare College, Fig. 1.4, a manifestement été construit avec un mauvais équilibrage, et le pilier côté ouest dans le lit de la rivière a basculé pendant la construction, entraînant le fléchissement de la chaussée sur la travée centrale.

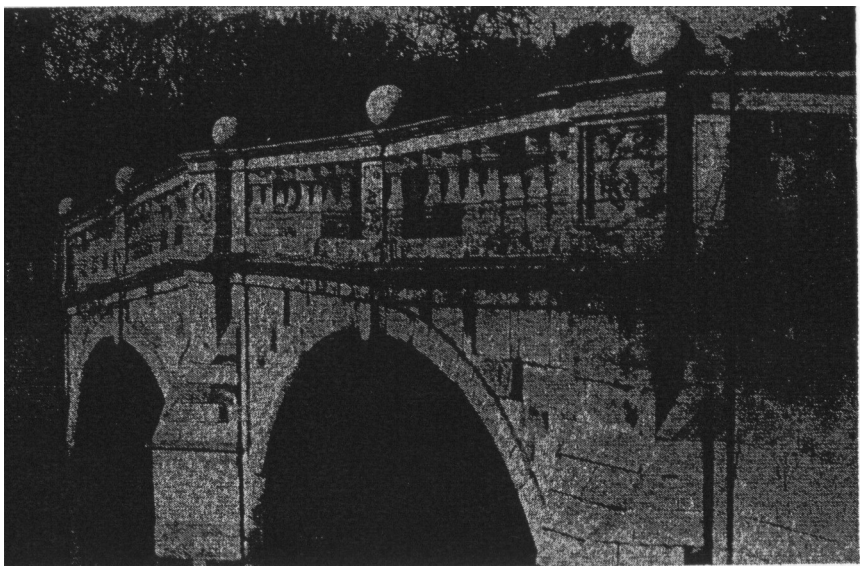

Fig. 1.4 Clare College Bridge, Cambridge; Thomas Grumbold, 1638-40.
On remarque le fléchissement au sommet (crown) de la travée principale.

Dans un petit pont, le remblai peut être composé de maçonnerie de blocage (rubble=moellon), de terre ou de gravier or hoggin, amassés jusqu'à la hauteur voulue pour supporter la surface de la

route. Le remblai est maintenu par des murs-allège (spandrel walls) construits sur the arch rings sur les deux faces du pont. Le remblai n'agit pas sur la structure bien qu'en pratique, une charge appliquées sur la surface de la route puisse 'se répandre' (may 'spread') au travers du remblai avant qu'il ne s'applique aux extrados de la voûte. Dans des ponts plus grands, une série de murs maçonnés parallèles peuvent être construits sous les épaules (over the haunches), et ces murs-allège (spandrel walls) vont supporter la chaussée.

L'élévation représentée sur la Fig. 1.2 peut être également considérée comme une coupe transversale du pont (The elevation of Fig. 1.2 may be taken equally as a section through the bridge). Les arch rings parallèles ne sont pas nécessairement indépendants ; les voussoirs ont habituellement des longueurs axiales (axial lengths) différentes, de sorte que les arch rings voisins les verrouillent et forment une voûte en berceau prismatique continue (continuous prismatic arch barrel). Cependant, on ne peut pas en déduire que l'épaisseur de the arch ring visible sur la face externe du pont représente l'épaisseur du berceau entre les faces. Clare College Bridge, Fig. 1.5, par exemple, semble avoir an arch ring d'une épaisseur radiale constante de 0,30 m. En fait, derrière ces voussoirs apparents la maçonnerie est moins bien taillée et mesure seulement 0,15 m d'épaisseur ; l'arche principale est en réalité moitié moins épaisse que ce qu'elle paraît. Cette supercherie n'est pas réalisable dans le cas de travées plus larges.

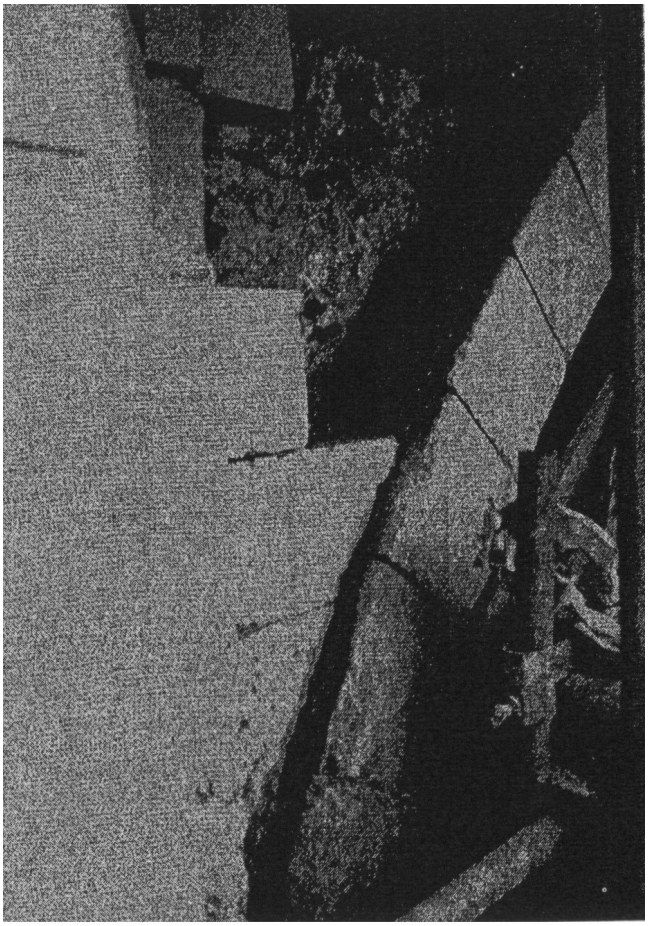

Fig. 1.5 Clare College Bridge, Cambridge. L'épaisseur des voussoirs apparents est de 0,30 m, mais celle du berceau principal (main barrel) n'est que de la moitié.

Les problèmes résultants sont les suivants. Le profil et l'épaisseur d'un arc sont connus, de même que les charges ; charges mortes dues au poids propre de la voûte et du remblai, et charges utiles apportées par le trafic. (La 'plus mauvaise' position sur le pont pour placer des charges vives données devra être déterminée) Comment le pont supporte-t-il ces charges ? Quelles sont les forces entre les voussoirs ? Quelle est la poussée sur les sommiers (abutments) ? Avec des techniques permettant de répondre à ces questions et à des questions similaires, on peut estimer la sécurité d'un pont donné ou dessiner une voûte pouvant supporter une charge connue.

LE POLYGONE FUNICULAIRE

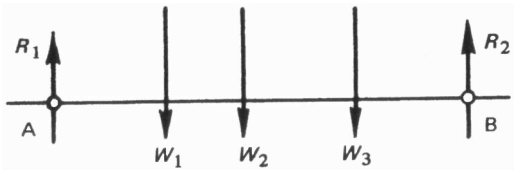

Fig. 1.6

Un outil bien connu d'analyse des voûtes est le polygone funiculaire dont la construction sera rendu claire grâce à un exemple simple. La Fig. 1.6 représente trois forces parallèles W_1, W_2 et W_3 (qui seront interprétées plus loin comme représentant un système simple de charges sur un pont) ainsi que deux autre forces parallèles R_1 et R_2 appliquées aux points A et B. Le système est supposé en équilibre, de sorte que

$$W_1 + W_2 + W_3 = R_1 + R_2, \tag{1.1}$$

Une seconde équation représente l'équilibre des moments. Si l'on imagine les forces W comme appliquées sur une chaînette de poids négligeable (Fig. 1.7(a)) le profil de la chaînette peut alors être déterminé graphiquement. En supposant que la composante horizontale H de la tension de la chaînette est connue, alors un triangle de forces (Fig. 1.7(b)) donne la direction du segment AP de la chaînette.

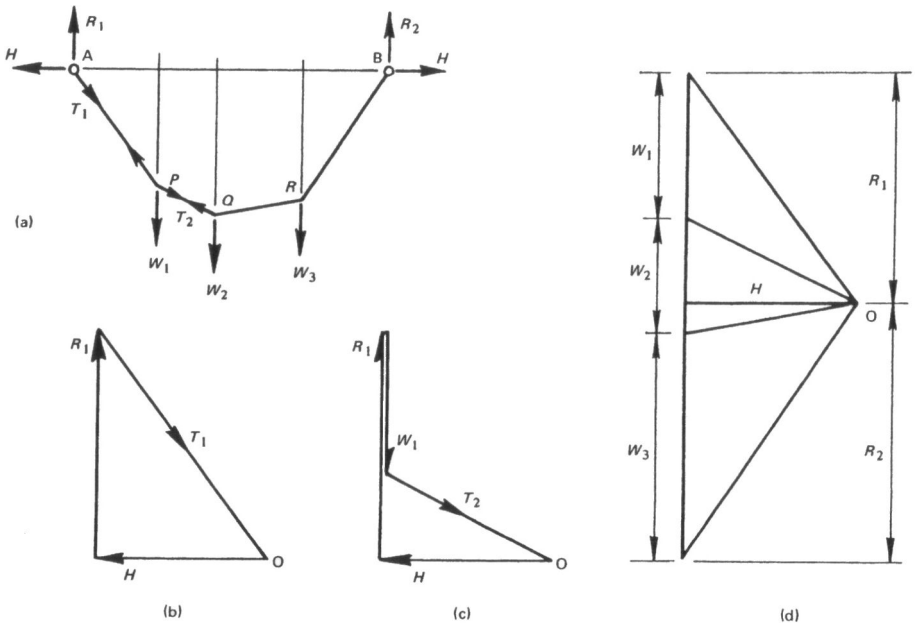

Fig. 1.7

Le segment PQ de la chaînette est soumis à la même force horizontale H et à une force verticale (R_1 - W_1) ; la Fig. 1.7(c) représente la construction permettant de trouver la direction de la chaînette (et la valeur T_2 de la tension). Les Figs. 1.7(b) et (c) peuvent clairement être combinées, et la Fig. 1.7(d) montre le polygone des forces complet correspondant aux charges W_1, W_2 et W_3 et les réactions R_1 et R_2 ; dans ce cas particulier de charges parallèles, le polygone des forces correspond à la ligne verticale représentée associée à la ligne horizontale qui représente la composante horizontale H de la tension de la chaînette. Il est clair que la construction de la Fig. 1.7(d) satisfait (1.1). Le point O du polygone des forces est situé à une distance H de la ligne verticale et les lignes issues de O radiating from O donnent la direction des différents segments de la chaînette.

Du point de vue de la statique, les problèmes de la chaînette pendante et de la voûte sont les mêmes. La Fig. 1.8 correspond exactement aux Figs. 1.7(d) et (a), et l'on voit qu'un assemblage de tronçons droits weightless AP, PQ, QR et RB tenus par leurs extrémités pourrait être disposés de manière à transmettre les charges W_1, W_2 et W_3 aux sommiers A et B, les tronçons travaillant en compression (tandis que la chaînette de la Fig. 1.7 est en tension). L'assemblage des tronçons serait en équilibre bien que l'équilibre soit instable. Le polygone funiculaire APQRB représente la ligne de poussée dans une voûte supportant les charges W_1, W_2 et W_3 ; c'est l'épaisseur des voussoirs qui entourent la ligne de poussée qui confère sa stabilité à la voûte.

Les polygones funiculaires des Figs 1.7(a) et 1.8(b) ont été dessinés en partant du principe que la valeur de la réaction horizontale H (traction pour la chaînette, compression pour la voûte) était connue. Sur la Fig. 1.9 on a retracé la Fig. 1.8 à laquelle on a superposé un autre polygone funiculaire correspondant à une plus petite valeur de H, dite H'.

Il ressort de l'étude des triangles de forces telle que celle réalisée sur la Fig. 1.7(b) que le polygone funiculaire AP'Q'R'B de la Fig. 1.9(b) est une version étirée du polygone initial APQRB, et que les ordonnées dans chaque section sont dans le rapport H/H', c'est-à-dire

$$\frac{P'p}{Pp} = \frac{Q'q}{Qq} = \frac{H}{H'}, \qquad (1.2)$$

(En ce qui concerne l'analogie de la chaînette, une chaînette plus longue supportera son poids avec une traction horizontale plus faible ; une voûte à faible courbure (shallow arch) subira des poussées plus fortes à ses sommiers qu'une voûte dont l'élévation est plus importante.)

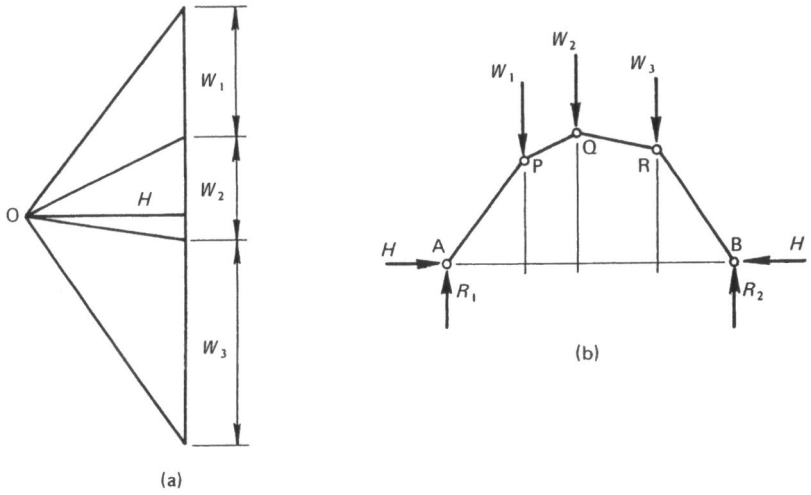

Fig. 1.8

On a supposé en dessinant les polygones funiculaires des Figs. 1.7, 1.8 et 1.9 que la statique avait préalablement été calculée afin de s'assurer de l'équilibre du système ; c'est-à-dire que les valeurs des réactions R_1 et R_2 avaient été déterminées avant de commencer le dessin. Comme le montre la Fig. 1.10, cette analyse préliminaire n'est pas nécessaire. Sur cette figure, les valeurs des charges W_1, W_2 et W_3 sont les mêmes que précédemment, mais le point O du polygone des forces a été placé de façon aléatoire. Le polygone funiculaire correspondant APQRS est alors tracé à partir du point A fixé et il apparaît que le point S ne coïncide pas avec le point B. Cependant, le polygone funiculaire peut être ramené à la forme des Figs. 1.8 et 1.9 en traçant le segment AS. La parallèle OX dans le polygone des forces l'emplacement du point O' pour lequel le polygone funiculaire correspondant passe par A et B. De plus, on peut remarquer que les polygones funiculaires APQRS et AP'Q'R'B ont mêmes les dimensions dans le plan vertical est qu'ils sont reliés par un cisaillement pur, c'est à dire un déplacement tangentiel sans modification des longueurs des segments.

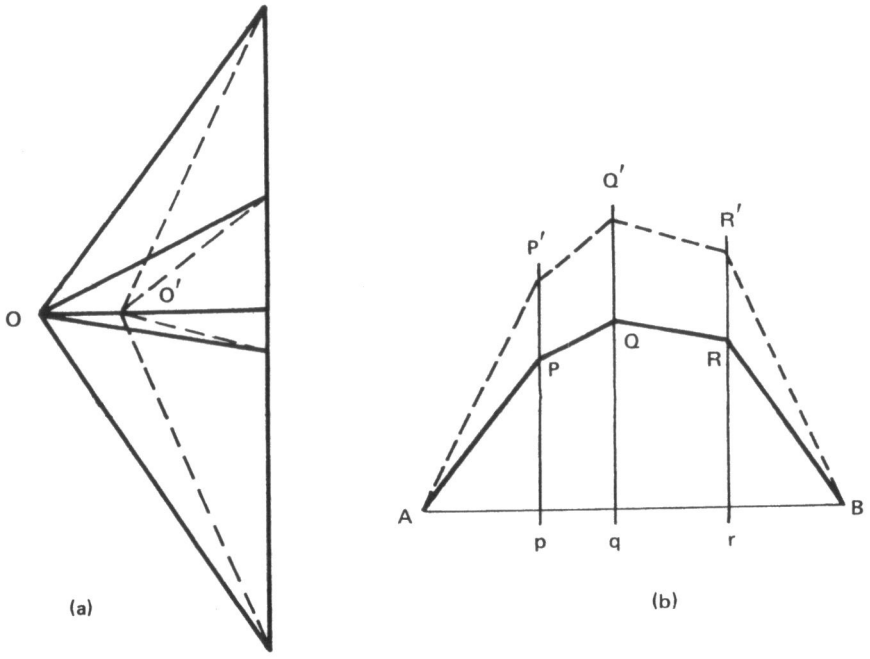

Fig. 1.9

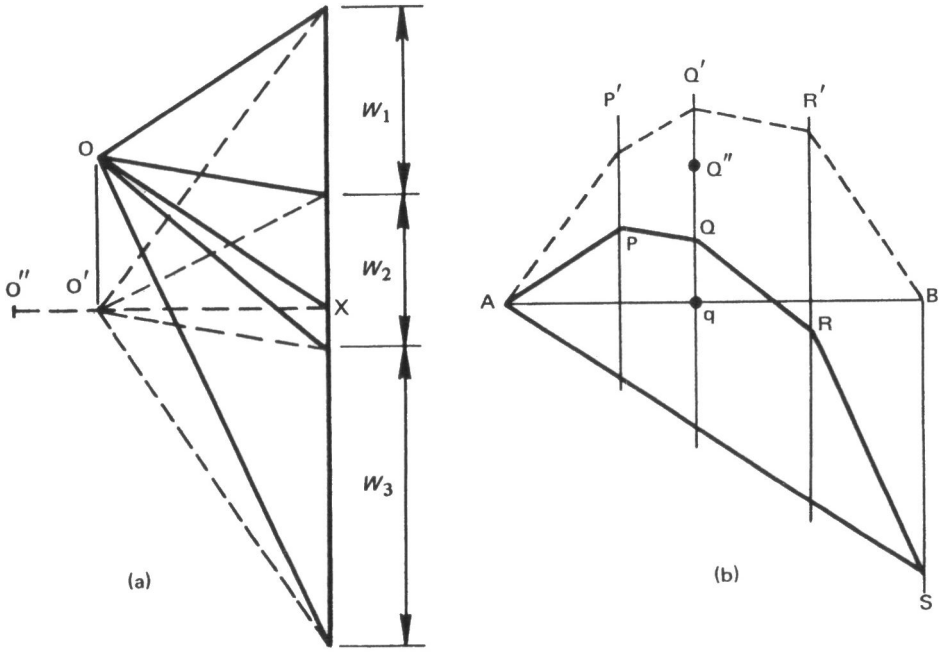

Fig. 1.10

Les Figs. 1.9 et 1.10 illustrent une méthode totalement graphique pour tracer un polygone funiculaire en passant par trois points donnés. Si en plus des points A et B on fait passer le polygone funiculaire de la Fig. 1.10(b) par un point Q" donné, le point O' du polygone des forces de la Fig. 1.10(a) sera déplacé horizontalement jusqu'en O", où

$$\frac{O''X}{O'X} = \frac{qQ'}{qQ}, \qquad (1.3)$$

L'ARC À TROIS ARTICULATIONS (PIVOTS)

L'axe médian d'une voûte est représenté sur la Fig. 1.11 ; ni la voûte ni sa charge ne sont nécessairement symétriques. Les deux moitiés de la nervure d'arc (arch rib) sont reliées entre elles et

aux sommiers (abutments), par des pivots (pins) sans frottements. Une telle voûte à trois pivots est biensûr une forme de construction parfaitement satisfaisante ; de plus, la voûte est calculée et statique et (par exemple) les réactions en A et B dues aux charges W_1 etc. peuvent être déterminées en une seule étape en décomposant (resolve) les forces et en en mesurant (taking) les moments. (On notera au passage que les valeurs de ces réactions ne seront pas affectées par de faibles mouvements des sommiers (abutments). Tant que la géométrie globale de la voûte est peu modifiée, les équations statiques seront également peu modifiées.)

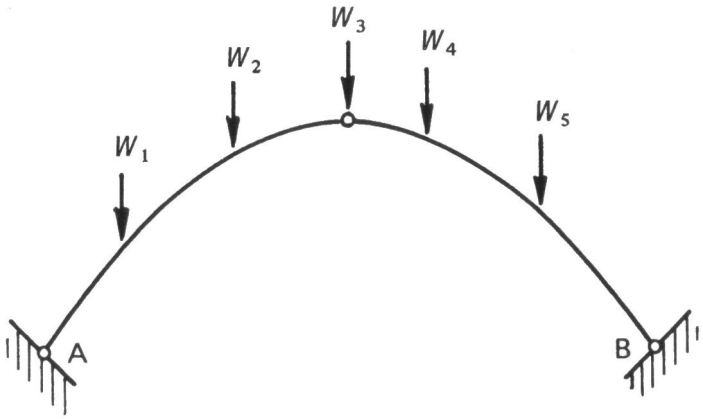

Fig. 1.11

Pour éviter d'avoir à écrire les équations statiques, les réactions peuvent être déterminées graphiquement. On verra immédiatement que les lignes de poussée dans la voûte, c'est-à-dire le polygone funiculaire, doivent passer par les trois pivots (pins), de sorte que les techniques illustrées par la Fig. 1.10 pourront être utilisées pour tracer les diagrammes de la Fig. 1.12.

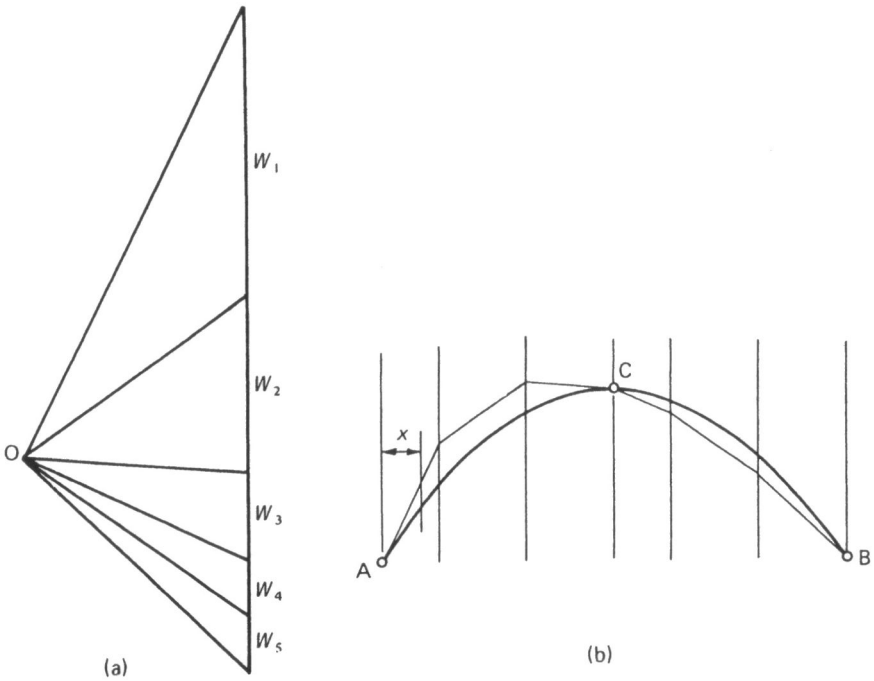

Fig. 1.12

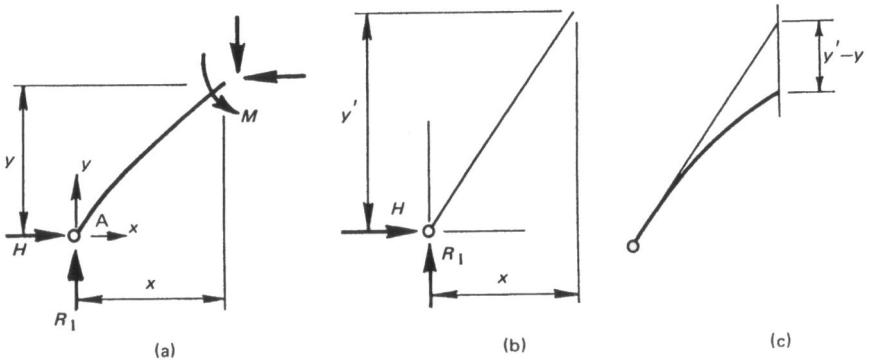

Fig. 1.13

On remarque que la ligne de poussée de la Fig. 1.12(b) ne coïncide pas, excepté au niveau des trois pivots, avec l'axe médian de la voûte et on peut en déduire une interprétation structurale simple. Sur la Fig. 1.13(a) l'arc (arch rib) a été 'coupé' à une distance horizontale x du pivot de sommier (abutment pin) A et les forces horizontale et verticale ainsi que le moment de flexion M ont été tracés à l'intersection en respectant l'équilibre. En développant (By taking) les moments, on trouve

$$M = -Hy + R_1 x, \tag{1.4}$$

soit, en réarrangeant,

$$M = H\left(\frac{R_1}{H}x - y\right), \tag{1.5}$$

La Fig. 1.13(b) représente le segment correspondant de la ligne de poussée et l'on voit que la quantité $R_1 x/H$ est égale à l'ordonnée notée y'. La Fig. 1.13(c) représente à la fois l'axe médian de la voûte et la ligne de poussée et la relation (1.5) ce qui implique que le moment de flexion dans l'arc (arch rib) est égal à la composante *horizontale* (H) de la poussée sur les sommiers (abutment thrust) multipliée par la distance *verticale* entre l'arc (arch rib) et la ligne de poussée.

Cette propriété a été démontrée dans les Figs. 1.12 et 1.13 en se référant à une portion particulière de la voûte, mais elle est en fait générale. Les distances verticales entre l'axe médian de la voûte et la ligne de poussée de la Fig. 1.12(b) donnent, dans une certaine mesure, les moments de flexion au cœur de l'arc (arch rib). De plus, comme un pivot sans frottements ne peut pas transmettre un moment de flexion, la ligne de poussée doit effectivement passer par les pivots A, B et C.

Comme le montre la Fig. 1.12(b), les moments de flexion dans la moitié gauche de la voûte fléchissent (are sagging) (on note que les charges W_1 et W_2 sont plus grandes que les autres), alors que les moments de flexion dans la moitié droite ont une flèche négative (are hogging). (Les signes des moments de flexion peuvent être vérifiés au moyen d'un simple exemple idéalisé. Dans la Fig. 1.14 une seule charge ponctuelle agit (a single point load acts) sur la voûte. La ligne de poussée correspondante dont la forme est équivalente à celle de la chaînette pendante doit correspondre aux deux lignes droites représentées.)

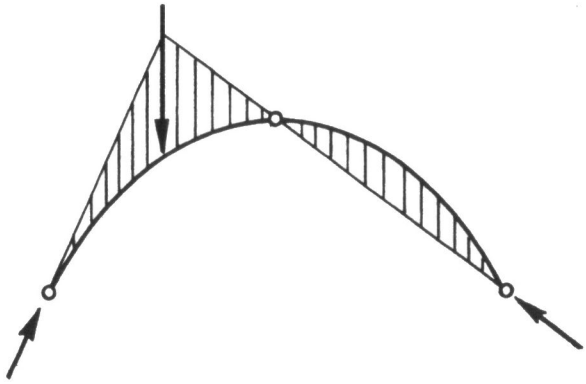

Fig. 1.14

LA RÈGLE DU TIERS MÉDIAN

Les charges et les constructions des Figs. 1.11 et 1.12 étaient appliquées à une voûte à trois pivots. La Fig. 1.15 représente les mêmes charges appliquées à un arc à voussoirs ayant le même axe médian que précédemment et la Fig. 1.16 représente le polygone funiculaire de la Fig. 1.12(b) dessiné pour la voûte de la Fig. 1.15. Evidemment, le polygone funiculaire représente une ligne de poussée en équilibre avec les charges données ; en général, cette ligne de poussée ne sera pas symétrique, ni même placée de façon symétrique à l'intérieur de la voûte.

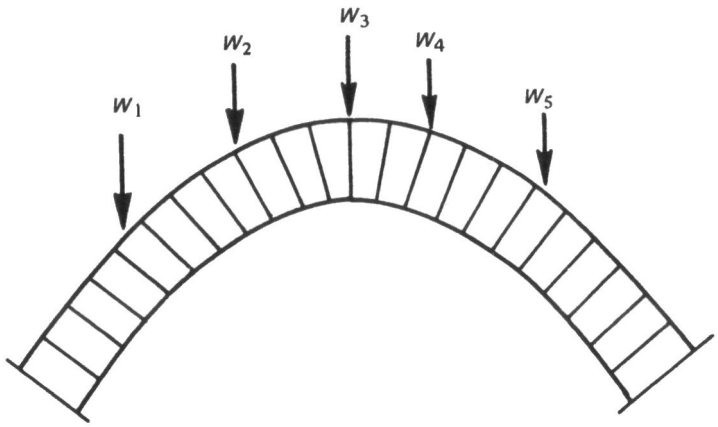

Fig. 1.15

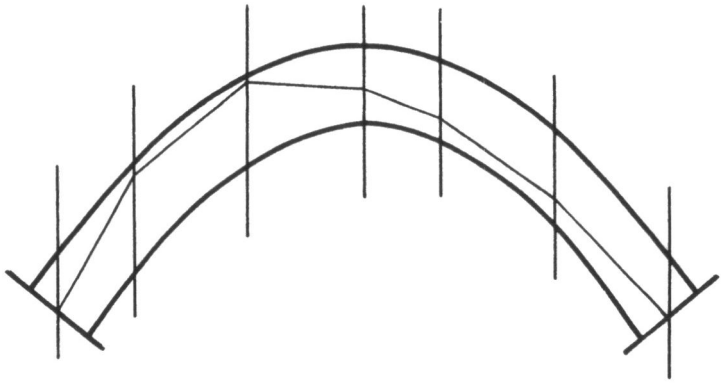

Fig. 1.16

L'hypothèse selon laquelle la ligne de poussée équilibre les charges peut être poursuivie. Si l'on 'coupe' la voûte en un point, par exemple le long du joint entre deux voussoirs, l'équilibre peut être maintained en introduisant une poussée au niveau de la coupe transversale agissant le long de la ligne du polygone funiculaire. Deux coupes ont été faites sur la Fig. 1.17 et la section de voûte est en équilibre sous l'action des forces tracées. On verra que la poussée dans la voûte n'est pas nécessairement transmise suivant la normale aux faces en culée (abutting faces) des voussoirs. Au

contraire, il existe une force normale à chaque section couplée à une force tangente (tangential force) et la seconde tend à faire glisser un voussoir sur l'autre. Cet effet de glissement instantané est faible et on le négligera entre une pierre et la suivante ; la question est traitée plus en détails dans le Chapitre 2. La question présente est celle de la poussée normale.

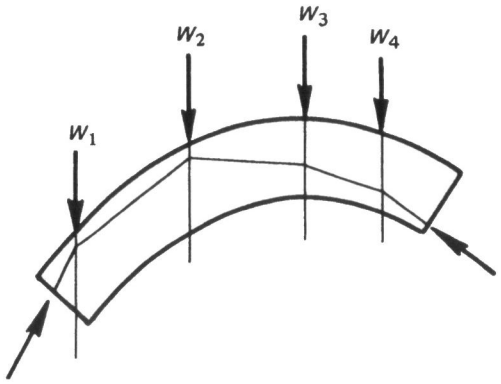

Fig. 1.17

Pour permettre une meilleure compréhension des actions structurales (structural action), la Fig. 1.18(a) représente un empilement de dalles de pierres identiques (dalles de pavement) posées l'une sur l'autre sans mortier de liaison. Les dalles elles-mêmes sont supposées élastiques et reposent sur une base rigide ; elles sont surmontées d'une dalle rigide à laquelle sera appliquée une charge verticale. Ainsi, sur la Fig. 1.18(b) une charge ponctuelle est appliquée au centre de l'empilement de dalles ; la théorie élémentaire de l'élasticité montre que toutes les dalles sont compressée de la même manière et qu'une contrainte uniformément distribuée sera transmise aux fondations. Dans la Fig. 1.18(c), la charge a été quelque peu éloignée du centre et la distribution de contraintes simplement prévue par la théorie élastique est représentée. Cette distribution est linéaire et lorsque la charge est à la limite du 'tiers médian' (Fig. 1.18(d)) la contrainte devient nulle à un des bords de l'empilement.

Si l'on continue d'éloigner la charge du centre, Fig. 1.18(e), l'empilement de dalles reste une 'structure' dans le sens où il peut continuer de supporter la charge appliquée de l'extérieur (externally-applied load). Cependant, comme les dalles sont supposées assemblées sans mortier, elles ne pourront pas transmettre les contraintes de traction et la théorie de courbure élastique en présence de forces de compression doit être modifiée. D'après la théorie élastique, la distribution effective de contraintes de compression de la Fig. 1.18(e) est toujours linéaire, mais dans les zones où la théorie de courbure prévoirait des tractions, les dalles tendent à se séparer.

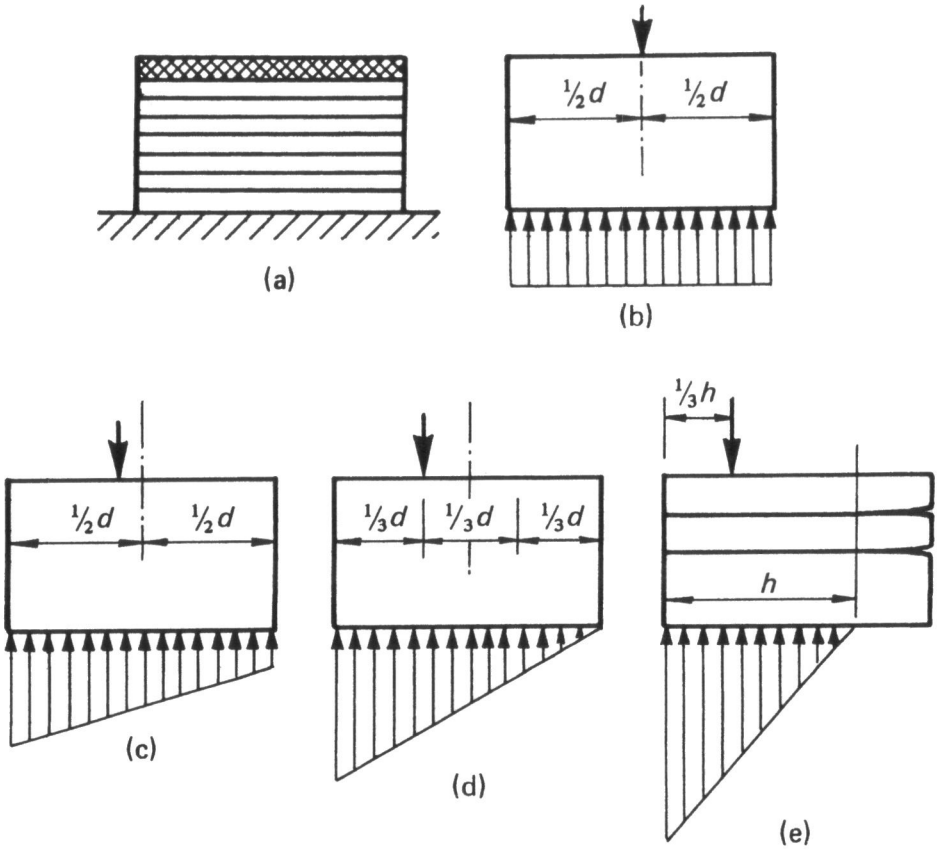

Fig. 1.18

Ainsi, si la charge appliquée reste à l'intérieur du 'cœur' de la section, les contraintes seront en compression sur toute la section. Pour une section rectangulaire, le cœur a une épaisseur d'un tiers de l'épaisseur totale ; si la section a une autre forme, le cœur aura une autre proportion de l'épaisseur totale. Pour une voûte en berceau c'est le tiers médian qui est pertinent et des ingénieurs du dix-neuvième (et du vingtième) siècle ont établi que la 'règle du tiers médian' est une nécessité première du dessin. Sur la Fig. 1.16, on aurait la certitude que le dessin est convenable si la ligne de poussée pouvait se trouver non pas à l'intérieur de la voûte (arch ring) mais bien à l'intérieur d'une voûte (arch ring) imaginaire plus étroite comme représenté sur la Fig. 1.19, laquelle aurait une épaisseur égale à un tiers de l'épaisseur réelle. (on peut noter que si le pole du polygone des forces était légèrement déplacé, à la fois horizontalement et verticalement, comme dans la Fig. 1.10, alors le polygone funiculaire de la Fig. 1.16 pourrait être déplacé jusqu'à la position tracée sur la Fig. 1.19. Ces deux lignes de poussées montrent deux manières différentes d'équilibrer les même charges *W* sur la voûte de la Fig. 1.15.)

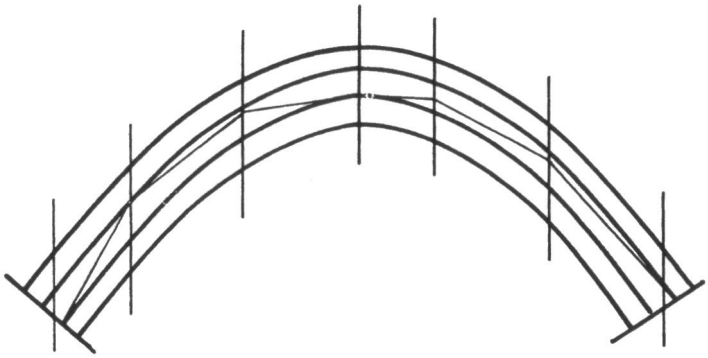

Fig. 1.19

Le critère du tiers médian a été établi sur le principe que les prévisions de la théorie élastique est observée en pratique ; les imperfections du monde réel, ou peut-être un simple coup d'œil à la

photographie de la Fig. 1.3, feraient douter de l'existence d'un comportement élastique linéaire. De plus, on a considéré que la traction devait être évitée étant donné que l'idée que la fissuration du mortier entre les voussoirs serait dangereuse n'a pas été justifiée. En fait la règle du tiers médian est parfois, du moins en théorie, assouplie à la règle de la moitié médiane ; l'arc intérieur de la Fig. 1.19 a été légèrement agrandi.

La restriction découlant de la Fig. 1.19 semble dériver d'arguments théoriques basés sur des suppositions douteuses. C'est néanmoins la bonne restriction à appliquer au dessin d'un pont, comme nous le verrons dans le prochain chapitre. En particulier, il pourrait sembler que la voûte réelle de la Fig. 1.19 a une sorte de facteur géométrique de sécurité correspondant à la voûte plus étroite. La Fig. 1.19 représente une voûte à l'intérieur d'une voûte ; si l'on peut montrer, d'une manière ou d'une autre, que la voûte la plus étroite est satisfaisante, alors on peut s'attendre intuitivement à ce que la voûte réelle soit également satisfaisante. La véracité de cette intuition est également démontrée dans le prochain chapitre.

Une préoccupation sera alors de voir s'il est possible ou non de construire des lignes de poussée, c'est-à-dire des polygones funiculaires, qui entrent dans des voûtes de dimensions données. De telles démonstrations peuvent être faite de manière purement analytique ; les calculs sont décrits plus loin dans ce livre. Il existe cependant une construction élégante qui démontre le problème de façon purement graphique.

LA CONSTRUCTION DE FULLER

La voûte de la Fig. 1.15 est représentée par son axe médian (centre line) sur la Fig. 1.20(a) de même que la ligne de poussée de la Fig. 1.16 (cf. Fig. 1.12(b)). Cependant, la ligne de poussée de la Fig. 1.20(a) ne doit pas nécessairement être une ligne particulière ; comme nous le verrons, le point O du polygone de forces (Fig. 1.12(a)) peut être placé à n'importe quelle positions convenable pour commencer la construction de Fuller.

La Fig. 1.20(b) fournit les mêmes informations que la Fig. 1.20(a), mais l'échelle horizontale a été déformée. Chaque portion de chaque voûte (entre les points de charge) a été étirée ou compressée de telle manière que la ligne de poussée prenne simplement la forme de deux lignes droites tandis que l'axe médian de la voûte (à l'origine probablement parabolique) a pris la curieuse forme tordue représentée. Cependant, les distances verticales entre l'axe médian de la voûte et la ligne de poussée sont les mêmes respectivement pour chaque segments sur les Figs. 1.20(a) et (b).

La dégénérescence du polygone funiculaire en deux lignes droites est la caractéristique importante de la construction de Fuller. Pour une série de charges données, une fois la forme déformée de la voûte tracée, voir Fig. 1.20(b), le point O du polygone de forces est déplacé, le polygone funiculaire continuera d'être représenté pas deux lignes droites ; ceci découle de la question discutée plus haut dans ce chapitre des propriétés du polygone de forces et du polygone funiculaire.

Ainsi, la Fig. 1.20(c) représente le profil déformé de la voûte d'épaisseur limite (corriger le texte anglais). On peut désormais déterminer s'il est possible ou non d'équilibrer les charges données avec une ligne de poussée inscrite dans la voûte. Il faut simplement démontrer que les deux lignes droites (représentées en pointillés sur la Fig. 1.20(c)) peuvent être représentées à l'intérieur de la voûte déformée. Ceci est clairement possible pour la voûte représentée, mais également ce ne serait clairement pas possible pour une voûte de plus faible épaisseur. De plus, dans le but de cette démonstration il n'est pas nécessaire de positionner un point O correspondant du polygone de forces.

La Fig. 1.20 a été redessinée dans une certaine mesure sur la Fig. 1.21. pour des raisons pratiques, les réactions verticales aux sommiers ont été déterminées par la statique, de sorte que le polygone funiculaire $Aa_1a_2 \ldots a_5B$ a été tracé sur une ligne de base horizontale AB ; les points A et B reposent sur l'intrados de la voûte. La valeur de la composante horizontale *H* de la poussée a été choisie arbitrairement. Chacun des points A' et B' sont ensuite pris sur la ligne de base et le polygone funiculaire déformé est constitué par les deux linges droites $A'a_2$ et $B'a_2$, où a_2 est (comme précédemment) le point le plus haut sur le polygone funiculaire. Ainsi le point a_5 sur le polygone funiculaire original vient en a'_5, et le point b_5 correspondant sur l'intrados est déplacé de la même distance horizontale en b'_5.

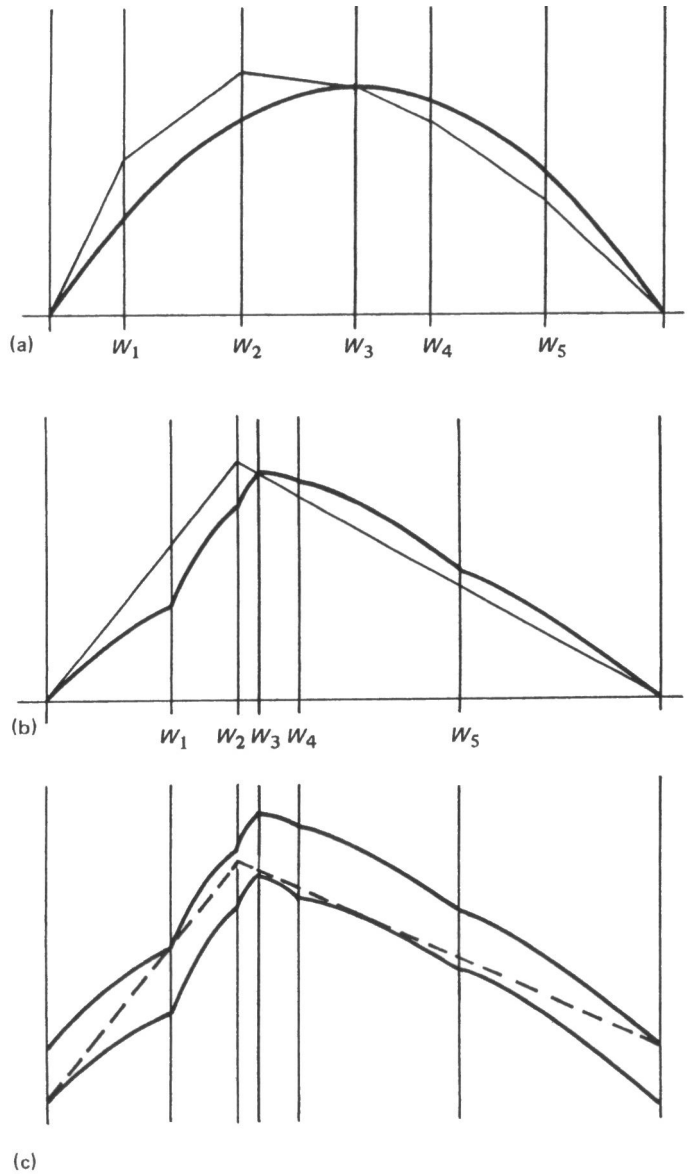

Fig. 1.20

Les lignes de construction sont représentées sur la Fig. 1.21 uniquement pour les intrados, mais les extrados déformés sont aussi représentés. Une fois de plus, la Fig. 1.21 contient les mêmes informations que la Fig. 1.20(c). Pour la voûte réelle, un polygone funiculaire avec des charges données peut être dessiné et complètement inscrit dans la maçonnerie si, sur la Fig. 1.21, deux lignes droites peuvent être tracées dans l'épaisseur de la voûte déformée.

L'idée qu'une voûte doit avoir une épaisseur minimale pour supporter une ligne de poussées pour des charges données (et la possibilité de déterminer cette épaisseur minimale) est la clé pour établir un facteur de sécurité pour des constructions pratiques. Ceci va être discuté dans le chapitre suivant.

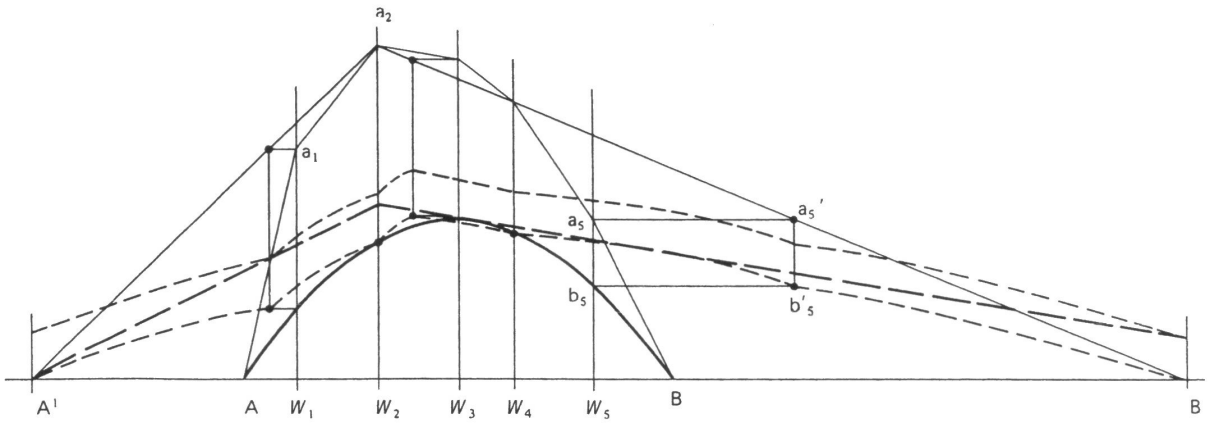

Fig. 1.21

2

Les théorèmes plastiques

La théorie des structures est basée sur l'établissement de trois différents types d'équations. En premier lieu il faut faire des hypothèses pour exprimer le fait qu'une structure donnée est en *équilibre* sous des charges appliquées données. Deuxièmement il est possible d'établir des hypothèses sur les *déformations* de la structure. Enfin, il peut être nécessaire d'introduire dans l'analyse les *propriétés matérielles* de la structure. Ainsi dans l'analyse élastique conventionnelle les forces internes peuvent s'écrire en terme de charges appliquées à l'extérieur ; les déformations internes peuvent être calculées comme étant linéairement dépendantes des forces internes, et les déplacements de la structure qui en résultent doivent être compatibles avec n'importe quel (internally or externally imposed restraints). Une structure est statiquement déterminée si les forces internes peuvent être établies immédiatement par de simples considérations d'équilibre en termes de charges appliquées ; elle est statiquement indéterminée si des forces ne peuvent pas être établies de cette façon. Ce livre ne traite pas des solutions élastiques pour des structures statiquement indéterminée, mais il faut noter que ces solutions peuvent être établies de différentes manières et que les trois types de master equation peuvent être utilisées en termes de différentes quantités inconnues.

On a remarqué que la voûte de la Fig. 1.11 (supposée avec trois attaches sans frottements) était une forme statiquement indéterminée de structure. Pour une charge W_1, W_2… donnée, les réactions en A et B peuvent être établies de sorte que la charge extérieure soit parfaitement déterminée. Le polygone funiculaire de la Fig. 1.12(b) est unique puisque il est obligé de passer par les trois points A, B et C (c'est-à-dire que la position du point O du polygone de forces de la Fig. 1.12(a) peut être déterminée sans ambiguïté) ; ainsi les forces internes, par exemple le moment de courbure de chaque section de la voûte, peuvent être évaluées directement. Tous ces calculs peuvent être faits sans faire référence à des notions de déformation et sans informations sur les propriétés du matériau constituant la voûte. Ainsi il n'est pas nécessaire de faire d'hypothèses sur les déformations internes de la voûte ni de restrictions sur les déplacements.

Cependant, ces remarques sous-entendent, selon le postulat habituel de la théorie structurale, que les déplacements sont petits. L'axe médian de la voûte de la Fig. 1.12(b) ne doit pas nécessairement conserver *exacement* sa forme originale lorsqu'elle est chargée et les sommiers A et B peuvent éventuellement give way slightly under the abutment thrust. Ces déformations ne sont cependant pas assez importantes pour être remarquées ; put in a loose way l'aspect déformé de la voûte chargée est suffisamment semblable à l'aspect original pour qu'il ne soit pas nécessaire de prendre en compte les modifications de géométrie lorsqu'on établit les équations d'équilibre.

On peut biensûr évaluer numériquement de telles restrictions sur les déformations. Dans l'optique de cette analyse, il faut admettre qu'un déplacement d'un point quelconque sur l'axe médian de la voûte d'un millième du span ou d'un centième du span will not upset les équations d'équilibre. Cependant le fait que les équations d'équilibre sont très peu affectées ne définit pas à ce stade les effets que ces petites déformations pourraient avoir sur le comportement général de la voûte. Does a small spread des sommiers, même invisible à l'oeil nu, cause harm à la voûte ? Quel est l'effet d'un pilier enfoncé dans une rivière différemment de ses voisins ? Nous allons voir que la théorie plastique fournit des réponses à ces questions (fairly strong answers to such questions).

LE PROBLÈME STRUCTURAL

Toute théorie des structures, qu'elle soit élastique ou plastique, doit traiter des cas statiquement indéterminés. C'est-à-dire qu'il n'y a en principe pas de difficultés à utiliser les forces internes

statiquement déterminées de la voûte de la Fig. 1.12(b) pour calculer les déplacements (en supposant que les propriété du matériau sont connues) et le dessinateur peut déterminer facilement les magnitudes des contraintes ou de n'importe quelle autre quantité significative. By contrast, the arch of Fig. 1.15, having the same centre line and carrying the same loads as the three-pin arch, is statically-indeterminate. The line of thrust may be close to that sketched in Fig. 1.16, but there are no longer three fixed points which can be used to locate it. The prime structural problem, stated here in terms of the voussoir arch, consists in fact in determining the position of the line of thrust, so that the internal structural forces can be found.

The other structural equations must of course be used in order to solve the problem. That is, the *equilibrium* statement for the voussoir arch is represented by the funicular polygon and by the force polygon, but no information is provided from considerations of statics which may be used to determine the position of the pole O of the force polygon (as, for example, in Fig. 1.12(a)). All that can be determined from statics is the general shape of the line of thrust in Fig. 1.16, but not its precise location.

For the purpose of a plastic analysis, as opposed to an elastic analysis, of the voussoir arch, very little need be said concerning the *deformation* of the structure. As noted above, displacements will be assumed to be small, but a general analysis of the strains suffered by the arch is not necessary. As will be seen, the geometry of the way an arch might collapse must finally be studied, and in fact this study helps to determine possible positions for the funicular polygon.

The *material properties* of the masonry in a voussoir arch must be defined carefully, to provide the third of the statements necessary for the establishment of a theory of structural action. There are three key assumptions:

Sliding failure cannot occur
It is assumed that friction is high enough between voussoirs, or that the stones are otherwise effectively interlocked, so that they cannot slide one on another. It turns out that this is a perfectly reasonable assumption, although it is certainly possible in practice to find occasional evidence of slippage in a masonry structure.

Masonry has no tensile strength
Although stone itself has a definite tensile strength, the joints between voussoirs may be dry or made with weak mortar. Thus the assumption implies that no tensile forces can be transmitted within a mass of masonry. In accordance with common sense, and with the principles of the plastic theorems (which are discussed below), this assumption is 'safe'; it may be too safe, that is, unrealistic if, for example, the interlocking of the stones which prevents sliding also enables tensile forces to be transmitted locally.

Masonry has an infinite compressive strength
This assumption implies that stresses are so low in masonry construction that there is no danger of crushing of the material. The assumption is obviously 'unsafe', but it is not, in fact, at all unrealistic. It is found that, for a wide range of bridges of the type considered here, mean stresses are indeed low; clearly check calculations must be made for any given structure. General implications of this assumption are pointed out below.

Thus a picture emerges of masonry as an assemblage of stones cut to pack together in a coherent structural form, with that form maintained by compressive forces transmitted within the mass of the material. These forces will arise, in the 'dead' state of the structure, from the self-weight of the material and (for example) from the weight of any superincumbent fill in the spandrels of the arches of a bridge. Live loading will equally be carried by compressive forces, and in all cases these forces are supposed to be high enough for friction to provide interlocking against slip.

The question then arises as to how such a masonry assemblage might fail in any meaningful structural sense. If the masonry is infinitely strong, then it would seem that a calculation of levels of stress will not lead to a criterion of failure. The idea that tension is not permissible is, however,

significant. In Fig. 2.1(a) the joint Mm between two particular voussoirs has somehow been identified as a 'critical' joint (how the joint is identified will be seen later). It would seem that the joint could be considered critical if the thrust transmitted between the voussoirs approached the surface, as say the extrados m, permitting the 'hinge' of Fig. 2.1(b) to form. (Equally, a hinge might form by turning about the point M in the intrados.) The hinge of Fig. 2.1(b) corresponds to the final limit of the sequence shown in Fig. 1.18, in which the eccentric load has reached the edge of the pile of paving slabs.

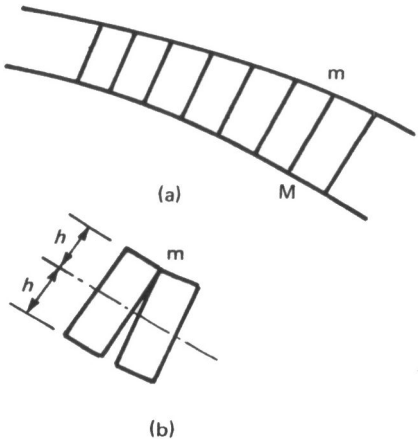

Fig. 2.1

Now the stress resultants, that is, the structural action at any joint such as Mm between voussoirs, will be specified in terms of the magnitude, direction and point of application of the force transmitted across the joint. In fact, if the tangential component of the force is not of importance (since slip is assumed not to occur), then what is needed is a knowledge of the value of the normal force N across the joint together with the value of its eccentricity (say e) from the centre line. It is convenient to work, temporarily, with a 'bending moment' $M = Ne$ as the second variable, so that the stress resultants N, M define the state of the structure at any particular section.

The hinge of Fig. 2.1(b) will form when the eccentricity e of the normal thrust just has the value h, that is when $M = hN$. The lines $M = \pm hN$ are shown as OA and OB in Fig. 2.2, and they represent, for any given joint between voussoirs, the condition that a hinge is in existence. A general point (N, M) in Fig. 2.2 which lies within the open triangle AOB represents a thrust passing between voussoirs at an eccentricity less than h, that is, the line of thrust lies within the masonry at that point and no hinge is forming. If the general point lies on OA or OB, then a hinge is forming in either the extrados or the intrados of the arch, and the thrust line lies in the surface of the masonry. The general point cannot lie outside the open triangle AOB, since equilibrium across the joint would then be impossible for a material assumed to be incapable of carrying tension.

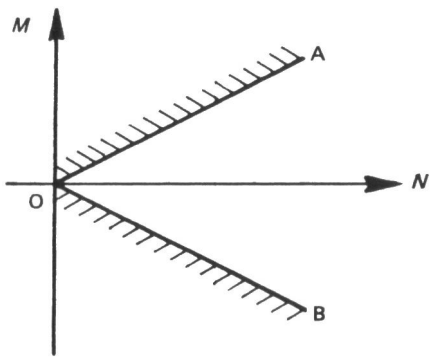

Fig. 2.2

The construction of Fig. 2.2 involved the assumption that the masonry had infinite compressive strength. As the line of thrust approaches the edge of a voussoir (cf. Fig. 1.18(e)), so the stress on the diminishing area of contact will increase, and a real stone with a finite crushing strength

will not permit the sort of line contact at a hinge illustrated in Fig. 2.1(b). Thus the lines OA and OB in Fig. 2.2 cannot quite be reached; they are replaced by the slightly curved lines of Fig. 2.3. The full boundary is formed by the parabolic arcs OCD, OED in Fig. 2.4, and the general point (N, M) representing the thrust at any point in the arch is constrained in reality to lie within this boundary.

The assumption of generally low mean compressive stresses in fact constrains the point (N, M) to lie within an area such as OCE in Fig. 2.4; it is this area which is enlarged in Fig. 2.3, and for which the real curved boundaries depart only slightly from the approximately straight lines.

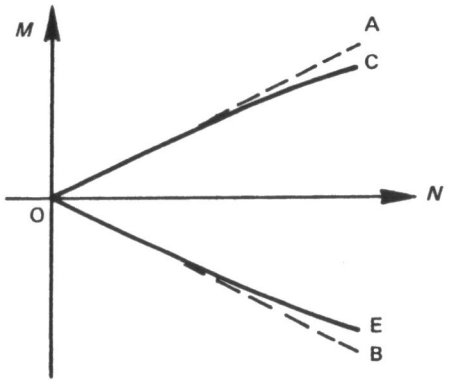

Fig. 2.3

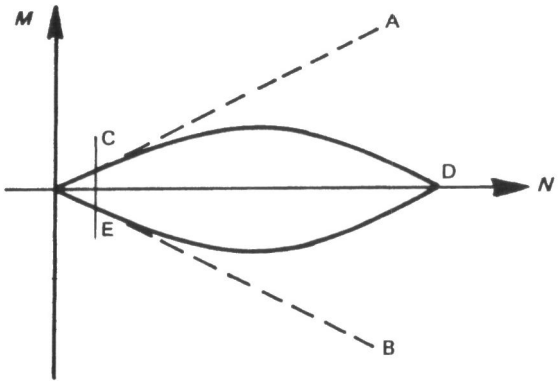

Fig. 2.4

The constraining boundaries of Figs. 2.2, 2.3 and 2.4 are examples of yield surfaces in the theory of plasticity, and the whole discussion can now be pulled within the framework of that theory. Figure 2.2 will be used as the basis for the development of the principles, although the results will clearly be slightly unsafe. They may in fact be made absolutely safe by the device sketched in Fig. 2.5. If it is thought that the mean axial stresses will not exceed say 10% of the crushing strength of the material, then the straight lines OA, OB of Fig. 2.2, that is, $M = \pm hN$, may be replaced by the straight lines OC, OE of Fig. 2.5, given by $M = \pm 0.9\,hN$ (cf. Fig. 2.3). Thus the real arch having a (local) ring depth of $2h$ is replaced, for the purposes of analysis, by a hypothetical arch of depth $2(0.9h)$; this kind of 'shrinking' is, as will be seen, of some importance in the gauging of the safety of masonry arches. The assumption that mean stresses are less than 10% (or any other percentage) of the crushing strength can be checked at the end of the calculations.

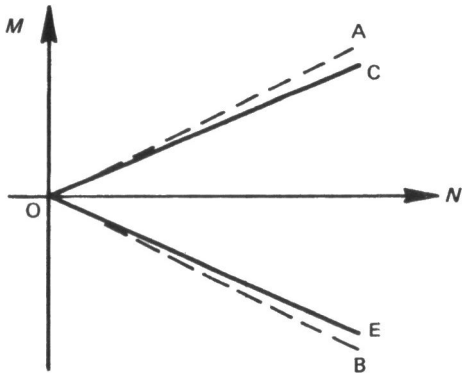

Fig. 2.5

Thus it will be assumed that the general point (*N*, *M*) is confined to lie within the open triangle AOB in Fig. 2.2. This implies, as has been seen, that the thrust line for the arch must lie within the masonry. In turn, this means that the pole O of the force polygon must be located in such a position that the corresponding funicular polygon (that is, the thrust line) does indeed lie within the masonry. No guidance, other than this requirement, has yet been given for locating the 'actual' position of the pole O and the corresponding 'actual' position of the thrust line. (The reason for suspicion as to the use of the word 'actual' will become clear.)

However, a very powerful statement can be made by translating the 'safe' (or lower-bound) theorem of plasticity into terms applicable to masonry. It is this: If a thrust line can be found, for the complete arch, which is in equilibrium with the external loading (including self weight), and which lies everywhere within the masonry of the arch ring, then the arch is safe. The importance of this theorem lies in the fact that the thrust line found in this way needs not be the actual thrust line. To demonstrate that the arch will stand as a structure it is necessary to show only that there is at least one satisfactory internal force system; viewed anthropomorphically, the arch is at least as clever as the analyst, and it will discover for itself an equally satisfactory position for the pole of the force polygon.

The conclusions of the safe theorem are positive; having found any one satisfactory thrust line, the designer knows that his arch cannot collapse, and he is relieved of any necessity to examine possible modes of failure. This anti-insomnious comfort of the safe theorem has always been appreciated by the experienced designer, even if he has not been able to formulate precisely that theorem on the basis of plastic theory. It is the designer's job to derive a 'reasonable' set of equilibrium forces on which to base his calculations, and he is accustomed to using whatever aids he can to arrive at values for those forces.

Thus to assess the actual state of a masonry arch, the traditional elastic approach will make certain assumptions about the abutments, for example that they are rigid, or that they give way according to certain specified rules when subjected to load. With some definite assumptions of this sort, an elastic analysis can be made of the structure (or indeed, an inelastic analysis, if the complications of real material properties can be accommodated). The designer will then have derived a set of forces compatible with his assumptions, and certainly in equilibrium with the applied loads. To describe this set of forces as the actual state of the structure is, however, to conclude too much from the analysis.

If from no other cause, the passage of time will ensure inevitably the destruction of the designer’s assumptions; an abutment will give way slightly, or a pier will settle, and very small movements of this sort can alter markedly the equilibrium state of the structure, However, it does not seern reasonable to suppose that a settlement of a few millimetres in a span of a few metres, even if it has an apparently large effect on the position of the thrust line in the arch, can really have any measurable effect on the final strength of the arch.

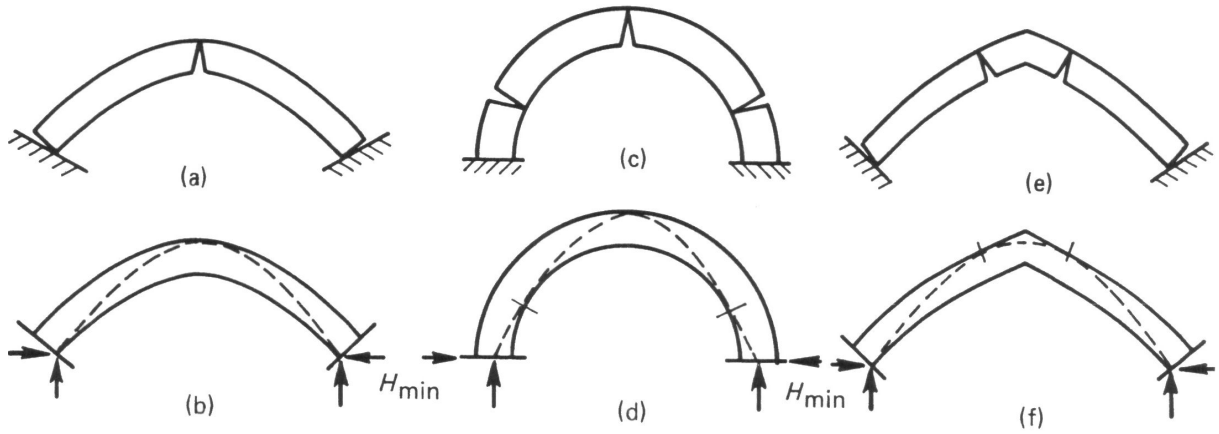

Fig. 2.6

It is precisely this common-sense view that is justified by the safe theorem. Small deformations of the arch, not apparent to the eye, can cause the thrust line to shift violently within the masonry (as will be illustrated below, Figs. 2.6(f) and 2.8(b)). The safe theorem states that once it has been shown that there is a single position of the thrust line lying within the masonry, then (to continue the anthropomorphic view) no matter how the thrust fine thrashes about in response to the changes in the external environment, it can never escape from the masonry.

The matter is one of overall geometry. A defect of a few millimetres in a few metres is a defect of the order of one part in a thousand, that is, of the order of the thickness of a pencil line in a drawing of the arch. On the drawing board the perfect arch and the defective arch appear to be the same. A funicular polygon drawn for the perfect arch and found to be satisfactory will be equally satisfactory for the defective arch.

THE GEOMETRICAL FACTOR OF SAFETY

As has been remarked, words like 'satisfactory' and 'safe' may be clear, but they carry no numerical meaning. The statement that an arch is 'safe' if it can be shown to contain a proper funicular polygon does not indicate the extent of that safety. Some progress can be made towards the derivation of a numerical assessment by considering the ways in which an arch might fail. As a first step, some light will be shed by a study of the way in which an arch can adapt itself to small movements of its supports.

A voussoir arch, made of rigid material and otherwise obeying the assumptions of material behaviour listed above, may be imagined to be fitted exactly between abutments. If the abutments then spread, the arch could accommodate itself to the increased span by forming three hinges as in Fig. 2.6(a), one at the crown in the extrados, and one at each abutment in the intrados. If the arch is a full semi-circle, then the hinges in the intrados will move away from the springings (Figs. 2.6(c) and 2.7) but in either case the arches of Figs. 2.6(a) and (c) have become, effectively, three-pin arches. The funicular polygons for these arches can be drawn immediately, since the line of thrust must pass through the hinge points, and schematic fines (for an assumed symmetrical loading) are sketched in Figs 2.6(b) and (d).

The pointed arch of fig. 2.6(e) will, in theory, form four hinges if the span increases. Now the three-pin arch is a well-known structural form; in the light of remarks below on conditions for formation of a collapse mechanism, care must be taken to avoid alarm at the sight of the four hinges of Fig. 2.6(e). Figure 2.6(f) shows the corresponding thrust line, and it is evident that if there is a slight asymmetry, either geometrically or in the loading, then one of the hinges in the extrados near the crown will not form. The two hinges are in effect a single hinge, split and displaced, but remaining of the same sign (that is, with their hinge lines both in the extrados); two neighbouring hinges of the same sign can always be regarded in this way as a split hinge, one component of which will be suppressed by any slight asymmetry. (There are other ways in which supernumerary hinges may be formed, but such hinges can again be detected by appealing to notions of symmetry.)

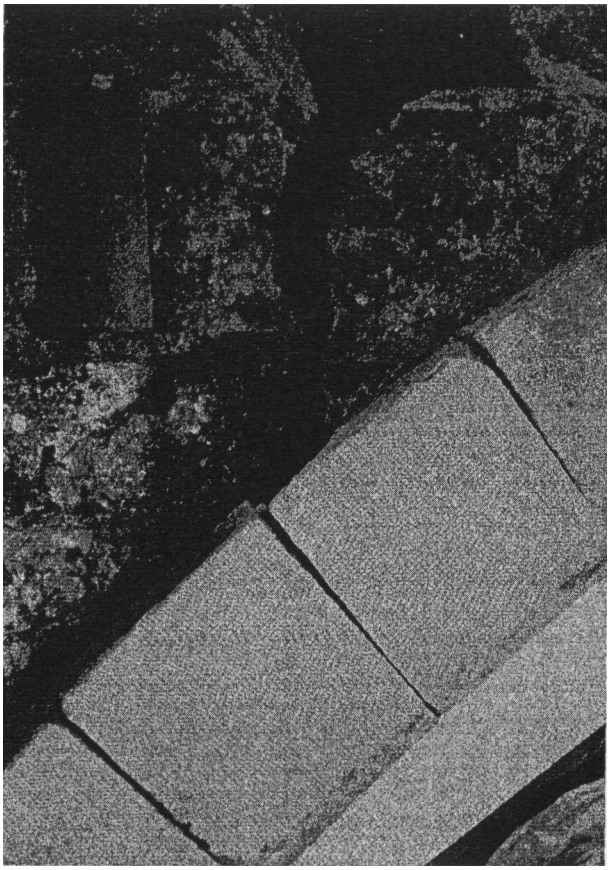

Fig. 2.7 Clare College 1 Bridge, Cambridge. Another view of the region shown in Fig. 1.5. The increase in span of the central arch has led to the formation of hinges between voussoirs.

The pole of the force polygon which leads to the funicular polygon of say Fig. 2.6(f) lies as close as possible to the force polygon. That is, the value of the abutment thrust, H_{min}, has its least possible value. There is, correspondingly, a maximum possible value H_{max} which can be determined from a study of Fig. 2.8. The abutments of the arch are now too close, and three hinges have again been formed to accommodate the decreased span.

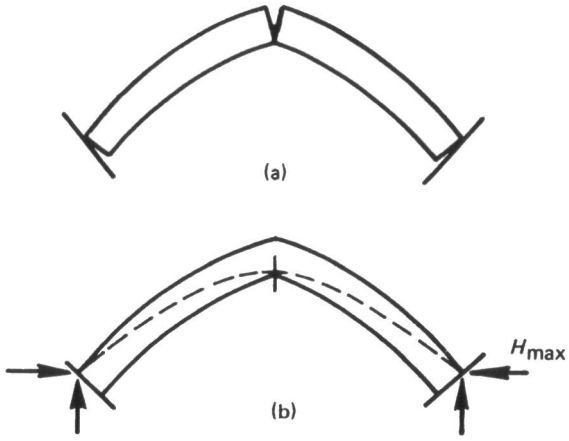

Fig. 2.8

Figures 2.6(f) and 2.8(b) represent pictorially the two extreme configurations of the funicular polygon. The movements which bring about the formation of the hinges are supposed to be small, but it is clear that these small movements can force the thrust line to adopt two widely different positions. However, for each limiting position of the thrust line the corresponding value of the abutment thrust can be calculated, and H_{max} and H_{min} represent upper and lower bounds on that value. Thus, despite

the uncertainty in practice as to the precise support conditions for the arch, it is at least possible to obtain numerical limits for at least one structural quantity; the safe theorem is not so blunt a tool as it might appear.

Figure 2.9 (a) shows a semi-circular arch for which the funicular polygon is contained comfortably within the masonry, and which is, therefore, 'safe'. It is evident that a thinner arch ring could accommodate the same funicular polygon, that is, that a thinner arch could carry safely the same loads, but it is also clear that there is a limit to the amount that the arch ring could be reduced. This limit is reached in Fig. 2.9(b), and the arch is on the point of collapse by the formation, of a mechanism of four hinges; five hinges are shown in the absolutely symmetrical arch of Fig 2.9(c).

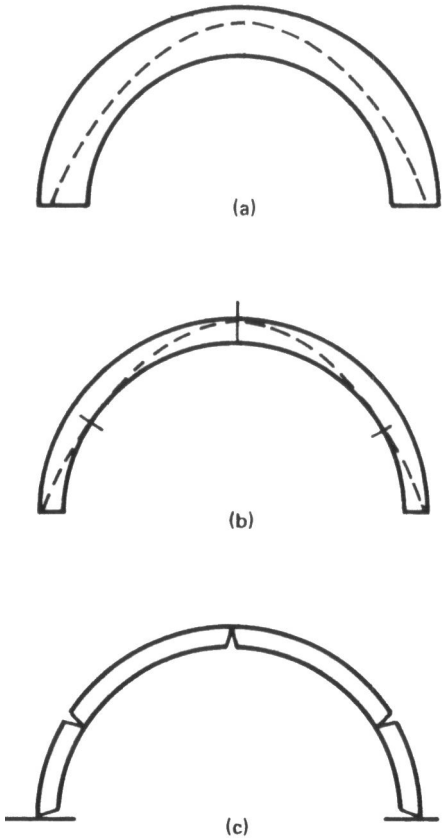

Fig. 2.9

The thinnest possible arch of Fig. 2.9(b) could be thought of as being contained within the actual arch of Fig. 2.9(a), and the amount by which the actual arch must be 'shrunk' to reach its thinnest possible state leads to the idea of a geometrical factor of safety. The concept of an arch within an arch was discussed in the first chapter; Fig. 1.19 shows the thrust line contained within the middle third of the arch ring. However, the middle-third arch arises from a study of the elastic behaviour of the material, whereas the geometrical factor of safety arises from a study of diagrams such as Fig. 2.9(a) and (b), in which the geometries of the funicular polygon and of the arch itself are compared.

Thus a design rule based upon a geometrical factor of safety of 3 is exactly equivalent in practice to the middle-third rule, although the two rules have been devised in very different ways. However, the value of 3 is, from the point of view of the geometrical factor of safety, arbitrary. It may be that some other value, perhaps smaller than 3, would be appropriate for practical arch design. In this connection, it should be noted that the establishment of a reasonable value for the geometrical factor of safety is not in itself sufficient to give assurance of an adequate margin for the safety of a given arch. If live loads are reasonably high, then indeed, as will be seen, the geometrical factor may be all that is necessary for a practical design, but (to take a trivial example) if only dead loads act on the arch, then the centre line of the arch may have been designed to coincide exactly with the dead-load line of thrust. In this case the geometrical factor of safety for the given loading is theoretically

infinite, whatever the thickness of the arch, although a thin rib, even of the correct shape, will be in a practical sense potentially unstable.

Thus a second measure of safety might arise from some assessment of the resistance of the arch to the action of a disturbing load (say a superimposed point load). In practice the 'live-load' test could be combined with the geometrical test. A suitable value of point load could be selected, and the minimum thickness of arch determined to contain a thrust line for both the original loading and the test loading. It is this sort of approach that is examined in Chapter 4.

Finally, a strength test could be devised. It has been assumed that stress levels are low, but this must be checked for any given design. A value of permitted stress will, in itself, lead at once to a minimum thickness of arch ring for given loading. For spans which are very large, or for arches of low rise which therefore have high thrusts, it may be that the strength of the material will govern the design. For bridges of usual dimensions, however, a limiting value of stress will usually not be the critical criterion, unless a very high factor of safety on stress is imposed. Instead, it is a mechanism of collapse, arising from suitably disposed hinges between the voussoirs, that is likely to form the basis of the assessment of safety.

MECHANISMS OF COLLAPSE

It has been noted that the three-pin arch is a satisfactory structural form; it is statically determinate, and the funicular polygon for given loading is unique. It is a fourth hinge which converts the statically-determinate three-pin arch into a mechanism. In Fig. 2.10(b) an idealized semi-circular arch is supposed to be acted upon by its own weight and by a single point load. As this point load is imagined to increase slowly in magnitude, the self-weight of the arch will have less and less effect on the shape of the funicular polygon; in the limit, the thrust line will consist of the two straight lines shown (cf. Fig. 1.14). For the particular dimensions sketched in Fig. 2.10(b) it is evident that a sufficiently large point load cannot be supported by two straight thrust lines lying wholly within the masonry; as the point load increases in magnitude, a stage will be reached when the arch collapses by the mechanism of four hinges sketched in Fig. 2.10(c).

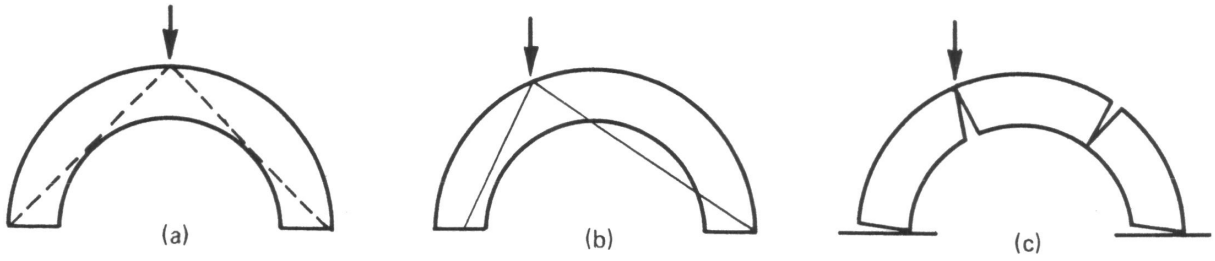

Fig. 2.10

The idealized arch has been drawn with very particular proportions; in Fig. 2.10(a) it will be seen that straight thrust lines *can* be drawn within the masonry to support a point load placed at the crown. The safe theorem would thus imply that the arch can carry a point load of any intensity at the crown (provided the strength of the material against crushing is not exceeded). The counterpart of this theorem is that there is no arrangement of hinges, for which one hinge, is at the crown, which will lead to a 'four-bar chain' mechanism of the type indicated in Fig. 2.10(c).

The four-bar chain is the basic mechanism for collapse of an arch. There are in fact many structures for which no pattern of hinges can be devised to lead to a four-bar chain, and such structures are, within the framework of the assumptions about material behaviour, infinitely strong. The flat arch between rigid abutments of Fig. 2.11(a) is one such 'perfect' structure; there is no arrangement of hinges in the extrados and intrados of the arch which gives rise to a mechanism of collapse. The flat arch can carry any pattern of loading, and each of the other arches in Fig. 2.11 is a development of the flat arch.

Use will be made of these ideas of mechanisms of collapse, on the one hand, and of safe positions of lines of thrust, on the other, to make an assessment of the strength of actual arches.

Before these ideas are developed, however, they may perhaps be illuminated by a brief review of the history of the analysis of arches.

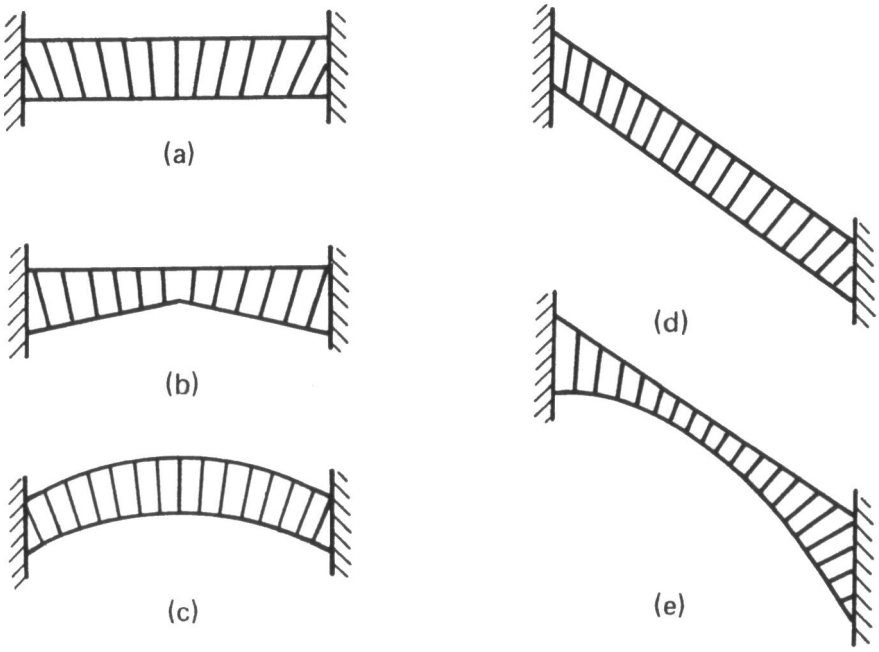

Fig. 2.11

Fig. 2.12 Flat arches at the Colosseum, Rome, 1st Century AD.

3

Some historical notes

THE STATICS OF THRUST

It was noted in Chapter 1 that the statics of the problem of the hanging chain were the same as those of the arch; the same techniques of force and funicular polygons can be used for each (cf. Figs 1.7 and 1.8). As early as 1675 Robert Hooke had concerned himself with 'the true Mathematical and Mechanical form of all manner of Arches for Building', and had published the statement 'Ut pendet continuum flexile, sic stabit contiguum rigidum in.versum' - 'as hangs the flexible line, so but inverted will stand the rigid arch'. However, while Hooke had gained this insight into the behaviour of the arch, he had not in fact solved the statics of the problem, and his publication was in the form of an anagram, to establish priority should another scholar stumble on the same idea.

Hooke had already demonstrated to the Royal Society some experiments on model arches, but it was not until after his death, in 1703, that the solution to the anagram was published. In the mean time, however, David Gregory had applied the newly-invented calculus to determine the shape of a hanging chain, and in 1697 he published the mathematical derivation of the catenary. He made mistakes in this work, which was intended to supply the proofs to otherwise unsupported statements of Huygens, Leibniz, and John Bernoulli, made in 1690-91. It is, however, Gregory's commentary (in a translation by Ware) that is of present interest:

> In a vertical plane, but in an inverted situation, the chain will preserve its figure without falling, and therefore will constitute a very thin arch, or fornix; that is, infinitely small rigid and polished spheres disposed in an inverted arch of a catenaria will form an arch; no part of which will be thrust outwards or inwards by other parts, but, the lowest part remaining firm, it will support itself by means of its figure… And, on the contrary, none but the catenaria is the figure of a true legitimate arch, or fornix. *And when an arch of any other figure is supported, it is because in its thickness some catenaria is included*. Neither would it be sustained if it were very thin, and composed of slippery parts.

The statement in italics (which were added by Ware) is, of course, nothing less than the safe or lower-bound theorem of plasticity, and the idea was used brilliantly by Poleni in 1748 in his analysis of the cracked dome of St Peter's. Figure 3.1 reproduces Poleni's Plate D, and gives evidence of his comprehensive grasp of the existing state of knowledge. At the bottom right is Hooke's hanging chain, and above is the fornix of "small rigid and polished spheres" (this last based closely on an illustration in a book of 1717 by Stirling).

The meridional cracks at St Peter's had effectively divided the dome into portions approximating half spherical lunes (orange slices) of the type shown schematically in the right-hand sketch of Fig. XIII in Fig. 3.1. Poleni sliced the dome, hypothetically, into fifty such lunes, and he considered the stability of an arch formed by two individual opposing lunes; he stated explicitly that stability would be assured if "our chain can be found to lie entirely within the thickness of the arch", and further, that if each individual arch were stable, then so also would be the complete dome. These two statements are correct.

The actual shape of the chain was found experimentally by Poleni, by loading a flexible string with weights each of which was proportional to that of a segment of the tune. This experimental line of thrust did indeed lie within the thickness of the dorne, and Poleni concluded that the meridional cracking was not dangerous. Moreover, the analysis furnishes a value for the horizontal thrust of the

dome at its base, and Poleni agreed with a previous recommendation that additional ties should be provided at the base to contain this thrust.

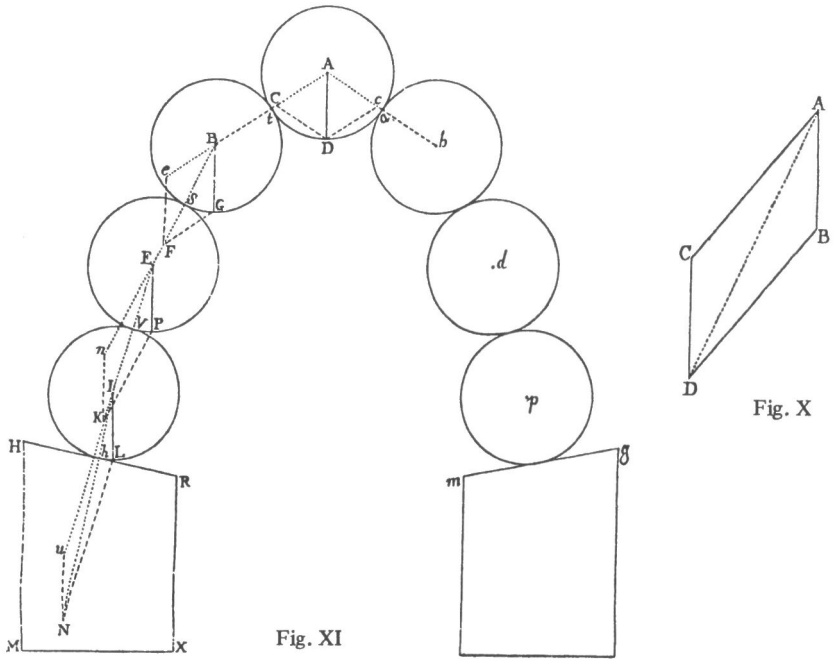

Fig. XI

Fig. X

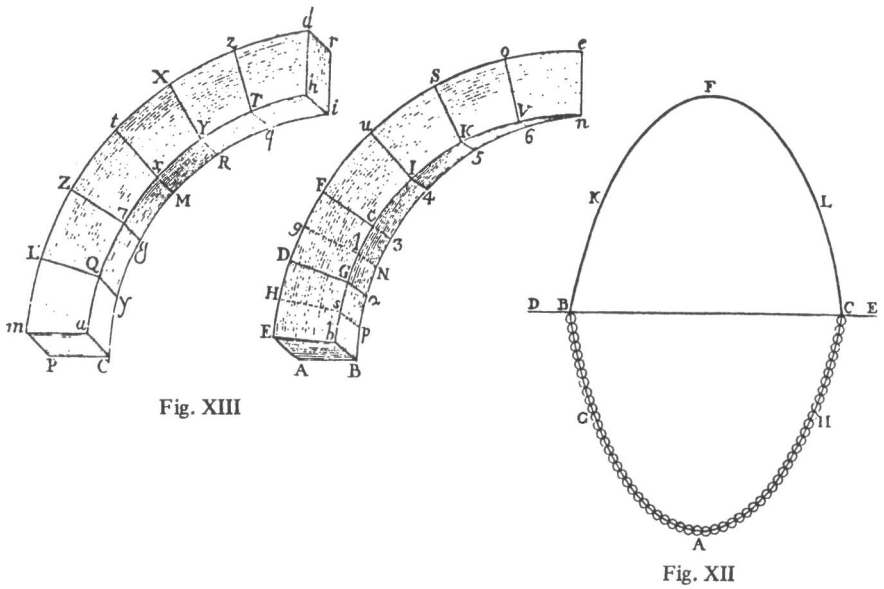

Fig. XIII

Fig. XII

Fig. 3.1

Almost exactly a hundred years later, in 1846, Barlow demonstrated models to the Institution of Civil Engineers illustrating the thrust of arches. One experiment was concerned again with the equivalence of the hanging chain and the inverted arch (Fig. 3.2); the semicircular arch shown has the minimum possible thickness, cf. Figs. 2.9(b) and (c). Further, the triangulation of forces at the left hand support of the chain in Fig. 3.2 was used by Barlow, as by Poleni before him, to calculate the horizontal component of the abutment thrust of the corresponding arch.

In another experiment, six voussoirs were assembled as in Fig. 3.3, with the 'mortar' in each joint in the form of four small pieces of wood, each of which could be withdrawn by hand. Three out of the four pieces at each joint were then indeed removed, in different configurations, and alternative positions of the thrust line were thus made 'visible'; the three lines shown in Fig. 3.3 may be compared with those of Figs 2.6(b), 2.8(b) and 2.9(a).

Thus Barlow was well aware that there are an infinite number of equilibrium states for a given masonry arch, and that the arch is, in fact, statically indeterminate. By 1879 notions of statical

indeterminacy were more fully developed, and Castigliano in his book applied the theorems which bear his name to the solution of the masonry arch. He knew that tension could not be transmitted between voussoirs assembled dry or with weak mortar. If, however, a section of the arch cracked (as in Fig. 1. 18(e)), then the flexural properties at that section would be affected, and Castigliano demonstrated a trial-and-error method of locating the position of the thrust line. His solution, therefore, was for an arch made of elastic/no tension material.

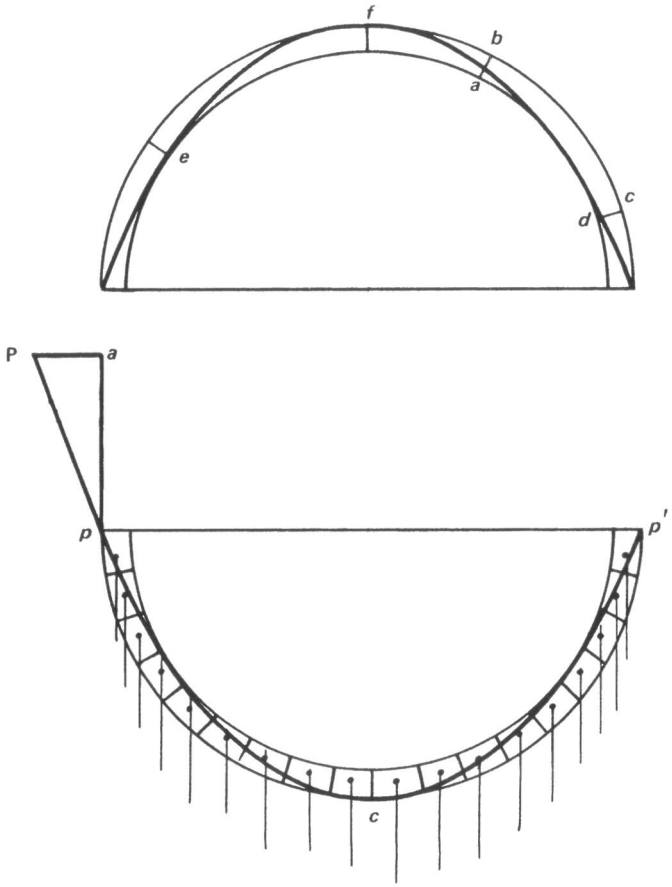

Fig. 3.2 (Barlow 1846).

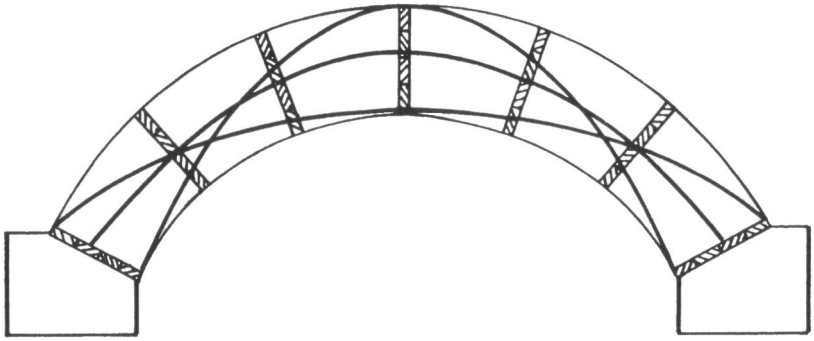

Fig. 3.3 (Barlow 1846).

Yvon Villarceau in 1854 was not bedevilled by such clear notions of statical indeterminacy, and he made no attempt to find 'the' solution to the problem of the position of the line of thrust. Instead, he developed a 'safe' design method by requiring the centre line of the arch to coincide with one of the possible thrust lines for the given loading. This inverse design method requires the numerical solution of the equations, and the results are given in the form of tables which can be used immediately in standard calculations by the bridge designer. Yvon Villarceau's work was elaborate, and his memoir to the French Academy was long, but the results were very accurate.

Inglis gives a simple closed-form example of the sort of inverse design made by Yvon Villarceau. Figure 3.4 shows a voussoir arch supporting a level roadway; the fill is supposed to be of

uniform density and to impose a purely vertical load on the arch ring. If the origin of coordinates is taken in the road surface on the centre line of the arch, and the equation of the arch centre line is $y = y(x)$, then the intensity of vertical load per unit horizontal length is ky. The problem posed by Inglis is the determination of the arch centre line so that it coincides with the thrust line resulting from this dead loading; that is, each element of the arch ring will be subjected to the forces of Fig. 3.5. From this figure, it will be seen that

$$\frac{d}{dx}(P\cos\psi) = 0, \tag{3.1}$$

or

$$P\cos\psi = H, \tag{3.2}$$

where H is the value of the horizontal component of the abutment thrust, and that

$$\frac{d}{dx}(P\sin\psi) = ky, \tag{3.3}$$

that is,

$$H\frac{d}{dx}(\tan\psi) = ky, \tag{3.4}$$

or

$$H\frac{d^2y}{dx^2} = ky, \tag{3.5}$$

Thus if the depth of the fill at the crown is a, then

$$y = a\cosh\alpha x, \tag{3.6}$$

where $\alpha = k/H$.

Finally, then, if the rise of the arch is h,

$$a + h = a\cosh\frac{\alpha \cdot l}{2}, \tag{3.7}$$

and the required equation of the arch centre line, that is, (3.6), becomes

$$y = a\cosh\left\{\frac{2x}{l}\cosh^{-1}\left(\frac{a+h}{a}\right)\right\}, \tag{3.8}$$

Equation (3.8) represents a family of curves with parameter h, and corresponds to the infinite number of possible positions for the thrust line. A practical design could, for example, specify the span l and the total height (a+h), but the value of h itself could be chosen by the designer.

As an example of the application of the 'Inglis equation' (3.8), it may be compared with the profile of an actual arch. Yvon Villarceau made redesigns of several existing bridges, including that of the Pont d'Iéna (Lamandé 1809). This five-arch bridge is of about 3 m rise in each 25 m span, and the ratio of h/a is about 2.0. The exact profile calculated by Yvon Villarceau differs from the Inglis profile of equation (3.8) by a maximum of about 20 mm. It is not possible to build a masonry arch of 25 m span whose profile can be guaranteed to an accuracy of 20 mm after decentering and subsequent settlement.

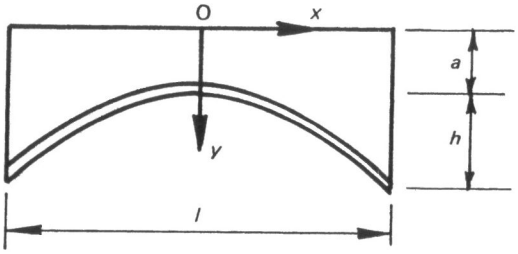

Fig. 3.4

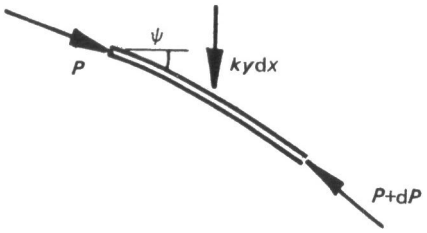

Fig. 3.5

MECHANISMS OF COLLAPSE

The notes above were all of work concerned in the main with the construction of lines of thrust; that is, it investigated the statics of the problem. However, the efficient methods of Yvon Villarceau, or of Inglis, while establishing the correct shape for the arch ring, give no information as to the thickness of that arch ring in order to ensure, in a practical sense, the stability of the arch. Side by side with the work on thrust other writers (and sometimes the same writer) were also demonstrating the ways in which a masonry arch might collapse.

Thus in his first attempt at the arch problem, in 1695, la Hire was concerned only with statics. The practical problem to be solved was the determination of the value of the arch thrust, so that, in turn, the abutments of the arch could be designed to stand firm against overturning. The difficulty in the analysis lay in the assumptions to be made about the behaviour of the voussoirs of the arch. In his 1695 analysis, La Hire took it that an individual voussoir was free to slide against its neighbour. He solved the problem by constructing a force polygon, involving the weights of the voussoirs, and the corresponding funicular polygon for the arch. For an arch of given shape with smooth voussoirs the funicular polygon is fixed, so that, working backwards, the force polygon can be deduced and finally the weights of the voussoirs found.

Now if the springing lines of the arch are horizontal it follows that the weights of the springing voussoirs must be infinite; a finite arch of this type with smooth voussoirs cannot stand. La Hire reached this conclusion, the result of an unrealistic assumption about the behaviour of the material, and he noted that in practice friction between the voussoirs would confer the necessary stability. Thus the arch problem was not much advanced in this work, although the important tool of the funicular polygon was developed.

La Hire returned to the problem in 1712, and here, apparently for the first time, consideration was given to the way in which a real arch might fail. He remarked that if the piers of an arch were too weak to carry the thrust, then the arch would break at a section somewhere between the springing and the keystone. The joint LM in Fig. 3.6 is taken to be critical, and the block LMF is then regarded as a single voussoir, as is the block LMI resting on the pier IBHS. Thus in Fig. 3.7 the thrust *P* can be found by considering the equilibrium of the top block (La Hire correctly directed this thrust tangentially to the intrados at L). Then, by taking moments about H for the lower portion of the arch and the pier, an expression to check the stability of the whole structure can be obtained.

La Hire gave no rule for finding the critical point L. The intrados hinges are analogous to those shown schematically in Fig. 2.6(c), but the thrust at the crown in Fig. 3.7 does not act at the extrados, and the third hinge is therefore not formed. However, La Hire's work is evidently a major

contribution; moreover, his estimate of the abutment thrust is greater than the minimum necessary for stability, so that his procedure is, as it happens, 'safe'.

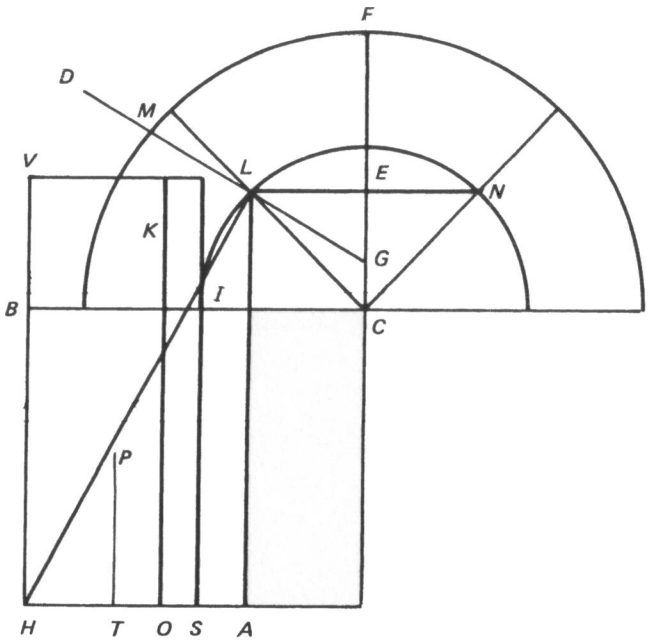

Fig. 3.6 (La Hire 1712).

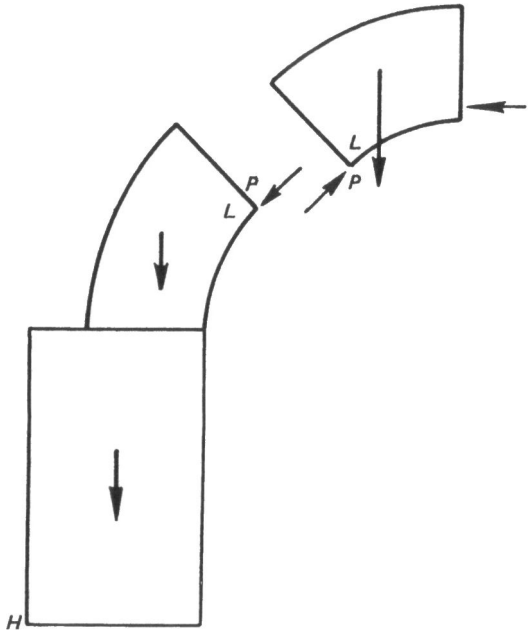

Fig. 3.7 (La Hire 1712).

The first civil engineering handbook, Bélidor's *Science des ingénieurs* of 1729, has a section on arches which is based firmly on the work of La Hire. However, there are some departures; the weakest section of the arch is taken to be always 45°, and the thrust (of value $\sqrt{2}W$ where W is the weight of the 'voussoir' LMF) acts not at the intrados L, but at the midpoint of LM. This last variation increases slightly the thickness of the piers for a given thrust $\sqrt{2}$W, and is therefore once again 'safe'. Bélidor did not in fact advance arch theory, but he established a set of practical design rules on the basis of existing work.

This was the background to Couplet's two remarkable memoirs on arch thrust of 1729 and 1730. The first of these papers really repeated much of La Hire's early work on frictionless arches, and consists of little more than an examination of lines of thrust and the calculation of corresponding forces. Couplet knew that all this was of little practical value, but he did give one interesting calculation of the forces on centering. This topic is of obvious constructional importance, but little

had been written, although Pitot in 1726 gave details of timber centers and attempted a theoretical analysis.

The problem posed by Couplet is that of a semicircular arch of uniform frictionless voussoirs resting on a smooth center; the final keystone (of very small width) has not been placed. In this state, Couplet determined the voussoir joint, say MV in Fig. 3.8, above which the voussoirs will require support from the centering, and below which they will be self-supporting. He deduced that the dividing joint lay at 30° from the abutment, but he failed to notice that the bottom group of voussoirs was not in equilibrium, and that his analysis demanded the development of tensile forces between the voussoirs and the centering.

It is the second memoir of 1730 which is the major contribution to arch theory. In his introduction Couplet was precise in the statement of two key assumptions about the way the material behaves. He noted that friction would in practice lock the voussoirs together against sliding, while offering no resistance to separation between voussoirs. He makes no mention of the strength of the stone of which the voussoirs are made, and by implication he assumed that ambient stresses are low so that crushing strength is of little importance.

Thus Couplet made in effect the three postulates necessary for arch theory to be embraced within the theory of plasticity: that masonry has no tensile strength, has infinite compressive strength, and that sliding between voussoirs does not occur. Further, his work demonstrates the two ways of approaching any structural problem, the first being through equilibrium (statics) in which thrust lines are considered, and the second through deformation (mechanisms) in which patterns of hinges are constructed.

Couplet's proof of his first theorem in his second paper contains exactly, these dual aspects of structural behaviour. The theorem states that an arch will not collapse if the chord of half the extrados does not cut the intrados, but lies within the thickness of the arch. Couplet has in mind an arch of negligible self-weight subjected to a single point load at the crown A (Fig. 3.9 (cf. Fig. 2.10(a)).

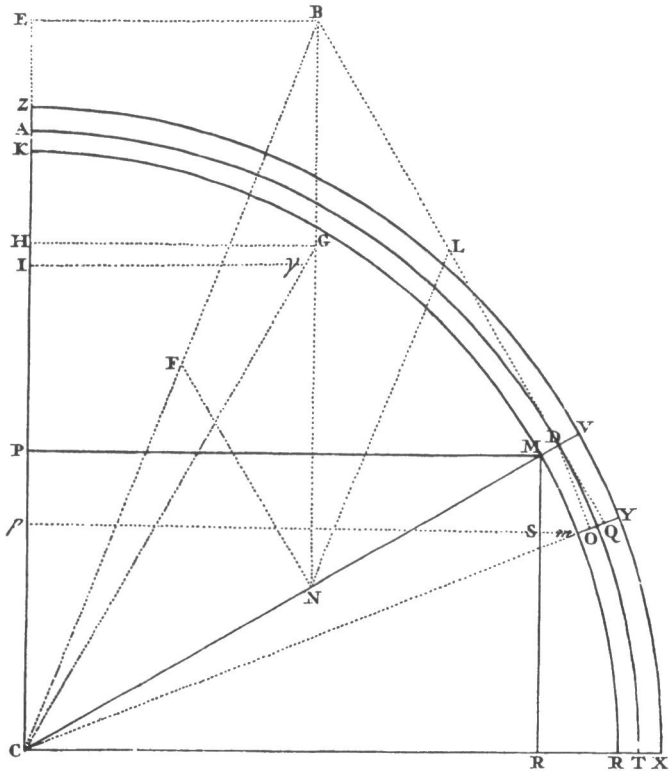

Fig. 3.8 (Couplet 1729).

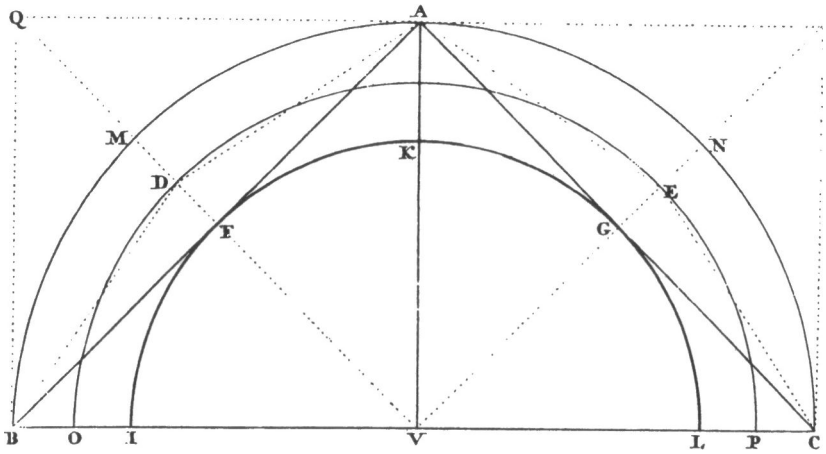

Fig. 3.9 (Couplet 1730).

Whatever the magnitude of the load, it can communicate directly with the abutments B and C, following the straight thrust lines AFB and AGC. Further, said Couplet, for the arch to collapse the angle BAC must open, and this can happen only by a spread of the abutments, which is ruled out by hypothesis; there is in fact no arrangement of hinges in the extrados and intrados which is both compatible with a thrust line for the load and which gives rise to a mechanism of collapse.

Couplet then remarked on the behaviour of the thinner arch BAC; ODEP. If the crown A were loaded sufficiently, then the angle DAE could now open and the angles ADB and AEC could close, it being supposed that the portions BMDO and CNEP have insufficient mass to resist overturning. However, the mode of collapse could be inhibited if the haunches were loaded. Moreover, Couplet noted that when such superimposed loading is omitted, then in the possible consequent failure the weakest points of the arch are often found to be half way between the springing and the crown.

With these preliminaries completed, Couplet tackled his first problem, namely to find the least thickness to be given to a semi-circular arch, carrying its own weight only. The arch, said Couplet, would collapse by breaking into four pieces, attached to each other by hinges (Fig. 3.10, cf. Fig. 2.9(c)). The hinges T and K at the haunches are placed at 45° from the springings (that is, 'half way') and, by considering the equilibrium of the arch in this state, a single equation can be found relating the thickness of the arch to its (mean) radius. Couplet solved this cubic equation numerically to obtain the required ratio of thickness to radius t/R as 0.101.

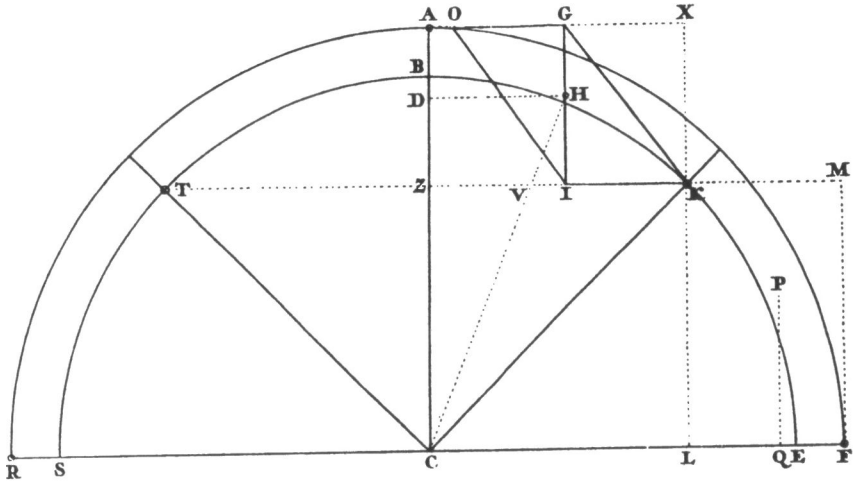

Fig. 3.10 (Couplet 1730).

Couplet's statics are evident in Fig. 3.10. For the equilibrium of the piece AK of the arch, the horizontal thrust at A combined with the weight acting through H leads to a thrust at K in the line GK. Now GK is not tangential to the intrados at K; Couplet missed this point, but the work is otherwise correct. The intrados hinges do not form at 45° from the springing but at about 31°;

however, the analysis is not very sensitive to their exact position, and the correct value of t/R is increased only to 0.106.

In his second problem Couplet repeated the above analysis for a circular arch embracing 120° rather than 180°. The third problem is concerned with the determination of the value of the arch thrust, and Couplet's solution is essentially a reworking of La Hire's analysis. He abandoned his 'collapse analysis', and instead he worked from a thrust line; specifically, he worked from the centre line SX of the arch, Fig. 3.11. The thrust at the crown acts horizontally at S, and the weight of half the arch in the line LR; a simple triangulation of forces then gives the magnitude of the abutment thrust, acting in the line LX. This calculation of abutment thrust is necessary for the solution of Couplet's fourth and final problem, namely the determination of the dimensions of the piers so that the whole structure is stable; this is the problem to which the whole of the work is directed.

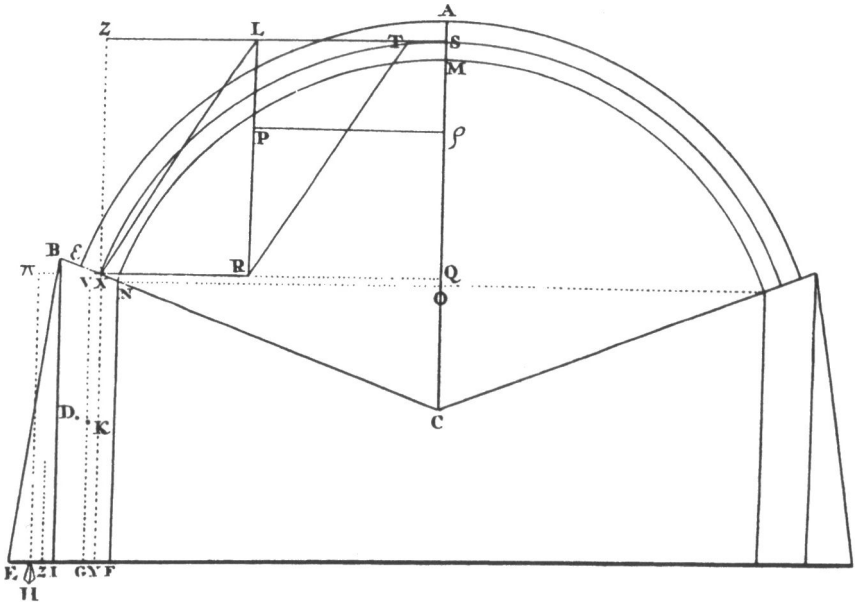

Fig. 3.11 (Couplet 1730).

This contribution of Couplet is outstanding. He had clear ideas of lines of thrust and of mechanisms of collapse caused by the formation of hinges, he stated explicitly his simplifying assumptions, and he used the ideas to obtain an essentially correct and complete solution to the problem of arch design. His work had an immediate impact, and found its way into standard texts (for example, that of Frézier in 1737-39).

In 1732 Danyzy obtained experimental confirmation of the correctness of Couplet's approach. The work was done in Montpellier, and published obscurely (and not until 1778). However, the experiments were noted, and Fig. 3.12 reproduces a plate from Frézier based on one of Danyzy's illustrations showing collapse of arches made from small plaster voussoirs. (Note Frézier's Fig. 241, which is half of Couplet's arch sketched in Fig. 3.9.). All the arches shown are on the point of collapse, the piers having minimum dimensions. Figure 235, for example, reproduces exactly (apart from the double hinge at the keystone) the collapse mechanism predicted by Couplet (Fig. 3.10). The flat arch of Fig. 240 (cf. Figs. 2.11) is, within the framework of the assumptions, infinitely strong; it can collapse only if the abutments give way.

Despite this publicity given to the work of Couplet, it was slowly forgotten; Poleni knew of it in 1748, but Coulomb betrays no knowledge of it in his famous memoir of 1773 on 'some statical problems'. However, Coulomb lived as a young man in Montpellier, and knew Danyzy there, so that it seems certain that he would have known of the collapse of arches by the formation of hinges. In fact if friction is large enough between voussoirs to prevent sliding (and this is a clear statement made by Coulomb) then he concludes that hinging is the only possible mode of failure.

In Fig. 3.13, from Coulomb, half an arch is maintained in equilibrium by a horizontal thrust H through the point f at the crown. If this thrust falls to a small enough value then the whole of the

portion GaMm of the arch might hinge about the point M in the intrados; for the arch in this state, it is a matter of simple statics to determine the corresponding value of the thrust as

$$H = \phi \frac{\mathrm{gM}}{\mathrm{MQ}}, \tag{3.9}$$

where ϕ is the weight of GaMm acting in the line g'g. Similarly, if the thrust is too high the portion GaMm could hinge about the point m in the extrados, and again the value of the thrust is calculable as

$$H = \phi \frac{\mathrm{g'q}}{\mathrm{mq}} \tag{3.10}$$

Thus Coulomb established limits between which the value of the horizontal thrust must lie if stability of the arch is to be assured. However, the critical section Mm has not yet been determined. Coulomb showed that, if various cross-sections of failure are considered (together with different positions of the point f at the crown through which the thrust acts), then the maximum value of H must be sought from (3.9), and the minimum from (3.10). All these ideas are correct.

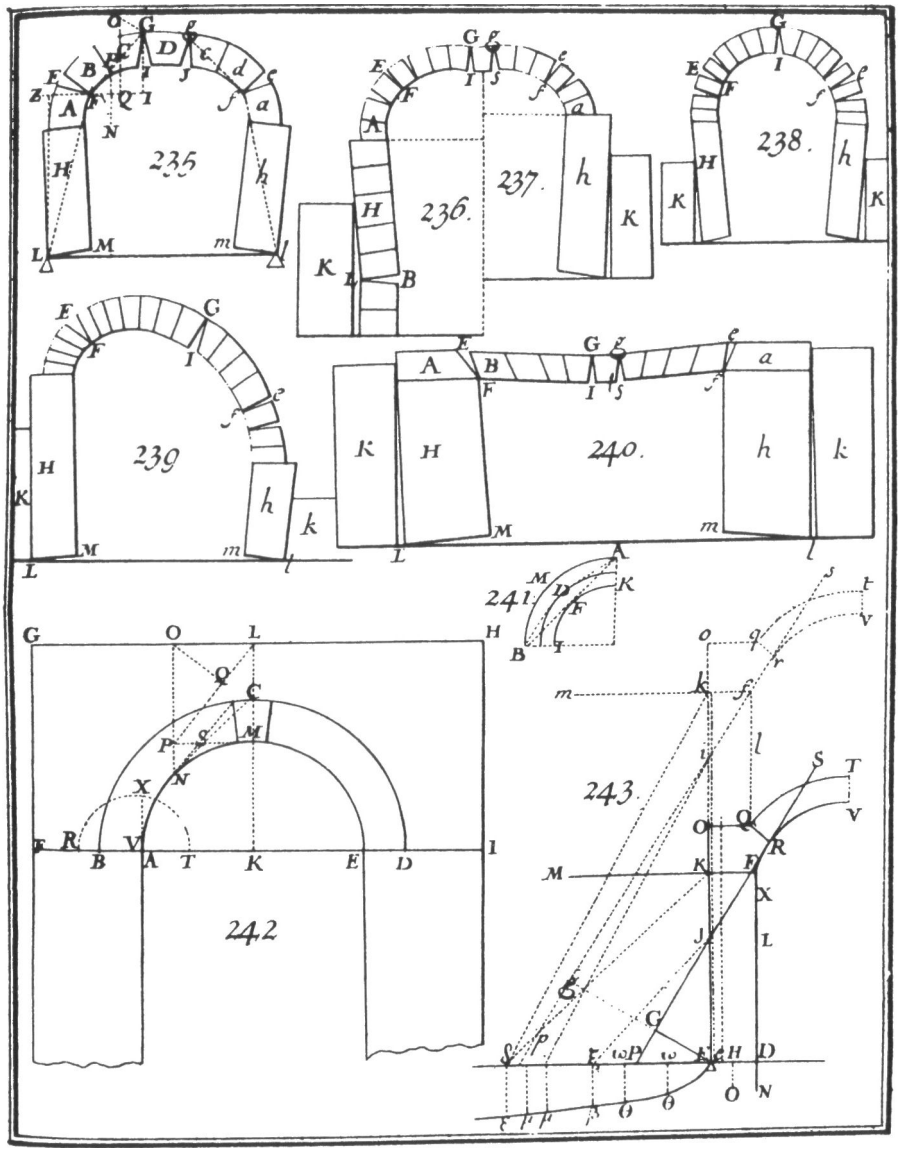

Fig. 3.12 (Frézier 1737-39).

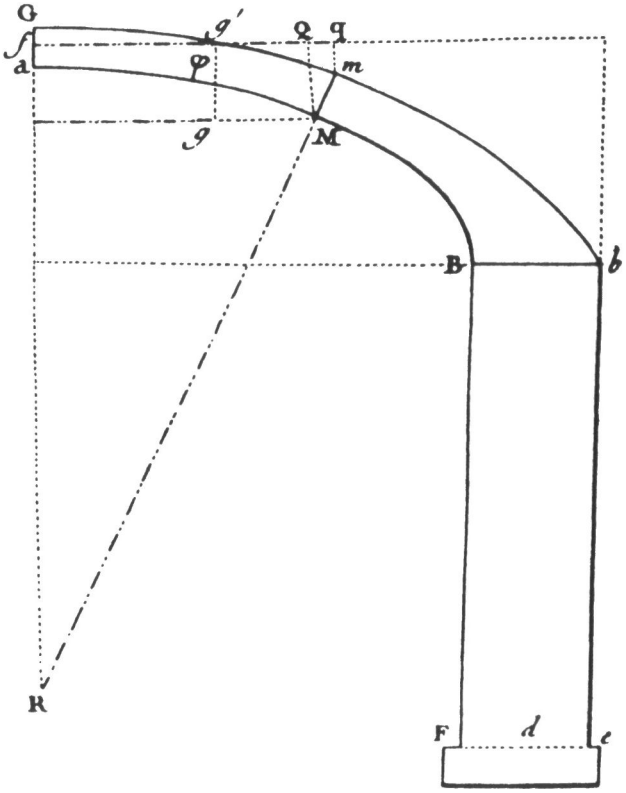

Fig. 3.13 (Coulomb 1773).

Coulomb's work, combining as it does clear statements of assumptions and material properties with notions of thrust lines on the one hand, and hinge mechanisms on the other, gives an extensive theoretical basis for arch analysis and design. However, there is no mention of the work in a volume of 1810 intended for the use of engineers in the Ponts et Chaussées; a paper by Boistard, in the volume edited by Lesage, mentions only the work of Couplet and Prony. (By contrast, Coulomb's work on soil mechanics – the thrust against a retaining wall – published in the same paper of 1773, was immediately taken up; Prony, for example, in 1802, elaborated Coulomb's theory of soil into a small book.)

Coulomb remarked that a method of trial and error to find the critical section will be very accurate, since the maximum or minimum is 'flat'; this insensitivity was noted above in the work of Couplet, and, by implication, Coulomb was able to correct the trivial error of placing the intrados hinge at the fixed location of 45°.

Thus Lamé and Clapeyron, who later achieved distinction in more than one field, were, in 1823, bright ignorant young army officers, who were called on to assess the stability of the dome of the cathedral of St Isaac in St Petersburg. In the course of this assessment they virtually reinvented the whole of Coulomb's theory; further, they recreated Poleni's slicing technique, and divided the dome into lunes for the purpose of their analysis. The theory of arches was, in fact, known to professors, if not to young students, and in 1833 Navier published his *Leçons* for the Ponts et Chaussées, so that the theory was then available also in the schools.

In England, Barlow's paper of 1846 to the Civils has been mentioned; Moseley developed his own (slightly cloudy) theory in 1843, by his own admission in ignorance of Coulomb's work. Information on arches was in fact available throughout the nineteenth century, and lines of thrust and the 'middle-third rule' were part of the designer's stock-in-trade. Fuller gave his construction for the thrust line in 1875, but the masonry arch was already obsolescent by the mid-nineteenth century (Séjourné published in six volumes early in the twentieth century a definitive catalogue of large span masonry bridges throughout the world). Rennie's London Bridge, now taken down, was completed in 1831, and Thomas Harrison's bridge at Chester, at 200 ft the largest masonry span in England, was built a year later. These were among the last of the masonry bridges. Iron Bridge at Coalbrookdale had been built in 1779; Telford had already projected a cast-iron span of 600 ft for the new London Bridge.

Fleeming Jenkin knew all about voussoir arches, but his long article on bridges for the ninth (1876) edition of the Encyclopedia Britannica devotes, rightly, most of the space to wrought iron and steel, and little to masonry. Indeed there seems to have been little further work on the masonry arch, and perhaps no need for further work, until well into the twentieth century; there was a renewed interest just before the second World War, due to the activity of Pippard. He made careful tests of model arches with steel voussoirs, and demonstrated that the slightest imperfection of fit (for example, at the abutments) converted an apparently redundant structure into a statically-determinate one. As will be seen in the next chapter, this led to some simplification of analysis, but Pippard's approach was still essentially that of an elastician, and he interpreted his results with respect to principles of minimum elastic energy. Coulomb, a century and a half earlier, had foreshadowed the limit principles and the techniques of plastic theory, but the full development of that theory came only after the second World War.

PRACTICE AND EXPERIMENT

Boistard, in his essay included in Lesage's collection of 1810 for the Ponts et Chaussdes, had covered much the same experimental grounds as Pippard, although the details of the tests were different. Moreover, they were wider in scope; not only did Boistard wish to establish modes of collapse under various loading conditions, he wished also to establish minimum abutment requirements at collapse (that is, he was interested in the value of the abutment thrust), and he wished to investigate the forces on the centering during construction.

Danyzy's tests of 1732 on arches with plaster voussoirs had not been concerned with this last constructional problem, although it was noted above that Couplet had made a theoretical contribution slightly earlier. Boistard worked on a larger scale than Danyzy; his voussoirs were cut from brick and polished, and the arches had spans of 8 ft. However, Boistard was content merely to record his observations, and he made no calculations.

The first model tests on arches seem to have been reported by Gautier in 1717; he used wooden voussoirs. Gautier gives numerical rules of proportion for bridges, relating thickness of abutments and thickness of internal piers (for multi-span bridges) to the span of the arch. He stated clearly five problems whose solution was needed:

(1) the thickness of abutment piers for all kinds of bridges;
(2) the dimensions of internal piers as a proportion of the span of the arches;
(3) the thickness of the voussoirs; between extrados and intrados in the neighbourhood of the keystone;
(4) the shape of arches;
(5) the dimensions of retaining walls to hold back soil.

(It was this fifth problem that Coulomb tackled, as well as the problem of arches, in his 1773 paper.)

Gautier's first problem was the fundamental problem of bridge design; what all investigators were trying to do, from La Hire onwards, was to solve the problem by the use of mechanics rather than empirically. Empirical rules did indeed exist for the design of abutments; the seventeenth century knew of 'Blondel's rule', which is described below (Bé1idor was concerned in pointing out the shortcomings of Blondel's rule), and similar rules can be found in the sixteenth century, for example in the writings of the Spanish architect Rodrigo Gil De Hontañon.

François Derand gave a clear account of Blondel's rule, and Fig. 3.14 is based upon one of Derand's plates in the edition of 1743. The intrados of the arch is divided into three equal chords AB, BC and CD in Fig. 3.14(a); CDF is a straight line with CD equal to DF, and the point F locates the outer edge of the supporting-pier. For the semi-circular arch the width of this abutment pier is one quarter of the span (Rodrigo arrives at this same proportion); Figs. 3.14(b) and (c) show the construction for arches of different shapes. Bélidor pointed out that the rule does not involve the thickness of the arch, nor the height of the piers. The second criticism, at least, is perhaps not of importance; Moseley demonstrated later that a finite width could be assigned to the piers to carry a given thrust, independently of their height. Moreover, the trend shown in Fig. 3.14 is at least

intuitively correct; low-rise arches will give rise to large thrusts, and must be provided with heavier abutments.

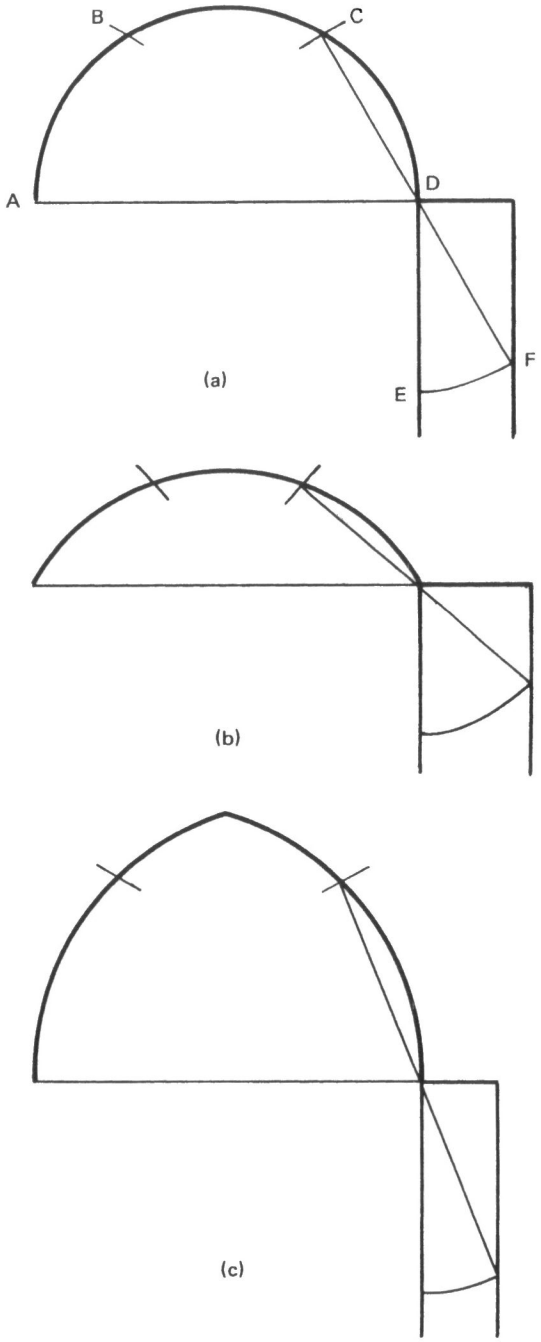

Fig. 3.14 (Derived from Derand 1743).

Blondel's rule says nothing of internal piers. The internal piers of medieval bridges had thicknesses large compared with the span (for example, old London Bridge, or the still existing bridge at Bideford, or the Pont d'Avignon); typically the ratio thickness/span might lie between 1/4 and 1/6. Such large obstructions to the flow of a river lead to a vicious circle of damage and repair: the increased flow through the restricted arches causes scour round the footings of the piers, and the piers must be enlarged by starlings to make good the damage; the flow is thereby further increased and the piers must be further enlarged. Gautier's own rule was 4/15 of the span for the abutment piers, but 1/5 for the internal piers.

There is evident in these ratios a tentative move towards the advance first taken fully by Perronet, in which the internal piers are drastically reduced in thickness. For a multi-span bridge with more or less equal spans, the internal piers carry little more than vertical forces, the horizontal thrusts from adjacent spans being roughly self-equilibrating. In his first major bridge over the Seine, the Pont

de Neuilly, 1768-74, Perronet reduced the internal piers to 1/9 of the span. The price paid during construction for this lightening of the masonry is that centers for all spans (five in number at Neuilly) must be erected simultaneously, and the centers cannot be struck until all arch rings, together with sufficient backing, have been constructed.

The bridge was entirely successful, not least in the operation of decentering, in which all five arches were released simultaneously in the presence of the King and Court. Perronet had a firm appreciation of the properties of his centering. He had calculated that each masonry span would sink 15 inches when released; in reality, the deflection was 13 inches immediately, followed by 10 $^1/_2$ inches, to make a total of nearly 2 ft in each span of 128 ft.

Perronet had been appointed in 1747 as the first director of the newly founded Ecole des Ponts et Chaussées, and his influence as a designer and teacher was very great. It was his pupil, Gauthey, who assembled and digested all the theoretical and experimental work on bridges known to the Ponts et Chaussées by the beginning of the nineteenth century. The three-volume Treatise (edited in 1809 by Navier) is a history of bridge-building, a survey of existing bridges, an architectural handbook, and, above all, a manual on the design and construction of masonry arches, together with their specification and costing.

The engineering problem of the masonry arch had been effectively solved, and further work tended to be written for the 'scientific' rather than the 'engineering' world. Thus Yvon Villarceau's paper, published in 1854, was presented to the Académie des Sciences in 1845; his inverse design method, presented in the form of tables, coupled with Gauthey's manual, could be used today with confidence and economy.

4

The strength of arches

There are many brick and masonry bridges in use, carrying road or rail traffic. Up until World War II highway loading was relatively light; since that time, vehicles have increased considerably in weight, and it can no longer be assumed that a medieval bridge will be capable of carrying every vehicle now on the roads. Instead, those responsible for the maintenance of such bridges are concerned to establish their safety and, in particular, to try to estimate safe values of live load for a given bridge. The problem was tackled in a systematic way by the Military Engineering Experimental Establishment (MEXE) just after the War, in an attempt to establish a military load classification system; this work was then developed, in 1967 (and revised in 1973), by the Ministry of Transport, and they issued a technical memorandum which is described briefly below.

These studies of masonry arches were based on Pippard's pre-war papers, and he himself developed his analysis and reported his findings in *Civil engineer in war*, in 1948.

PIPPARD'S 'ELASTIC' METHOD

Pippard started from his observation that a very slight spread of the abutments of a voussoir arch would normally produce 'pins' or hinges at the abutments. However, he ignored the fact that a third hinge will also form, converting the arch into a statically-determinate three-pin structure (cf. Fig. 2.6(a)); instead, he analysed a two-pin arch.

The bridge to be treated is shown in Fig. 4.1; the surface of the fill is horizontal and, for the purpose of analysis, the arch ring is replaced by the two-pinned centre-line rib of Fig. 4.2. This is the first in a series of simplifications made by Pippard in order to derive reasonable values for the structural quantities; his assumptions are not always explicit, but the analysis summarised by him in 1948 may be reconstructed from his book of 1943.

Thus Pippard, like Castigliano before him, was concerned with an 'elastic' solution to the arch problem. Unlike Castigliano, however, Pippard was content to analyse a hypothetical rib coinciding with the centre line of the arch, and he did not follow in detail the cracking of the masonry at the abutments. In fact, Castigliano's solutions for various alternative assumptions as to the behaviour of the mortar all gave values of abutment thrust within 4% of a mean value. This apparent insensitivity is commented upon below; it may be noted here that the assumption of simple pins at the abutments will not have any marked effect on the value of the abutment thrust.

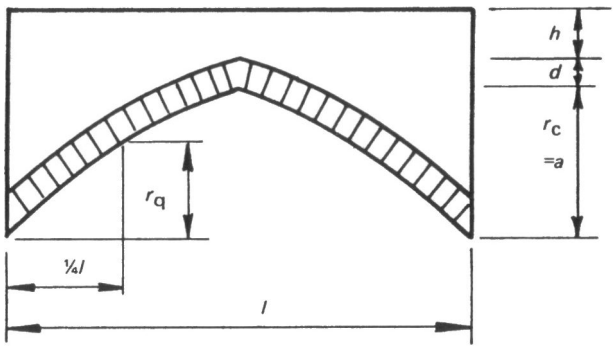

Fig. 4.1

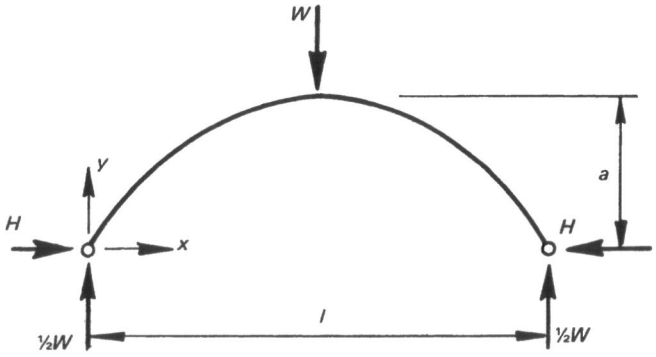

Fig. 4.2

If, therefore, a point load W is placed at the crown of the arch rib, (Fig. 4.2) – and this was the case considered by Pippard – then the bending moment M_x, at any section can be written in terms of the unknown, abutment thrust H. The shape of the arch rib must of course be known, and Pippard took the arch to be parabolic; that is, he confined his analysis to the case for which $r_q/r_c = 3/4$ in Fig. 4.1. The strain energy U for the arch can now be formulated in the usual way as

$$U = 2\int_{x=0}^{x=\frac{1}{2}l} \frac{M_x^2}{2EI}\mathrm{d}s, \tag{4.1}$$

where ds is an element of arc length of the arch. Thus the value of H is given by the solution of the equation

$$\frac{\partial U}{\partial H} = \int_{x=0}^{x=\frac{1}{2}l} \frac{M_x}{EI}\frac{\partial M_x}{\partial H}\,\mathrm{d}s = 0, \tag{4.2}$$

To simplify the integral, Pippard supposed that the section of the arch rib varied in such a way that

$$I = I_0 \frac{\mathrm{d}s}{\mathrm{d}x}, \tag{4.3}$$

so that (4.2) becomes

$$\int_0^{\frac{1}{2}l} M_x \frac{\partial M_x}{\partial H}\,\mathrm{d}x = 0, \tag{4.4}$$

Equation (4.3) implies that the section of the arch rib increases from the crown towards the abutments.

The solution of (4.4) for the loading case of Fig. 4.2 gives a value H_L of the live-load abutment thrust:

$$H_\mathrm{L} = \frac{25}{128}\left(\frac{l}{a}\right)W, \tag{4.5}$$

Correspondingly, the value of the bending moment at the crown of the arch is

$$M_\mathrm{L} = -\frac{7}{128}Wl, \tag{4.6}$$

where the negative sign indicates that the thrust line lies above the arch rib (sagging bending moment); the solution is illustrated in Fig. 4.3.

Equations (4.5) and (4.6) are the essential results which, when combined with corresponding expressions resulting from the self-weight of the arch ((4.7) and (4.8) below), were used by Pippard to estimate the safe value of live load for an arch of any shape. It should be noted, however, that these results have been obtained, using an elastic method of analysis, for a two-pin arch, for a rib of parabolic shape, and for a cross-section which varies in accordance with (4.3). In point of fact none of these assumptions will have much effect on the value of the abutment thrust H_L. However, since the bending moment at the crown of the arch is determined by the difference in ordinates between the line of thrust and the arch centre line (that is, by the dimension 7a/25 in Fig. 4.3), a relatively small change in the value, of H_L can have a much larger effect on the value of bending moment.

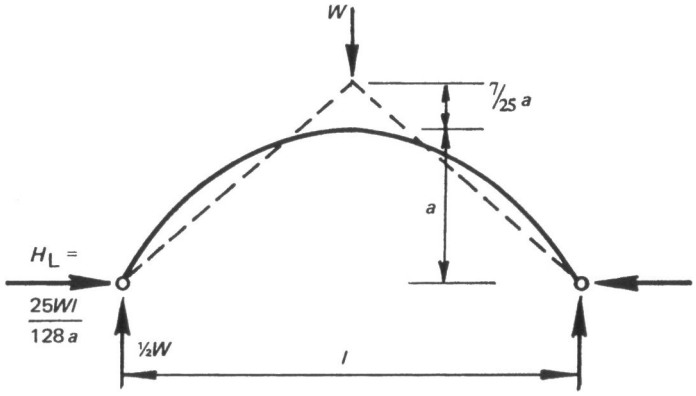

Fig. 4.3

Further, Pippard confined his analysis to that for a single point load at mid-span. The 'worst' location for a point load is investigated further below. Pippard was aware that in theory an arch rib is weakest under the action of a point load at about quarter-span rather than at the crown. However, he argued – reasonably – for the use of the result for the central load on the grounds of the distribution of the load from the road surface through the fill to the arch proper. If a conventional 90° wedge angle is taken for the dispersion of the load, then the effective width of the arch when the load acts at the crown is $2h$. A greater width of arch will be available to carry the point load at quarter span, since the load will be dispersed through a greater thickness of fill.

The numerical values resulting from (4.5) and (4.6) must be superimposed on the corresponding quantities arising from the dead weight of the arch and fill. Pippard took it that the appropriate width of bridge is $2h$; that is, he analysed the 'rib' contained within the bridge that is concerned, at least at the crown, with carrying the live load. He assumed further that the fill has no structural strength, so that it imposes purely vertical loads on the arch (this was the assumption made by Inglis, and noted in Chapter 3, Fig. 3.5), and that the fill has the same unit weight σ as the arch ring. A further strain-energy analysis then gives values of the dead-load thrust and bending moment at the crown as

$$H_D = \frac{\sigma l^2}{a}\left(\frac{a}{21} + \frac{h+d}{4}\right), \tag{4.7}$$

$$M_D = \frac{1}{168}\sigma l^2 a h, \tag{4.8}$$

Thus the combined effects of the point live load at the crown and the dead weight of the arch (of width $2h$) are a thrust and a central bending moment with values

$$H = \frac{l}{a}\left\{\sigma l h\left(\frac{a}{21} + \frac{h+d}{4}\right) + \frac{25}{128}W\right\}, \tag{4.9}$$

$$M_c = \frac{1}{4}l\left(\frac{\sigma l a h}{42} - \frac{7}{32}W\right), \tag{4.10}$$

The remarks about the sensitivity of the value of bending moment to the assumptions that have been made in deriving that value apply even more to the dead-load analysis. The dead-load line of thrust is a smooth symmetrical curve lying close to the parabolic arch centre line (as it must to minimize the strain energy); for typical values of h, d and a, (4.7) and (4.8) show that the line of thrust lies below the arch centre line at the crown by only a few per cent of the rise a. Thus for a typical small bridge with $h=d=1/4a$, say, (4.7) and (4.8) give $M_D/H_D=a/29$.

Moreover, the two sensitive quantities are combined in (4.10), and it is this, value of bending moment that was used by Pippard to derive his rules of assessment. As larger and larger values of W are imposed at the crown of the bridge, so the resultant line of thrust departs more and more from the centre line of the arch; the first term in (4.10) remains constant, while the second increases. The implication is that tensile stresses will eventually develop.

Thus a first criterion applied by Pippard is derived from the middle-third rule. Or rather, Pippard argued that a less restrictive criterion might be based on a middle-half rule, in which case the limiting value of W would be given by the solution of

$$\frac{M_c}{H} = -\frac{1}{4}d \tag{4.11}$$

which leads to

$$W_1 = \frac{32\sigma l h\left\{2a^2 + 4ad + 21d(h+d)\right\}}{21(28a - 25d)} \tag{4.12}$$

However, Pippard also investigated the case where the compressive stress in the masonry reached a maximum permitted value, and thus he considered a second condition. Since the arch ring has depth d and effective width $2h$, the limiting stress f will be reached when

$$f = \frac{H}{2dh} - \frac{3M_c}{hd^2} \tag{4.13}$$

and substitution of (4.9) and (4.10) gives

$$W_2 = \frac{\frac{256fhd}{l} + 128\sigma l h\left(\frac{a}{28d} - \frac{1}{21} - \frac{h+d}{4a}\right)}{\left(\frac{25}{a} + \frac{42}{d}\right)} \tag{4.14}$$

Pippard studied expressions (4.12) and (4.14), which give limiting values of W on the alternative assumptions of zero tensile stress (in fact relaxed by the 'middle-half rule to allow some unspecified tensile stress) and a limited compressive stress. He took a range of numerical examples, and he had available the results of full-scale tests made by the Building Research Station. As a result, he considered it safe to discard (4.12), and to use the less restrictive (4.14). That is, the value of W_2 (for the values of the constants chosen by Pippard) is generally larger than that of W_1, and Pippard allowed even his middle-half rule to be violated.

For small arches the cover h is often less than 2 ft, so that the effective corresponding arch rib will be less than 4 ft wide; two such ribs can be thought of as existing independently within the barrel of an actual arch. Thus the safe axle load W_A for a vehicle of normal track width may be taken as

$$W_A = 2W_2 \,, \tag{4.15}$$

From (4.14) and (4.15) Pippard constructed tables for a single standard arch of parabolic profile with a span/rise ratio $l/a = 4$. The unit weight of the arch and fill material was taken as $\sigma = 0.0625$ ton/ft^3, and the limiting compressive stress as f =13 ton/ft^2.

From these tables could be read the value of W_A for various values of span l, ring depth d and crown cover h. The significance of these tables is discussed below in the light of further developments made by MEXE.

THE MEXE/MOT METHOD OF ASSESSMENT

The Military Engineering Experimental Establishment found that (4.14) could be fitted quite well, for given values of σ and f, by a nomograph involving only the arch span l and the total depth (h+d) at the crown, and this idea was incorporated in the Ministry of Transport memorandum of 1967. Thus for an arch of given dimensions the provisional axle loading W_A can be read off immediately, as shown schematically in Fig. 4.4. The loading is designated provisional because the value of W_A is operated on by a series of modifying factors. In the first place, it was seen that (4.14), and the corresponding nomograph, were derived for the standard case a = $^1/_4 l$; the first modifying factor adjusts the value of W_A to allow for span/rise ratios different from the value 4. When l/a > 4 (that is for flat arches) the factor is progressively reduced from unity (to about 0.6, for example, for l/a = 8).

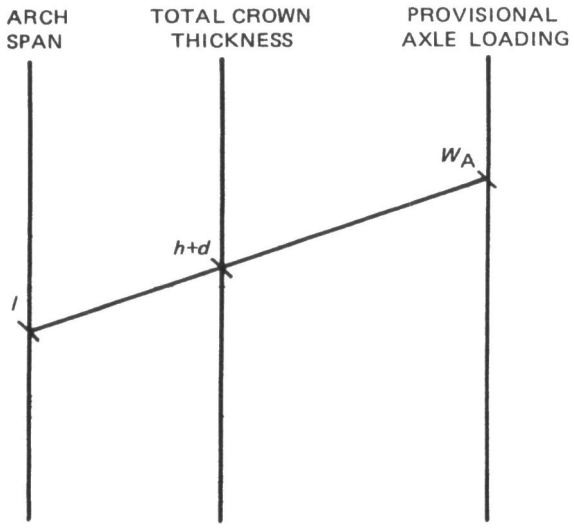

Fig. 4.4

Second, an adjustment is made to allow for a profile other than the standard parabolic, for which $r_q/r_c = {}^3/_4$, where r_q is the rise at quarter span, Fig. 4.1; for $r_q/r_c > {}^3/_4$ the factor is less than unity.

Third, the product of two further factors expresses an assessment of the quality of the material in the arch ring and in the fill; the resulting material factor can be greater or smaller than unity, and typically might lie between 0.6 and 1.2.

Fourth, a joint factor lying between $^1/_2$ and 1 is assessed from the width, depth and condition of the mortar between the voussoirs.

These four factors are applied to the provisional value of the axle loading, and can have a marked effect; four factors each of value 0.7 will reduce the permitted load to one quarter of the provisional value. Moreover, there is a fifth and final factor to be applied: the condition factor. The engineer is invited to specify a factor between zero and unity depending on his overall impression of

the state of the bridge (a factor of 0.4 or less implies that the bridge should be rehabilitated immediately).

The essential features of this MEXE/MOT approach to the assessment of masonry arches are that

(a) there is considerable emphasis on the geometrical properties of the bridge; in the nomograph, the arch span and the total crown thickness (h+d) serve to define a provisional value of the axle loading, and the actual shape of the arch is later introduced in the form of modifying factors. One curiosity is that the thickness d of the arch, ring does not enter directly into the calculations, although it does have a small effect on the value of the material factor;

(b) the arch is treated, in a late nineteenth-century way, as an elastic redundant structure. A long series of simplifying assumptions is made, but the state of the arch under given loading is evaluated using established elastic techniques;

(c) the final criterion for the load-carrying capacity of the arch is based upon the attainment of a limiting value of compressive stress.

The whole assessment depends, of course, on the values of the thrust and bending moment that have been evaluated at the crown of the arch. As has been noted, the value of the thrust will not be much affected by the various assumptions made in the elastic analysis, but the value of the bending moment is sensitive to these assumptions. On the face of it, therefore, this way of assessing the provisional value of axle load must be regarded with some suspicion.

However, the criterion of a limiting compressive stress does impose, as it turns out in practice, some uniformity in the assessment. The use of the middle-third rule as a limiting criterion would imply that, at the crown of the arch, the largest compressive stress would have been contributed to by 50% from the thrust and 50% from the bending moment; the middle-half rule makes these proportions 40/60. Pippard's examination of the expression for W_2, (4.14), in which he found that the middle-half rule was slightly violated for a wide range of practical cases, implies that the proportions are about 30/70 or perhaps 25/75. Thus, for this usual range of bridges, the horizontal thrust is contributing a roughly constant proportion, of between say 25 and 30%, of the maximum compressive stress at the crown; effectively, the design of the arch ring (that is, the assessment of carrying capacity) is based empirically almost entirely on the value of the thrust.

Thus, despite the apparently arbitrary nature of some of the steps, the Pippard analysis which led to the MEXE/MOT method is perhaps not so capricious as it might appear. If it were used as a method for design, then the dimensions of the arch ring would be fixed from the value of the thrust in the arch, so that stresses are kept, nominally, within permitted values, and this despite the fact that, paradoxically, the thickness of the arch ring is not a major parameter in the method. As with most sets of apparently empirical design rules, it is implicit that the structure under consideration is of a usual type. Certainly, it seems implicit that an arch of reasonable shape for a bridge with reasonable cover at the crown will be able to carry a reasonable range of live loading (the actual shape does have some effect on the design, by way of the various factors introduced in the analysis).

Further, the MEXE/MOT method finds a place for engineering judgement as to the nature of the materials and the state of the structure. However the method is, in the last analysis, an amalgam of practical experience backed by a theory of elastic behaviour which does not really apply to the masonry structure, and which is in fact largely discarded in the construction of a practical method of assessment.

Above all, the very real insights obtained in the eighteenth and early nineteenth centuries are disregarded; it is these insights into the behaviour of the voussoir arch, deepened now and made more secure by the basic plastic theorems, that make it possible to propose an alternative method of design.

A 'PLASTIC' METHOD OF ANALYSIS

The idea of the geometrical factor of safety discussed in Chapter 2 may be developed in order to give an alternative way of assessing the safety of an arch. It was seen that there were limiting configurations for the state of any given arch. For example, the idealized semi-circular arch carrying

its own weight only has the two limits of Figs. 4.5(a) and (b); in the first the abutment thrust has its least possible value H_{min}, and in the second the thrust has increased to its greatest possible value H_{max}. Neither 'elastic' theory nor 'plastic' theory indicates which of these two states is 'correct'; the actual state of the arch at any given time will depend on the current state of the environment (that is, on whether the abutments have given way slightly, or settled differentially, or approached each other).

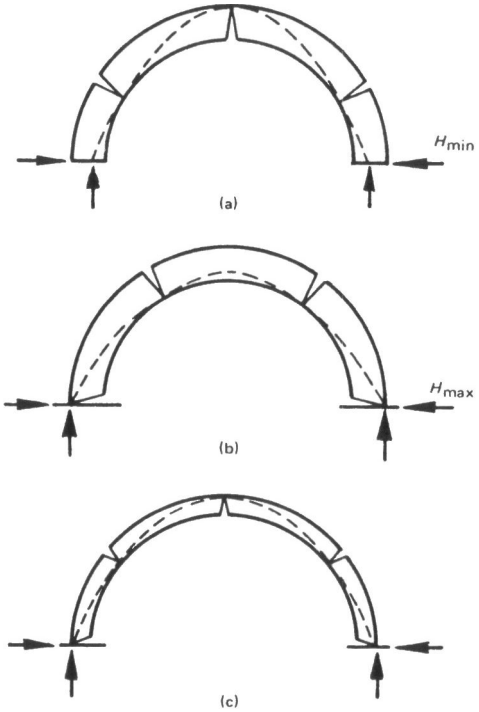

Fig. 4.5

What can be said, however, is that the values of H_{min} and H_{max} marked in Fig. 4.5 will be fairly close to each other; the values can be determined analytically (for this idealized example) or, more generally, by drawing funicular polygons by the methods of Chapter 1. If the thickness of the arch is reduced slightly the values of H_{min} and H_{max} will approach closer together, and it was seen that there is a limit, Fig. 4.5(c), cf. Fig. 2.9, where the arch has been shrunk to such a state that the position of the thrust line, and the corresponding value of the thrust H, is unique. As was noted in Chapter 2, the ratio of the thickness of the arch in Fig. 4.5(a) or (b) to that of Fig. 4.5(c) may be defined as the geometrical factor of safety.

Figure 4.6(a) shows the bridge of Fig. 4.1 with a point load carried at some general position. The funicular polygon equilibrating the dead weight of the arch and its fill, together with the point load P, may be drawn, and it will be supposed that this thrust line lies within the arch. The arch may then be shrunk to the state of Fig. 4.6(b) at which it is only just possible to contain the thrust line. During this process the pole of the force polygon may have to be shifted (if the problem is being tackled on the drawing board), and it will eventually be forced to lie in a unique position. This is because, as was seen, only one funicular polygon can be drawn to pass through three given points; the final formation of *four* hinges in Fig. 4.6(c), corresponding to the thrust line of Fig. 4.6(b), both fixes that thrust line and also gives one further piece of information, namely the thickness of the arch in its minimum state. The problem may in fact be solved by writing a set of simultaneous equations, as will be seen in Chapter 5; whatever method is used, a geometrical factor of safety may be calculated by comparing the arches of Figs. 4.6(a) and (b).

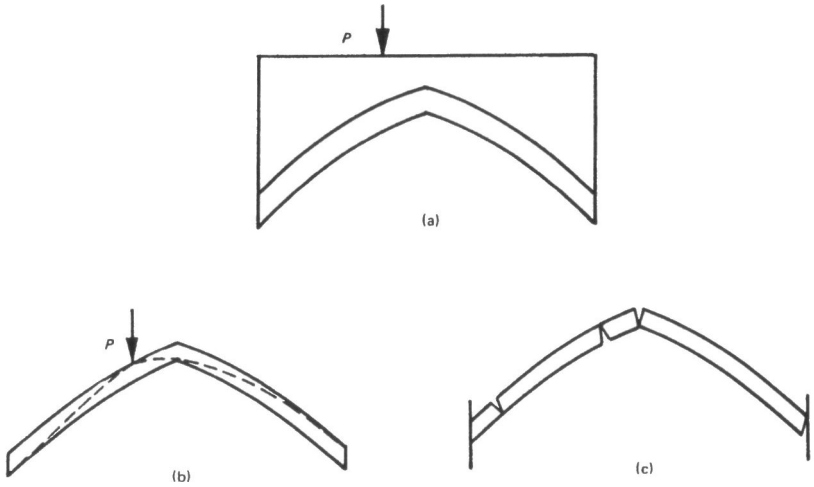

Fig. 4.6

The whole analysis may now be repeated for a different position of the live load *P*, and a new value of geometrical factor calculated. A numerical investigation of this sort is made in Chapter 5; Fig. 4.7 shows the essential results obtained from the analysis of a complete traverse of a bridge by a given live load *P*.

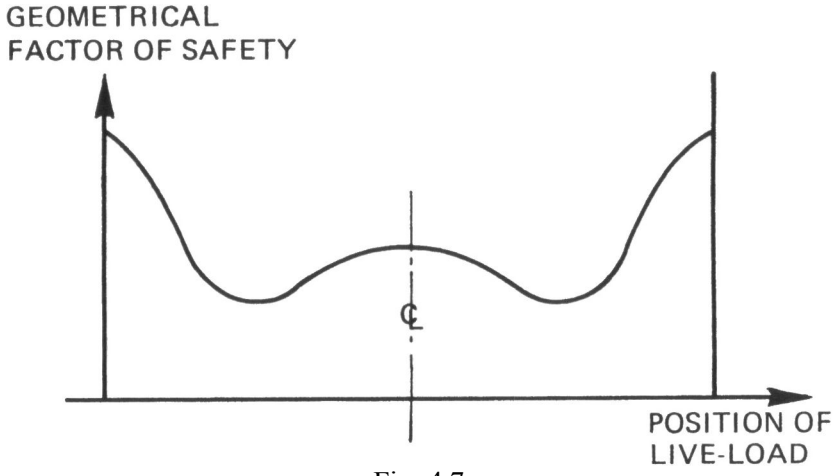

Fig. 4.7

The precise shape of the curve in Fig. 4.7 will depend on the geometry of an individual bridge and on the ratio of live load to dead load, but the general features will be as sketched. In particular, the minimum value of the geometrical factor of safety will occur when the live load is at about quarter span, and this minimum value is reasonably 'flat'; There is encouragement, therefore, to assume that, for the purpose of developing a quick approximate method of analysis, the worst position of the live load is exactly at quarter span. Further, it will be assumed that the mechanism of collapse of the minimum-thickness arch will be that indicated by the position of the thrust line in Fig. 4.8, over a wide range of different shapes of arch (cf. Fig. 4.6).

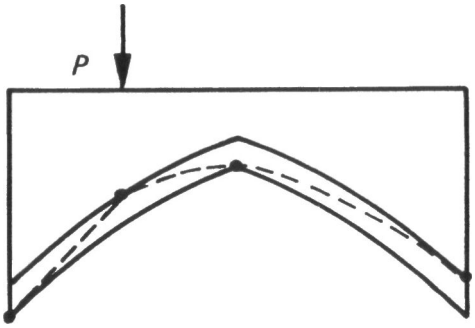

Fig. 4.8

Figure 4.9 shows the dimensions of the arch. The arch ring is not necessarily of uniform thickness, and is shown in its minimum configuration with all the 'shrunk' thicknesses bearing the same ratio to the corresponding actual values at each section of the span. The road surface is horizontal. The fill is assumed to have no strength and to transmit the live load P without dispersion to the arch ring; both fill and arch ring have unit weight γ. The calculations are normalised with respect to the rise h_c of the arch, so that the parameter $\alpha = h_q/h_c$ gives some measure of the shape of the arch, the parameter $\beta = h_0/h_c$ gives a measure of the depth of the bridge (ring plus fill) at the crown, and $\tau = t/h_c$ is a measure of the vertical thickness of the arch ring at quarter span.

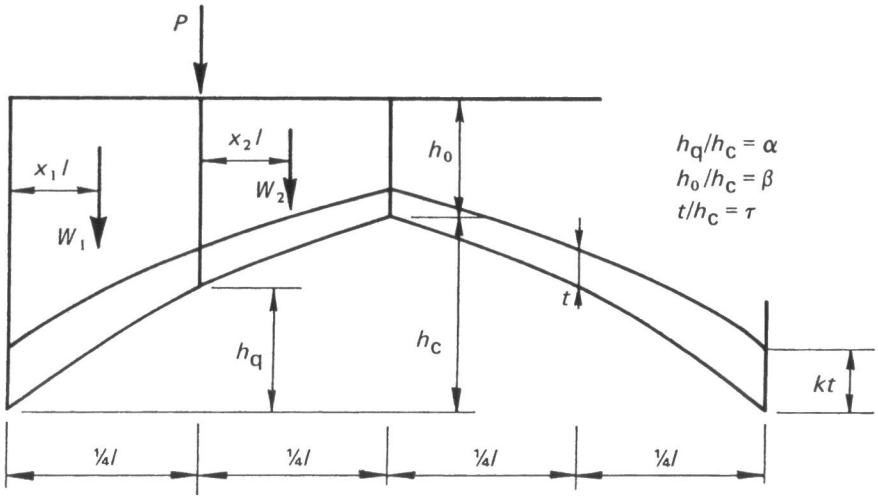

Fig. 4.9

The end quarter of the bridge has a dead weight W_1 with a centre of gravity as shown in Fig. 4.9; W_2 is shown similarly. The position of the funicular polygon is known at the four sections indicated in Fig. 4.8 when the arch is on the point of collapse. As has been discussed, these four known locations enable the funicular polygon to be fixed uniquely, and also furnish a single relationship between the quantities marked in Fig. 4.9. There are various ways of establishing this relationship, but perhaps the easiest is to write statical equations of equilibrium. The way this can be done is shown numerically in Chapter 5; for the quantities marked in Fig. 4.9, with the collapse mechanism of Fig. 4.8, the required relationship is

$$P = 16\frac{W_2x_2\{\alpha+(1-\tfrac{1}{4}k)\tau\}-(W_1x_1+\tfrac{1}{4}W_2)\{(1-\alpha)-(1+\tfrac{1}{4}k)\tau\}}{(3-2\alpha)-(2+k)\tau} \qquad (4.16)$$

Equation (4.16) gives the value of live load P which would just cause collapse of the arch. When $(3 - 2\alpha) = (2 + k)\tau$, the collapse load is theoretically infinite. This corresponds to an arch of the proportions shown in Fig. 4.10, for which straight lines can be drawn to the springings from the extrados at quarter span (cf. Fig. 2.10(a)).

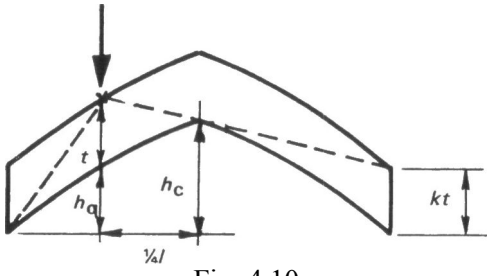

Fig. 4.10

As a further approximation made in order to get (4.16) into a form suitable for general application, the weight W_1 (and the corresponding value of x_1 defining the centre of gravity, Fig. 49) has been calculated from the trapezium of Fig. 4.11; the intrados of the arch ring has been replaced by a straight line. With a similar approximation for W_2, and for a unit width of bridge, (4.16) becomes

$$P = \frac{P}{\frac{1}{6}\gamma h_c} = \frac{(1+3\beta-\alpha)\{\alpha+(1-\gamma_4 k)\tau\}-(6+9\beta-5\alpha)\{(1-\alpha)-(1+\gamma_4 k)\tau\}}{(3-2\alpha)-(2+k)\tau} \qquad (4.17)$$

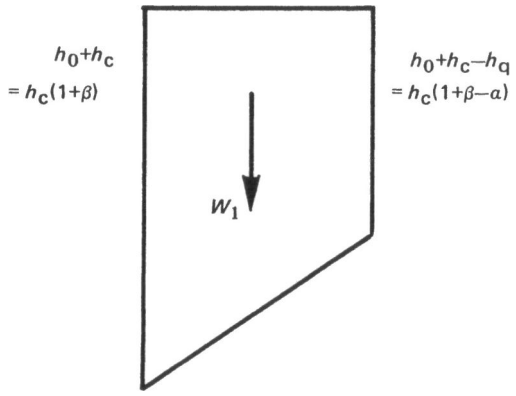

Fig. 4.11

Finally, in order to reduce by one the number of parameters in the equation, the constant k expressing the vertical thickness of the arch ring at the abutments, Fig. 4.9, will be taken as unity. Thus (4.17) gives the intensity of live load necessary to cause collapse of the bridge in terms of only three parameters, α, β and τ. The approximation $k = 1$ is, as a corollary of the lower-bound theorem, safe, but not excessively so. Figure 4.8 shows that the positions of three of the four hinges are fixed without involving the value of k, and the variation of the thickness of the arch at the fourth (abutment) hinge has a correspondingly small effect on the value of P. This physical argument is reinforced by an examination of the relative magnitudes of the quantities in (4.17); the magnitude of the non-dimensional ring thickness τ, with which k is always associated, is usually small compared with the values of α and β.

Equation (4.17) is the basis for a quick method of assessment of masonry arches. Table 4.1 gives numerical values (for $k = 1$) for

$$\begin{aligned} &\tau = 0.04\ (0.02)\ 0.30 \\ &\alpha = 0.60,\ 0.65,\ 0.68\ (0.02)\ 0.82,\ 0.85,\ 0.90 \\ &\beta = 0,1. \end{aligned} \qquad (4.18)$$

The value of P is a linear function of β, so that linear interpolation for a given value of β is exact. With the fairly close tabulation, no great errors are introduced by linear interpolation for α and τ. Examples of the use of Table 4.1 are given in Chapter 5.

The accurate analysis of an actual bridge arch may be made after a preliminary quick assessment from the Table. If the worst live load case is indeed that of a single live load, then the approximate method will usually give a result close to the exact value; the actual value can be checked by the drawing of funicular polygons, and again examples are given in Chapter 5. If however the specified design loading consists of a train of loads, then a graphical method must be used from the start.

In any case, both the approximate solution and the exact analysis will furnish, for a given bridge, estimates of its geometrical factor of safety. The choice of a suitable value for that factor remains an open question. The matter is reminiscent of the situation in the early days of the development of plastic theory as applied to steel frames; a suitable value of load factor (about 1.75)

was established by the comparison of plastic designs with conventional elastic designs. The Pippard method gives some help here, but what is needed is a comprehensive survey of existing bridges. In the mean time, a more limited experience indicates that a geometrical factor of 2 might be appropriate, and this factor has indeed been used in the practical rehabilitation of some masonry arches.

From the remarks made in Chapter 2, it will be appreciated that the adoption of a geometrical factor of 2 is equivalent to the adoption of a middle-half rule. If a purely graphical design were to be made, then the arch ring would be represented on the drawing board by a shrunk arch of half the actual thickness.

Table 4.1 Values of p (linear interpolation for β is accurate)

τ	$\alpha = 0.60$		$\alpha = 0.65$		$\alpha = 0.68$		$\alpha = 0.70$		$\alpha = 0.72$		$\alpha = 0.74$	
	$\beta = 0$	$\beta = 1$	$\beta = 0$	$\beta = 1$	$\beta = 0$	$\beta = 1$	$\beta = 0$	$\beta = 1$	$\beta = 0$	$\beta = 1$	$\beta = 0$	$\beta = 1$
0.04									-0.24	-0.11	-0.20	0.10
0.06							-0.24	-0.09	-0.20	0.12	-0.17	0.35
0.08					-0.24	-0.07	-0.20	0.15	-0.16	0.38	-0.13	0.62
0.10			-0.26	-0.15	-0.20	0.18	-0.16	0.42	-0.12	0.67	-0.08	0.93
0.12			-0.22	0.10	-0.15	0.46	-0.11	0.71	-0.07	0.98	-0.03	1.26
0.14			-0.17	0.37	-0.10	0.76	-0.06	1.03	-0.02	1.32	0.02	1.63
0.16	-0.24	0.04	-0.12	0.67	-0.05	1.09	0.00	1.39	0.04	1.71	0.08	2.04
0.18	-0.18	0.32	-0.06	1.00	0.01	1.46	0.06	1.79	0.11	2.13	0.15	2.51
0.20	-0.13	0.62	0.00	1.37	0.08	1.87	0.13	2.23	0.18	2.62	0.23	3.03
0.22	-0.06	0.97	0.08	1.78	0.16	2.33	0.21	2.73	0.26	3.16	0.31	3.63
0.24	0.01	1.34	0.16	2.24	0.24	2.85	0.30	3.30	0.36	3.79	0.41	4.31
0.26	0.09	1.77	0.25	2.76	0.34	3.45	0.40	3.95	0.47	4.51	0.53	5.11
0.28	0.18	2.24	0.35	3.35	0.45	4.13	0.52	4.71	0.59	5.34	0.67	6.05
0.30	0.28	2.78	0.47	4.03	0.58	4.92	0.66	5.59	0.75	6.34	0.83	7.15

Table 4.1 *continued*

τ	$\alpha = 0.76$		$\alpha = 0.78$		$\alpha = 0.80$		$\alpha = 0.82$		$\alpha = 0.85$		$\alpha = 0.90$	
	$\beta = 0$	$\beta = 1$	$\beta = 0$	$\beta = 1$	$\beta = 0$	$\beta = 1$	$\beta = 0$	$\beta = 1$	$\beta = 0$	$\beta = 1$	$\beta = 0$	$\beta = 1$
0.04	-0.17	0.32	-0.14	0.55	-0.10	0.79	-0.08	1.04	-0.04	1.44	0.02	2.18
0.06	-0.13	0.58	-0.10	0.83	-0.07	1.09	-0.04	1.36	0.00	1.80	0.06	2.61
0.08	-0.09	0.88	-0.06	1.14	-0.02	1.42	0.01	1.72	0.05	2.20	0.10	3.10
0.10	-0.04	1.20	-0.01	1.49	0.02	1.80	0.05	2.12	0.09	2.64	0.15	3.65
0.12	0.01	1.56	0.04	1.87	0.07	2.21	0.11	2.57	0.15	3.15	0.21	4.28
0.14	0.06	1.96	0.10	2.30	0.13	2.67	0.17	3.07	0.21	3.72	0.27	5.00
0.16	0.12	2.40	0.16	2.79	0.20	3.20	0.24	3.64	0.28	4.38	0.35	5.85
0.18	0.19	2.91	0.24	3.34	0.28	3.80	0.31	4.30	0.37	5.14	0.44	6.85
0.20	0.27	3.48	0.32	3.96	0.36	4.49	0.40	5.06	0.46	6.04	0.55	8.05
0.22	0.36	4.13	0.41	4.68	0.46	5.29	0.51	5.95	0.58	7.10	0.68	9.52
0.24	0.47	4.89	0.53	5.53	0.58	6.23	0.64	7.01	0.72	8.37	0.85	11.35
0.26	0.59	5.78	0.66	6.52	0.72	7.35	0.79	8.29	0.89	9.95	1.06	13.71
0.28	0.74	6.84	0.82	7.72	0.90	8.72	0.98	9.86	1.11	11.93	1.35	16.85
0.30	0.92	8.11	1.01	9.18	1.11	10.41	1.21	11.84	1.39	14.51	1.75	21.25

Example. For $l = 7.20$ m, $h_c = 2.66$ m, $h_q = 2.08$ m, $h_0 = 1.00$ m, $t = 320$ mm,
$\gamma = 1.67$ t/m^3, $\alpha = 0.78$, $\beta = 0.376$, $\tau = 0.12$, $\gamma l h_c/6 = 5.33$ t/m : from Table, $p = 0.73$
and therefore $P = 3.9$ t/m

5

Practical examples

THE LINE OF THRUST

A few examples of the analysis and design of actual bridges will illustrate the ideas developed in the previous chapters. Although the quick method of assessment given in Chapter 4 may well be useful in a preliminary analysis, it is evident that final calculations will involve the construction, on the drawing board or analytically, of funicular polygons. It was shown in Chapter 1 that a funicular polygon can be drawn by purely graphical means, but in fact labour is often saved by some preliminary calculation.

It is convenient to refer the calculations to an origin at the springing of the arch (cf. Fig. 1.13(a)). In Fig. 5.1 the solid line OA represents the intrados (or the centre-line, or any other reference line) of the arch ring, and the broken line represents the line of thrust, passing at a vertical distance Δ above the origin.

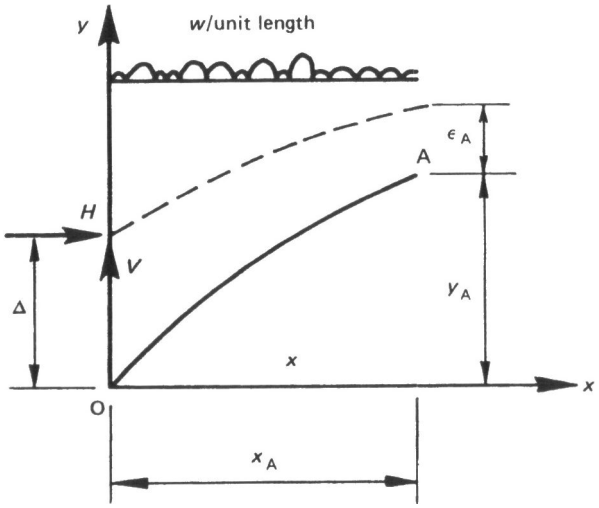

Fig. 5.1

At any section A of the arch, the vertical distance between the reference line OA for the arch and the line of thrust is $\in_A$. The (non-uniform) vertical loading acting on the arch has intensity w per unit horizontal length; then statical equilibrium (for moments taken about the right-hand end of the thrust line) requires that

$$(y_A + \in_A - \Delta)H + \int_0^{x_A} (x_A - z)w\,dz = Vx_A \,, \tag{5.1}$$

that is

$$\in_A = \Delta - y_A + \frac{V}{H}x_A - \frac{1}{H}\int_0^{x_A} (x_A - z)w\,dz \,, \tag{5.2}$$

In this equation, the quantities V and H are, as marked in Fig. 5.1, the components of thrust at the abutment. If their values have not yet been determined, then the three quantities Δ, V/H and $1/H$ in

(5.2) may well be regarded as the three redundant quantities for the arch, and (5.2) may be written for any section x (dropping the subscript A):

$$\in = \Delta - y + \mu x - \nu \int_0^x (x - z) w dz \,, \tag{5.3}$$

When an actual funicular polygon is drawn, the applied loads will be approximated by a series of point loads W_r, Fig. 5.2. If the section under consideration is taken at the nth load W_n, then the integral in (5.3) is replaced by the expression

$$x_n \sum_{r=1}^{n} W_r - \sum_{r=1}^{n} x_r W_r \,, \tag{5.4}$$

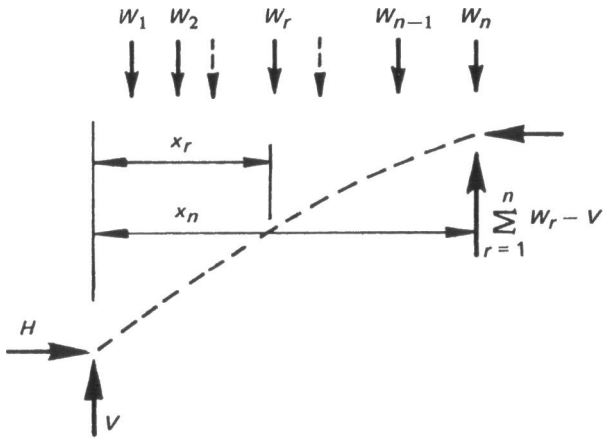

Fig. 5.2

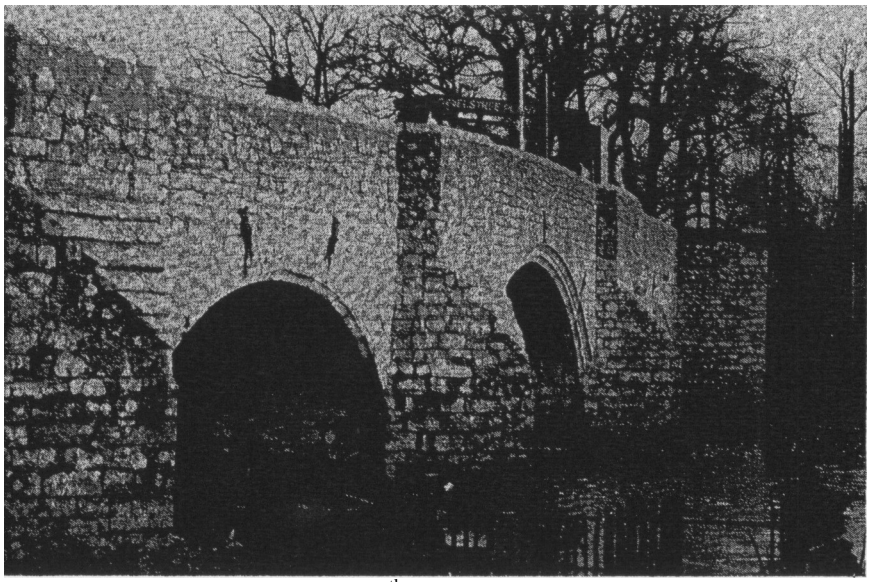

Fig. 5.3 Teston Bridge, Kent, 13th Century and later. The ties holding the spandrel walls above the arch barrel were removed in the rehabilitation of 1979.

This expression may be evaluated (in tabular form) for given loading; an example is given in Table 5.2 below. Equation (5.3) then gives the position of the thrust line relative to the arch centre line. If the position is known at any three sections, then the unknown quantities Δ, μ and ν may be determined, and the position is then calculable at any other section (see Table 5.3 below). A first example will illustrate how the equations may be set up and solved.

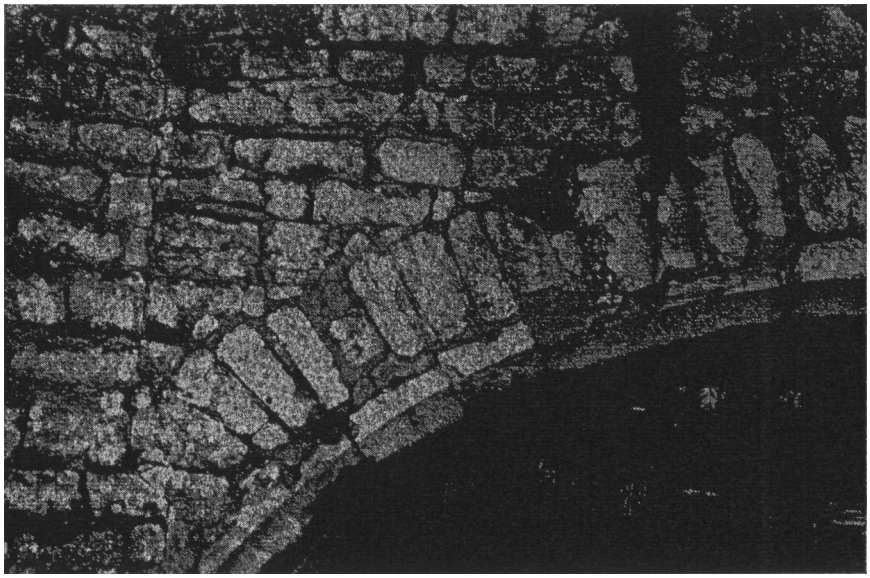

Fig. 5.4 Rough masonry of Teston Bridge, Kent, forming an arch ring of about 200-400 mm.

TESTON BRIDGE, KENT

Teston Bridge, Figs. 5.3 and 5.4, dates from the 13th century; it was rehabilitated in 1979 in such a way as to permit unrestricted use. To this end, four different conditions of loading were specified, and of these it turned out that the most critical was a singe axle of 11 ton; this load will be taken as a line load across the full width (3.5 m) of the bridge. With an allowance for impact, the line load has intensity 40 kN/m.

Such a knife-edge load is, of course precisely that envisaged in the development of the quick method of assessment (Fig. 4.8 leading to Table 4.1). The leading dimensions of the main navigation arch at Teston are marked in Fig. 5.5; they are l = 7200, h_c = 2660, h_q = 2080 and h_0 = 1000 mm. From these values,

$$\alpha = h_q/h_c = 0.78 ,$$
$$\beta = h_0/h_c = 0.376 , \qquad (5.5)$$

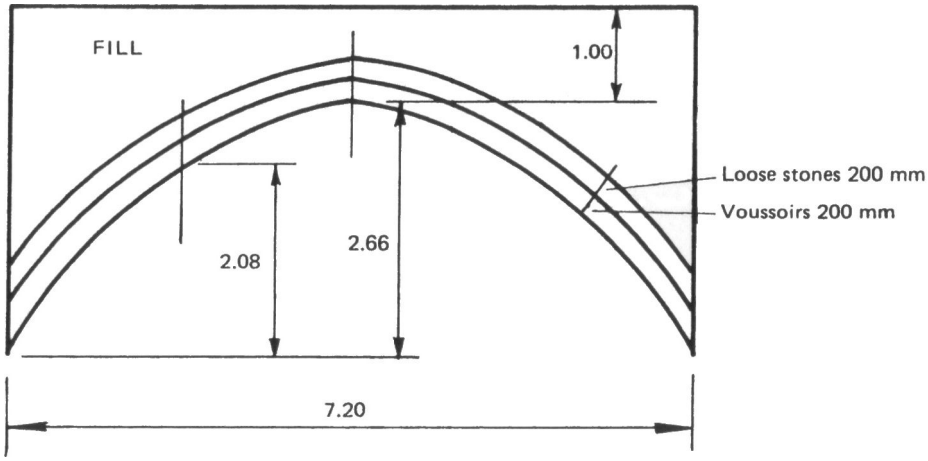

Fig. 5.5

The material weight (arch and fill) was taken as 16.7 kN/m^3, so that $^1/_6\gamma l h_c$ = 53.3 kN/m; the dimensionless point load has value p = 40/53.3 = 0.75. Table 4.1 then gives the value of τ required for the arch just to be stable as 0.122. The vertical thickness t of the arch at the quarter points should

therefore have a minimum value of 0.122 × 2660 = 325 mm, which corresponds to a radial thickness of about 280 mm.

It will be seen from the annotation in Fig. 5.5 that there might be some doubt as to the ability of the arch to carry the specified point load; with a geometrical factor of safety of 2, the arch ring should be about 560 mm thick. However, the next step is to make accurate calculations to confirm that the approximate minimum thickness of 280 mm is correct.

The span (7.20 m) of the arch was divided into twelve equal portions of 0.60 m, and the weights of each of the twelve sections was computed. The profile of the arch is given in Table 5.1, and the loads acting on the arch ring are shown in Fig. 5.6. Following the arguments relating to Fig. 5.1, moments will be taken about various points in the arch, and Table 5.2 records in an orderly way the loads and the moments of the loads. In this case, in order to simplify the equations, the calculations are referred to the right-hand end of the arch, and the unknown quantities V and H are introduced as shown in Fig. 5.7.

The way in which the calculations are made, and Table 5.2 used, is as follows. Figure 5.7 shows a point load P placed at the quarter point C, as in Fig. 4.8, and the hinge positions correspond also to those of Fig. 4.8. (It turns out that this hinge pattern is slightly incorrect, as will be seen.) The arch in Fig. 5.7 has the minimum *radial* thickness d to prevent collapse by the formation of hinges at the assumed points O, C, F and O'; the second set of numbers in Table 5.1 gives the *vertical* thickness of the arch ring at the various points in the arch.

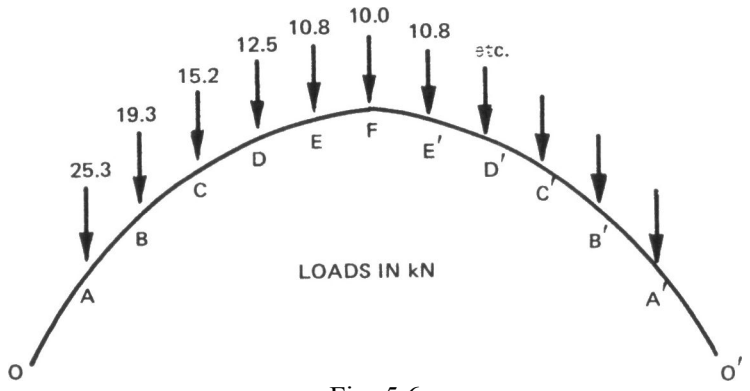

Fig. 5.6

Table 5.1

Point	O	A	B	C	D	E	F
Profile of intrados, m	0	1.03	1.65	2.08	2.37	2.56	2.66
(l/*d*)× vertical depth of ring	2.638	1.618	1.313	1.161	1.077	1.028	1.004

Table 5.2

Point	Load, kN	∑ load, kN	Distance, m	Product, kN m	∑ product, kN m
O'					0
A'	25.3	0	0.6	0	0
B'	19.3	25.3	0.6	15.18	15.18
C'	15.2	44.6	0.6	26.76	41.94
D'	12.5	59.8	0.6	35.88	77.82
E'	10.8	72.3	0.6	43.38	121.20
F	10	83.1	0.6	49.86	171.06
E	10.8	93.1	0.6	55.86	226.92
D	12.5	103.9	0.6	62.34	289.26
C	15.2	116.4	0.6	69.84	359.10
B	19.3	131.6	0.6	78.96	438.06
A	25.3	150.9	0.6	90.54	528.60
O		176.2	0.6	105.72	634.32

The analysis consists merely in taking moments about the hinge points F, C and O in turn for the whole portion of the arch lying to the right of the point in question; the data required for taking moments about C have been transferred from Table 5.1 to Fig. 5.7. Thus Tables 5.1 and 5.2 together may be used to give the following equations:

$$\left.\begin{aligned} \text{At F: } & 3.6\,V - (2.66 - 2.638d)H &&= 171.06 \\ \text{At C: } & 5.4\,V - (2.08 - 1.161d - 2.638d)H &&= 359.10 \\ \text{At O: } & 7.2\,V - (2.638d)H - 1.8P &&= 634.32 \end{aligned}\right\} \tag{5.6}$$

The unknown quantities V and H may be eliminated from these equations to give a single relationship between the required depth d of the arch ring and the value of the point load P:

$$d(1 + 0.00983P) = (0.0281 + 0.00757P)\,, \tag{5.7}$$

Thus for $P = 40$ kN, the value of d is determined as 0.237 m (that is, 237 mm). (It should be noted that the equations must be solved with care; small differences of large numbers are involved, and rounding errors can have a marked effect on the final results.)

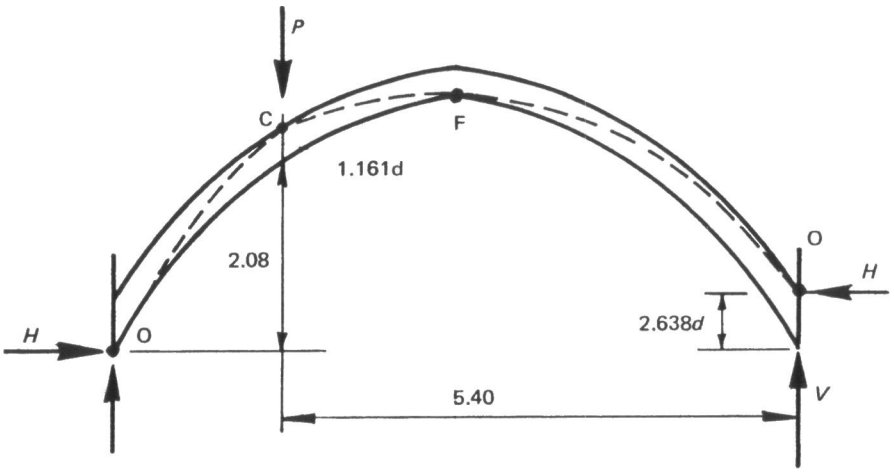

Fig. 5.7

The calculations made so far are 'unsafe' for two reasons. In the first place; the hinge pattern of Fig. 5.7 is an assumed pattern; there may be (and in fact there is) a more critical arrangement of hinges. Secondly, the worst position of the point load may not be at the quarter-span point C, but slightly away from quarter span.

The correctness of the hinge pattern of Fig. 5.7 is best confirmed by constructing the thrust line on the drawing board. However, this construction may also be made analytically by use of (5.3) and (5.4), where in fact the loading terms (5.4) are given in Table 5.2. If (x,y) are the coordinates of the intrados of the arch (and the values of y for x increasing in steps of 0.6 m are given in Table 5.1), and if the origin is taken at O in Fig. 5.7, then the general expression for the vertical distance $\in$ between the line of thrust and the intrados is given by

$$\in = (2.638d - y) + \frac{1}{H}\left[(7.20 - x)V - \{1.80 - x\}P - \Sigma\right], \tag{5.8}$$

In this equation, the brackets {} are 'Macaulay' brackets; the term is present in the equation only for $1.80 > x$. The last term Σ is taken from the last column of Table 5.2. (Equations (5.6) are, of course, just specific cases of the general equation (5.8), written in a slightly different order.)

The values of V and H, corresponding to the solution of (5.7) for $P = 40$ kN, are 91.3 and 77.6 kN respectively, and (5.8) may be solved for $\in$ at each section of the arch, with, of course, d set equal to 237 mm. The results are given in the first column of Table 5.3, and the values may be compared with the position of the thrust line sketched in Fig. 5.7. At C, for example, the line of thrust lies 276 mm above the intrados, and the radial thickness d of the arch at that point is 276/1.161 = 237 mm. Similarly, at O' the value of d is given by 626/2.638 = 237 mm, and there are zeros at points O and F.

Table 5.3

Point	$\in$, mm Trial 1 Fig. 5.7	Trial 2 Fig. 5.8
O	0	90
A	-65	0
B	85	122
C	276	289
D	179	187
E	86	90
F	0	0
E'	36	34
D'	79	77
C'	125	126
B'	193	200
A'	303	319
O'	626	657

Thus the equations have been solved correctly, but it is at once clear from Table 5.3 that the assumed hinge pattern is not correct. There is a negative value of $\in$ at point A, implying that the thrust line has emerged from the masonry. The obvious pattern of hinges for the next trial is shown in Fig. 5.8 (cf. Fig. 4.6), and the analysis may be repeated with hinges at A, C, F and O'. Equations (5.6) are replaced by

$$\left.\begin{aligned} \text{At F: } & 3.6\,V - (2.66 - 2.638d)H &&= 171.06 \\ \text{At C: } & 5.4\,V - (2.08 - 1.161d - 2.638d)H &&= 359.10 \\ \text{At A: } & 6.6\,V - (2.638d)H - 1.2P &&= 528.60 \end{aligned}\right\} \tag{5.9}$$

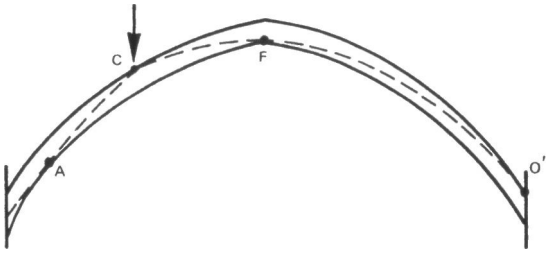

Fig. 5.8

The first two of these equations are identical with those of (5.6). For P = 40 kN, (5.9) solve to give d = 0.249 m; that is, the radial depth of ring is some 12 mm greater than that of Fig. 5.7. The correctness of the pattern of hinges may be confirmed by the construction of the funicular polygon, Fig. 5.9 (the intrados only of the arch is shown); alternatively, the second column of Table 5.3 gives numerically the information of Fig. 5.9.

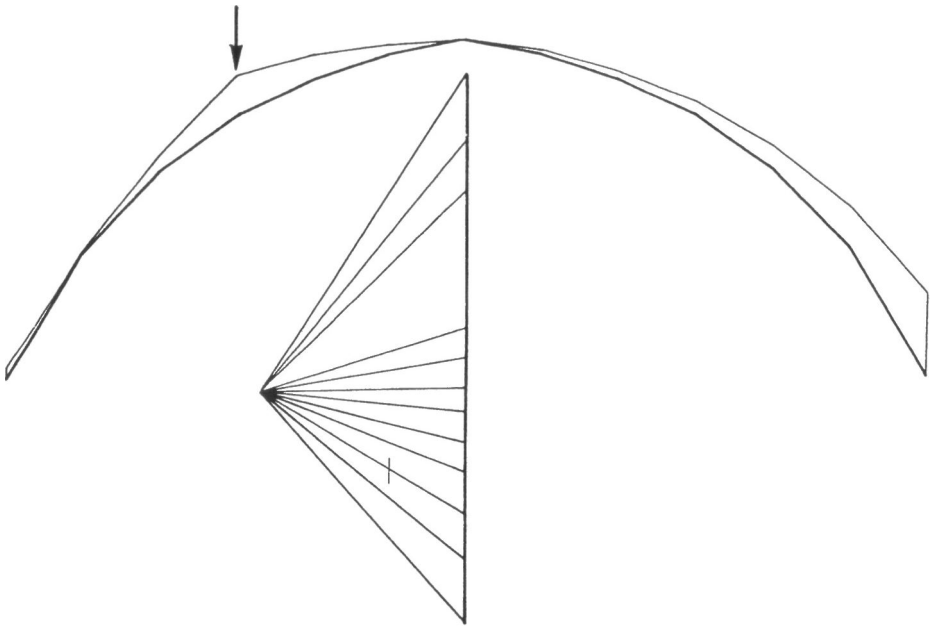

Fig. 5.9

The whole analysis must now be repeated with the load displaced to a possibly more unfavourable point in the span. Similar calculations made for the load placed at B and at D lead to the arch-ring depths given in Table 5.4 (the values have been rounded). Thus in fact, for this example, the load placed at quarter-span gives the most critical value of arch-ring depth, although the neighbouring point D (distant 0.6 m) is almost equally critical.

Table 5.4

Load position	B	C	D
Arch-ring depth (mm)	210	250	240

The quickly-assessed value of arch-ring depth of 280 mm has been reduced to 250 mm by the more accurate analysis. The final recommendation for the rehabilitation of the bridge was based on a geometrical factor of safety of 2; that is, the minimum required depth of 250 mm leads to a thickness of the actual arch of 500 mm.

The values of V and H quoted above indicate that the value of the (inclined) thrust at the abutment is about 150 kN/m; with an arch ring of 500 min depth, the corresponding mean stress is 0.30 N/mm^2. As is usual with masonry bridges of this size, this stress is low.

As an alternative to the single axle of 11 ton, the next most critical loading specified for the bridge related to a four-axle vehicle of total mass 30 ton and length about 5 m. This loading can be

investigated by the combination of analysis and drawing used for the single load; in equations similar to (5.6), for example, instead of the term 1.8*P* there would be contributions from all four axles. Because of the length of the vehicle, 5 m, compared with the span of 7.2 m, the live loading is more 'balanced' than the single point load; the worst positioning of the four axles leads to a required depth of arch of less than 200 mm.

THE 'QUICK' METHOD OF ASSESSMENT

The calculations summarized in the last section are typical of those for arches with spans of the order of Teston bridge, and the approximate method of assessment, given in Table 4.1, leads to a good estimate of the depth of arch ring required to carry a specified point load. As final examples of the use of this 'quick' method, data are presented below for the five-span neighbouring bridge in Kent, Twyford bridge, Fig. 5.10. This bridge has large piers and four river arches; there is a small fifth arch carrying, with shallow cover at its crown, a causeway over the flood plain. From a survey of the bridge average dimensions were evaluated for each arch; the arches are not in fact quite symmetrical and the roadway is not quite horizontal. These average dimensions are shown in Table 5.5, together with the derived values of the dimensionless quantities α and β. The unit weight of material was taken as 23 kN/m^3, from which the value $^1/_6\gamma l h_c$ was calculated for each span; the design line load was P = 30 kN/m, leading to the tabulated values of p.

Table 5.5

Span	l (m)	h_c (m)	h_q (m)	h_0 (m)	α	β	$^1/_6\gamma l h_c$kN/	p	τ	t(m)	d(mm)
1	4.40	2.12	1.70	1.44	0.80	0.68	35.8	0.84	0.07	0.148	130
2	5.31	2.77	2.15	0.83	0.78	0.30	56.4	0.53	0.11	0.305	260
3	5.13	2.73	2.29	0.93	0.84	0.34	53.7	0.56	0.06	0.164	140
4	5.13	2.22	1.79	0.83	0.81	0.37	43.7	0.69	0.09	0.200	170
5	4.11	2.04	1.61	0.42	0.79	0.21	32.1	0.93	0.18	0.367	320

The flood arch, No. 5, is most critical, mainly because of the thin cover. The design of this arch (that is, the establishment of the value of τ) must be carried out so that the required value of p, 0.93, is attained for α = 0.79, β = 0.21. Table 4.1 gives values of p (for β = 0, 1) for α = 0.78 and α = 0.80, and Table 5.6 may be drawn up for β = 0.21. Linear interpolation between α = 0.78 and α = 0.80 gives the final column of values for α = 0.79.

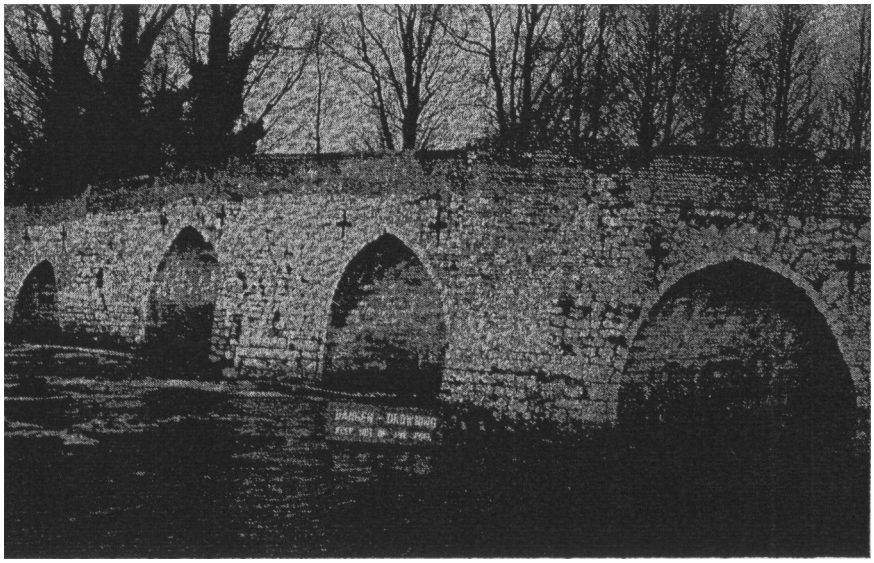

Fig. 5.10 Twyford Bridge, Kent, with river in heavy flow.

Table 5.6

	Values of p for $\beta = 0.21$		
	$\alpha = 0.78$	$\alpha = 0.80$	$\alpha = 0.79$
$\tau = 0.16$	0.71	0.83	0.77
$\tau = 0.18$	0.89	1.02	0.96
$\tau = 0.20$	1.08	1.23	1.16

It will be seen that, to two significant figures, $\tau = 0.18$ is the appropriate dimensionless value of arch-ring thickness for $p = 0.93$, and this is the value entered in Table 5.5. The penultimate column of this table gives the vertical thickness t at the quarter point of the arch; the arch ring is about 15% less in radial dimension, and the final column shows these thicknesses for the arch rings in each span.

If a geometrical factor of safety of 2 were specified, then the recommendation would be to build up the arch rings in the first four spans to say 250 mm, 550 mm, 300 mm and 350 mm respectively. In the case of the flood arch No. 5 a constant radial thickness of something over 600 mm is apparently needed, whereas the value of h_0, which includes both arch ring and cover at the crown, is only 420 mm. The analysis indicates, correctly, that extra dead weight applied to the arch would increase its strength against live loading.

However, it will be appreciated, from Fig. 5.8, that the thickness of the arch ring at the crown is of secondary importance; it is the thickness of the arch at the quarter points and at the springings that will control its strength when a live load is applied at a quarter point. In the case of arch No. 5 a first trial design would thus retain the crown thickness of 420 mm, but the arch ring could be increased to say 600 mm at the quarter points and further increased towards the springings. The resulting arch of non-uniform thickness would then have to be investigated for different positions of the line load, since it is possible that the quarter-span points would not remain the most critical.

THE DEAD-LOAD LINE OF THRUST

Investigation of the effect of live-loading on an arch (for example, the single knife-edge load considered in the previous examples) can often be made easier if the calculations are referred to the dead-load line of thrust (rather than to the centre line of the actual arch, or to the intrados). To illustrate the way in which such calculations can be made, the arch of Fig. 5.11 (a) is supposed to be subjected to the two idealized *dead* loads W shown; there are no other dead loads acting. Thus the dead-load line of thrust consists of the three straight lines shown in Fig. 5.11 (a), and, with the usual notion of an imaginary shrinking of the real arch, a corresponding geometrical factor of safety can be determined.

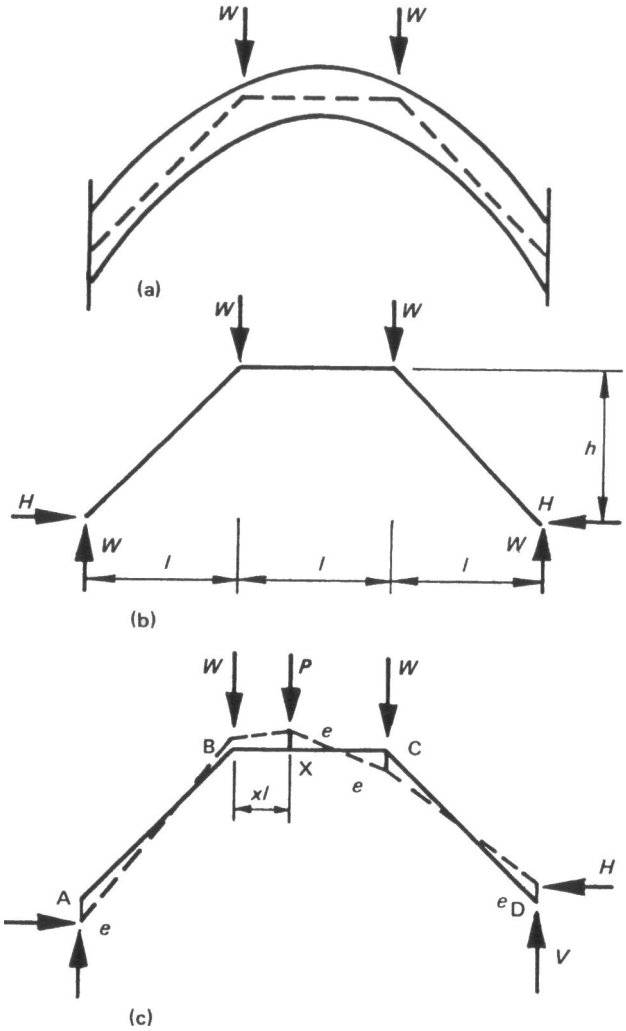

Fig. 5.11

The effect of a single concentrated live load P will now be considered, and for this purpose the real arch will be abandoned for the moment, and the calculations referred to the arch of Fig. 5.11(b). Thus in Fig. 5.11(c) the point load is shown acting in a general position (defined by the parameter x) on the 'dead-load arch'. The thrust line for the loading is also shown in Fig. 5.11(c), and it has been drawn in a special and unique position; its maximum departure (vertically) from the arch centre line is a quantity e (whose value is to be determined). An arch of the shape of Fig. 5.1l(b) and vertical thickness $2e$ could thus just contain the thrust line of Fig. 5.11(c), and moreover this is the thinnest arch that could contain the thrust line. If this arch of thickness $2e$ is fitted back into Fig. 5.11 (a), then the new geometrical factor of safety of the real arch, taking account of the live load P, is at once calculable.

The point of referring the calculation to the dead-load line of thrust will become apparent if the value of e in Fig. 5.1l(c) is determined. If moments are taken (in the way that led to (5.6)) at points on the thrust line corresponding to sections C, X and A on the arch, the following equations may be written:

$$\left.\begin{aligned} \text{At C: } Vl &= H(h-2e) \\ \text{At X: } Vl(2-x)-Wl(1-x) &= Hh \\ \text{At A: } 3V-3Wl-Pl(1+x) &= H(\text{-}2\text{e}) \end{aligned}\right\} \qquad (5.10)$$

As before, V and H can be eliminated from these equations, and the quantity e determined as a function of W, P and x:

$$e = \tfrac{1}{2}\,Ph\,\frac{(1-x^2)}{W(4-x)+P(2-x)(1+x)}, \tag{5.11}$$

However, if V and W are eliminated from (5.10), then the value of e is given by

$$e = \frac{1}{H}\,\frac{Pl}{2}\left\{\frac{1-x^2}{4-x}\right\}, \tag{5.12}$$

where the value of H may be written

$$H = \frac{Wl}{h-2e\left(\dfrac{2-x}{1-x}\right)}, \tag{5.13}$$

Equation (5.13) shows that, if e is small compared with h, then the value of the abutment thrust H is close to the dead-load value Wl/h; in effect, a relatively small live load P will not alter markedly the abutment thrust. If H can indeed be assumed to be fixed in value, then (5.12) shows that the eccentricity of the live-load thrust line from the dead-load thrust line depends only on the live load P; the loads W do not occur explicitly in (5.12), but are of course implicit in the value of H. More particularly, the product He, which gives the 'bending moment' in the arch referred to the dead-load line of thrust, is purely a function of the live load.

This matter is at once apparent if the analogous frame problem is studied, Fig. 5.12. If the frame were designed by the plastic theory, then the appropriate collapse mechanism would involve the four hinges at A, X, C and D; moreover, since the values of e have been set equal in Fig. 5.11, the values of M_p of the corresponding full plastic moments in Fig. 5.12 will be the same at all four hinges. (For an arch of variable thickness, leading to different values of eccentricity, as for example in Fig. 5.7, the values of M_p will differ from hinge to hinge. An example is given below, Fig. 5.19.)

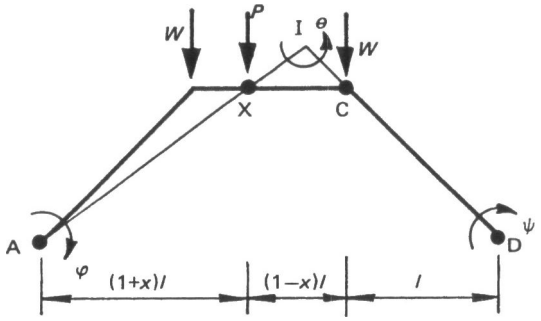

Fig. 5.12

The motion of the mechanism in Fig. 5.12 may be referred to a rotation θ of the portion XC of the arch about the instantaneous centre I. A straightforward analysis of the geometry of the motion leads to values ϕ and ψ of the rotations marked in Fig. 5.12 given by

$$\Phi = \Psi = \left(\frac{1-x}{2+x}\right)\theta, \tag{5.14}$$

Thus the work done by the loading on a small motion of the mechanism is

$$P(1+x)l\,\Phi + Wl\,\Phi - Wl\,\Psi,$$

and, by virtue of (5.14), the terms in W cancel.

This is, of course, a particular example of a general property. Since the centre line of the arch being considered coincides with the dead-load line of thrust, then any small inextensional deformation of the centre line will lead to zero virtual work of those dead loads. Thus any mechanism

of the type sketched in Fig. 5.12, referred to the dead-load thrust line, will involve work terms only for the additional live loading.

The total hinge rotation in Fig. 5.12 is $2(\theta + \phi + \psi)$, so that, using (5.14) and equating the work done by the loads to the work dissipated in the hinges, it is found that

$$M_p = \frac{Pl}{2}\left(\frac{1-x^2}{4-x}\right), \tag{5.15}$$

Thus (5.12) is recovered from this analysis of the analogous frame. Equation (5.15) is exact because it has been assumed that the plastic hinges lie on the centre line of the analogous arch. The actual hinges between voussoirs will occur slightly off the centre line (in fact at eccentricities e in Fig. 5.11), and the actual collapse mechanism will lead to some small extensional deformation of the centre line.

The maximum value of M_p in (5.15), that is, of He in (5.12), occurs for $x = 4 - \sqrt{15} = 0.127$ and is equal to

$$M_p = He = Pl\left(4 - \sqrt{15}\right) = 0.127Pl, \tag{5.16}$$

If e is indeed small compared with h so that H may be approximated by its dead-load value of $W1/h$, from (5.13), then

$$e = 0.127\frac{P}{W}h, \tag{5.17}$$

(For Teston bridge, considered earlier in this chapter, the appropriate value of W might be half the dead load on the arch, that is, 88.1 kN from Fig. 5.6 or Table 5.2, while the value of P was 40 kN. Thus 0. 1 $27P/W$ has value 0.06 in this case.)

The problem of Figs 5.11 and 5.12 has been worked through analytically, but it is more convenient to use graphical methods for arches of complex geometry. If graphical methods are used, then the dead loads may be ignored completely for the purpose of investigating the live load. For the problem just considered, in order to calculate the value of M_p at the hinge points of Fig. 5.12, it is sufficient to consider the action of the point load P acting alone. In Fig. 5.13(a) the thrust line has been positioned to give four equal bending moments, as before. In practice this would be done very quickly by trial and error; from the simple geometry of Fig. 5.13(a); it is found that

$$\frac{2e'}{h} = \frac{1-x}{2-x}, \tag{5.18}$$

The thrust line is shown separately, and in a general position, in Fig. 5.13(b); consideration of statics leads to the expression

$$T = \frac{P}{\frac{h_1}{l_1} + \frac{h_2}{l_2}}, \tag{5.19}$$

Thus for $h_1 = h + 2e'$, $h_2 = h$, $l_1 = (1 + x)l$, $l_2 = (2 - x)l$, the value of T is found to be

$$T = \frac{Pl}{h}\,\frac{(1+x)(2-x)}{(4-x)}, \tag{5.20}$$

so that, using (5.18) and (5.19),

$$Te' = \frac{Pl}{2}\,\frac{\left(1 - x^2\right)}{4 - x}, \qquad (5.21)$$

Once again (5.12) has been recovered, but this time with much less labour. This saving will be demonstrated by the calculations of the next example.

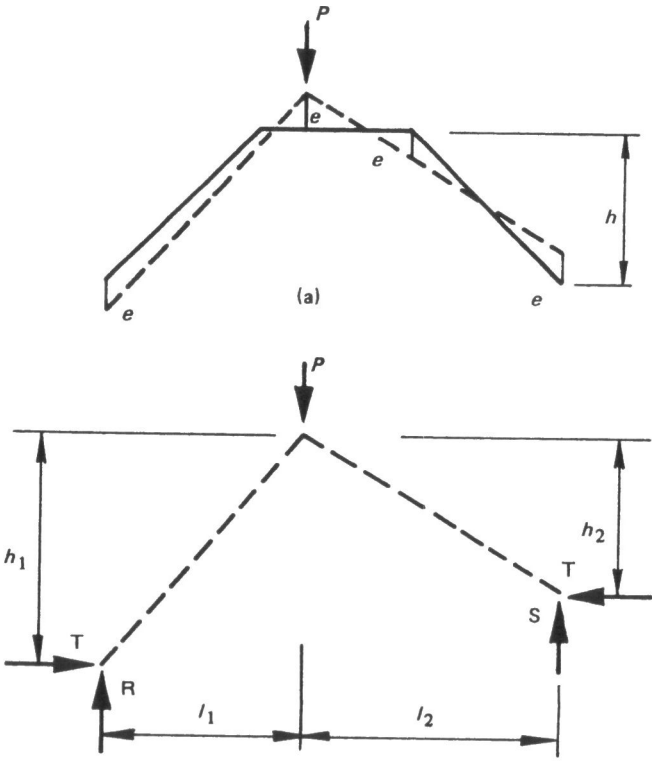

Fig. 5.13

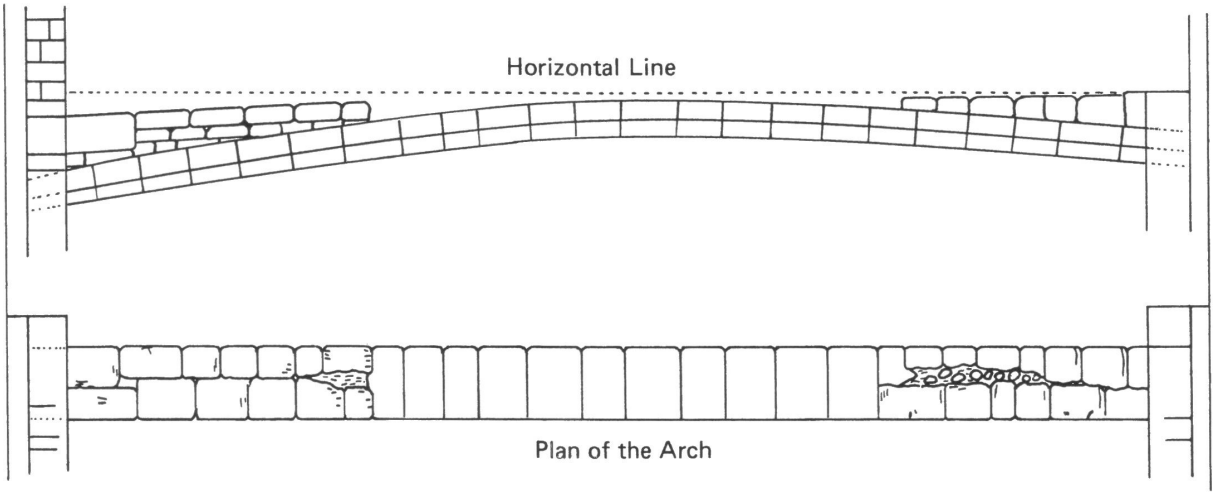

Fig. 5.14 Voûte de la cathédrale Lincoln (Nicholson 1842).

A STONE SPAN AT LINCOLN

Between the western towers of Lincoln Cathedral, and just above the nave vault, there is a thirteenth-century slender stone arch of span 8.54 m, Fig. 5.14. The northern springing of the arch is some 300 mm lower than the southern, due apparently to settlement. The rise of the arch relative to the chord was determined in 1836 as about 380 mm. The cross-section of the arch has a uniform profile, virtually rectangular, and is about 500 mm wide and 280 mm deep. The spandrels of the arch have stone backings which will contribute to the loading but which will be assumed not to act structurally. (The function of the arch is obscure; it may have served as a setting-out point for the construction of the nave vault in l240-50.)

The centre-line of the arch is shown to an exaggerated vertical scale (×6) in Fig. 5.15; it will be seen that the arch is two-centred and has a distinct point Also shown in Fig. 5.15 is a possible line of thrust for the self-weight of the arch plus its backings. In order to draw this dead-load line of thrust the arch was divided into 14 segments each of length 0.61 m, and the line of thrust has been positioned to lie as close as possible to the centre line of the arch. The difference between the two is ±33 min at sections 0, 3, 7 and 12 as marked in Fig. 5.15 and it may be concluded that an arch of the same shape as the actual arch at Lincoln but having a depth of 66 mm would just contain its own dead-load line of thrust. The geometrical factor of safety, against dead load only, is therefore 280/66 = 4.2.

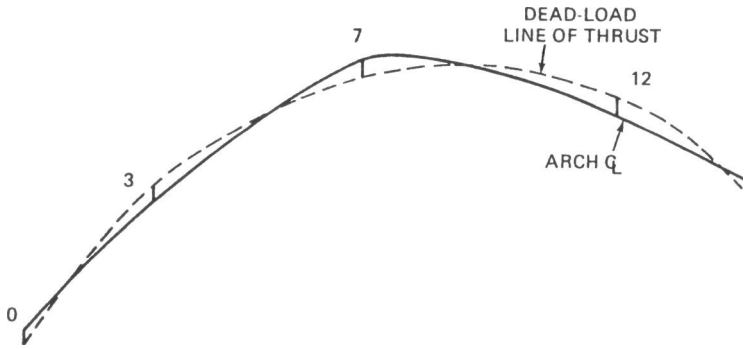

Fig. 5.15

The analysis also gives the value of the horizontal component of the abutment thrust as 87 kN. The arch has a cross-sectional area of about 0.14 m^2, so that the mean compressive stress is about 0.62 N/mm^2. The arch is made of oolitic limestone with a crushing strength of about 15 N/mm^2. The mortar beds between the voussoirs will of course have a lower strength; nevertheless the working value of the mean compressive stress seems satisfactory.

It was noted in 1842 that the arch vibrated perceptibly when jumped upon, and that it was the constant practice of visitors thus to prove its elastic properties (it still is). The effect of a point load placed anywhere on the arch will therefore be considered.

Figure 5.16(a) shows a unit point load placed on an arch having the profile of the dead-load line of thrust, and calculations will be made to determine the value of the 'full plastic moment' corresponding to collapse by formation of the hinges shown. On the drawing board the problem to be solved is that of Fig. 5.16(b), and it is clear that the value of *e* can be found very easily. Associated with the thrust line of Fig. 5.16(b) will be a certain horizontal, thrust *T*, whose value may be found from (5.19), Fig. 5.13; the product *Te* then gives the required value of full plastic moment. As the point load is traversed across the arch, the critical mechanism can switch to that of Figs. 5.17(a) and (b), but the analysis is equally straightforward.

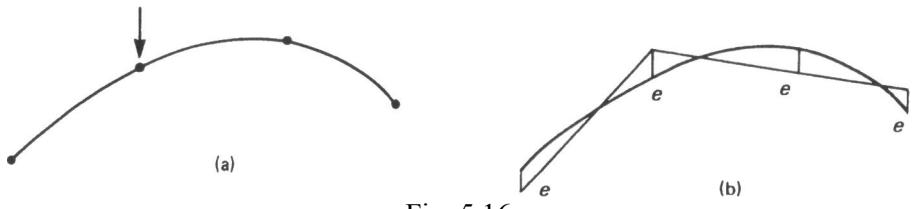

Fig. 5.16

Fig. 5.17

Figure 5.18 records the results of analyses made for 14 positions of a unit live load. The worst position of the load is as usual at about quarter span; the diagram is slightly asymmetrical, and the largest value of M_p is found to be 0.396 Nm for a load of 1 N. Thus, taking a point load of 2 kN (a heavy man jumping on the arch), and using the basic abutment thrust of 87 kN, the effect of the live load is to displace the dead load line of thrust by a maximum amount *e*, where

$$(0.396)\,(2) = (\in)\,(87)\,,$$

or

$$\in = 0.009 \text{ m}\,. \qquad (5.22)$$

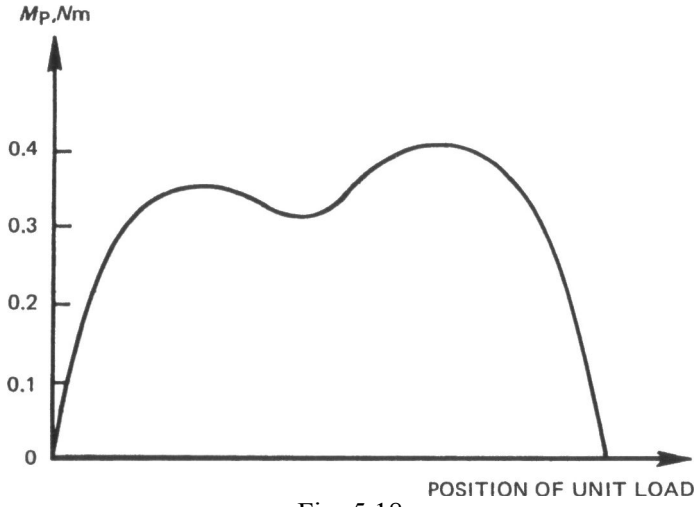

Fig. 5.18

This means that an arch of thickness 18 mm having the *broken-line* profile in Fig. 5.15 would just contain the line of thrust arising from the dead load on the Lincoln arch plus the live load of 2 kN in its worst position.

The thickness of 18 mm is simply additive to the thickness of 66 mm, found previously. That is, an arch of thickness 84 mm having the *full-line* profile (that is, the real profile) of Fig. 5.15 would just contain the lines of thrust arising from both dead and live loads. Thus the geometrical factor of safety, 4.2 against dead load only, is reduced by a man jumping in the worst position to 280/84 = 33.

PONTE MOSCA, TURIN

Mosca's bridge over the Dora Riparia, Turin, was constructed in 1827, and has a span of 45 m. Castigliano gives details of the bridge, and he gives tables of the quantities required for the analysis in a way similar to that shown in Table 5.2. As was mentioned in Chapter 3, Castigliano was concerned with the exposition of his theorems, and he treats the bridge at Turin as an elastic arch having three redundancies, whose values he proceeds to compute,

Castigliano shows that a cracked arch (that is, an imperfectly elastic arch) may also be dealt with by his methods, and he makes alternative calculations for the Turin bridge. In the first, full allowance is made for the elasticity of the mortar beds between the voussoirs, and the value of the

abutment thrust is calculated to be 352 990 kgf/m width of bridge. (It was noted above, (5.7), that it is necessary to solve the equations to an accuracy greater than is warranted by the data.)

A second calculation is made for dry construction (mortar beds of zero thickness), and Castigliano obtains the value of 324 710 kgf for the abutment thrust, a drop of some 8%. However, this solution involves the line of thrust falling outside the middle third near the springings, so that the masonry is partially cracked. (Castigliano remarks on a general tendency of arches of small rise to lift from their bearings near the extrados; the line of thrust approaches the intrados, with consequent possible overstressing of the masonry. This matter is mentioned again in Chapter 6.)

A final calculation allowing for the partially cracked masonry gives a thrust of 333 960 kgf.

As an alternative to these calculations, the geometrical factor of safety will be determined. Castigliano's drawing is reproduced in Fig. 5.19; the arch is symmetrical, so that one half only need be considered for the purpose of determining the effect of dead load. The radial thickness of the voussoirs increases from 1.50 m at the crown to 2.00 m at the springings; the *vertical* thickness at the springings is 2.23 m. As before, the arch will be imagined to be shrunk towards its centre line until the line of thrust can only just be contained. At this limit, there will be five critical sections, because of the symmetry of the arch; these lie at the springings and at the crown, and at about the two quarter points (cf. Fig. 5.15 for the asymmetrical arch of Lincoln). During the shrinking process, the relative thicknesses of the arch ring at the various cross-sections will be maintained constant.

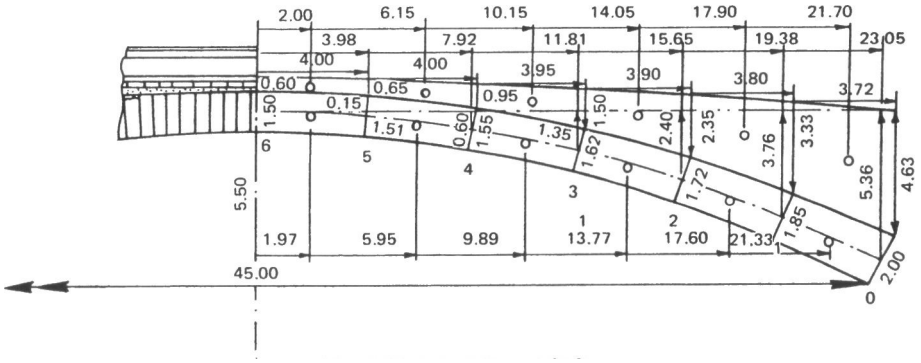

Fig. 5.19 (Castigliano 1879).

Castigliano divided the half-arch into six segments, Fig. 5.19. If the origin is taken at the crown, instead of at the springing (cf. Fig. 5.1), some simplification results; using the notation of (5.2), and with $V = 0$ by symmetry, the equations for the vertical distance between the thrust line and the arch centre line become

$$\left.\begin{aligned} 6(\text{crown}) \qquad & -\epsilon = \Delta \\ 3 \qquad & 1.20 = \Delta + 2.40 - \frac{1}{H}(800\ 470) \\ 0(\text{springings}) \quad & -0.49\,\epsilon = \Delta + 5.36 - \frac{1}{H}(2\ 021\ 937) \end{aligned}\right\} \qquad (5.23)$$

In the third of these equations, for example, the value 1.49ϵ contains the ratio 2.23/1.50 of the vertical thicknesses of the arch at the springings and at the crown; the eccentricity ϵ is thus referred to the actual ring thickness of 1.50 m at the crown. Section O lies 5.36 m below section 6 (the origin); the value 2 021 937 kgfm is taken from Castigliano's tables.

Equations (5.23) solve to give $\epsilon = -\Delta = 0.116$ m and $H = 373\ 000$ kgf; this last figure is some 5% higher than Castigliano's elastic value. The geometrical factor of safety against dead load is (1.50)/(2) (0.116) = 6.5.

The greatest mean stress in the arch occurs at the crown, where its value is 373/1.5 = 249 tf/m^2 (the corresponding value at the springings is 438/2.0 = 219 tf/ m^2.) Granite (of which the arch

ring is made) has typical strengths in the range 5000-18 000 tf/m^2; the nominal factor of safety on stress appears to be well over 20.

The dead-load line of thrust is now substituted for the actual centre-line of the arch for the purpose of computing the effect of live load. A graphical technique is again best, and a typical critical position of the thrust line is shown (schematically, vertical scale ×4) in Fig. 5.20. The eccentricities e of this thrust line are not constant; instead, the values e_1 etc. are proportional to the vertical depth of the arch ring at the corresponding sections. The final results are presented in Fig. 5.21; the largest value of M_p is 1.72 tfrn for a unit (tonne) load. Thus, taking a live load of 10 tf/m width of bridge the value of M_p is 17.2 tfm. The basic abutment thrust is 373 tf, and the live-load eccentricity, referred to the crown depth as before, is therefore 17.2/373 = 0.046 m. If the dead load eccentricity of 0.116 m is added in, then the geometrical factor of safety is reduced to (1.50)/(2)(0.162) = 4.6 for this particular value of live load.

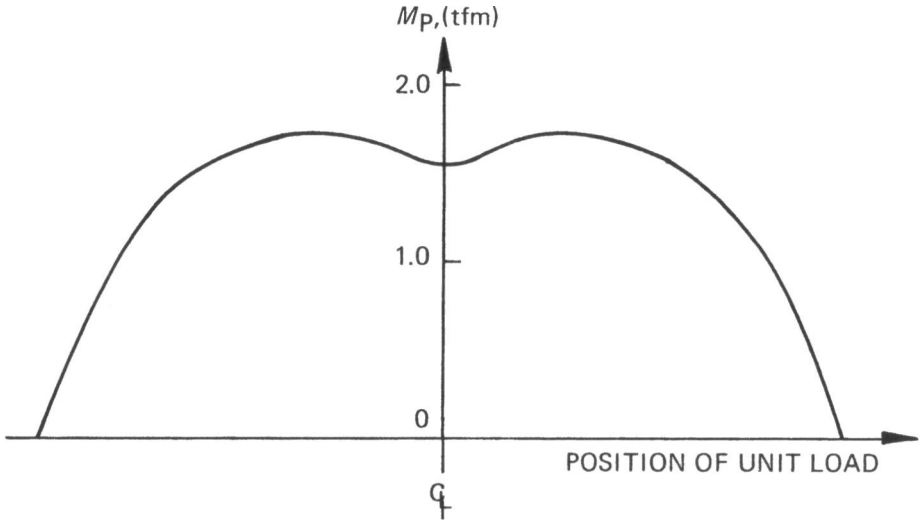

Fig. 5.20

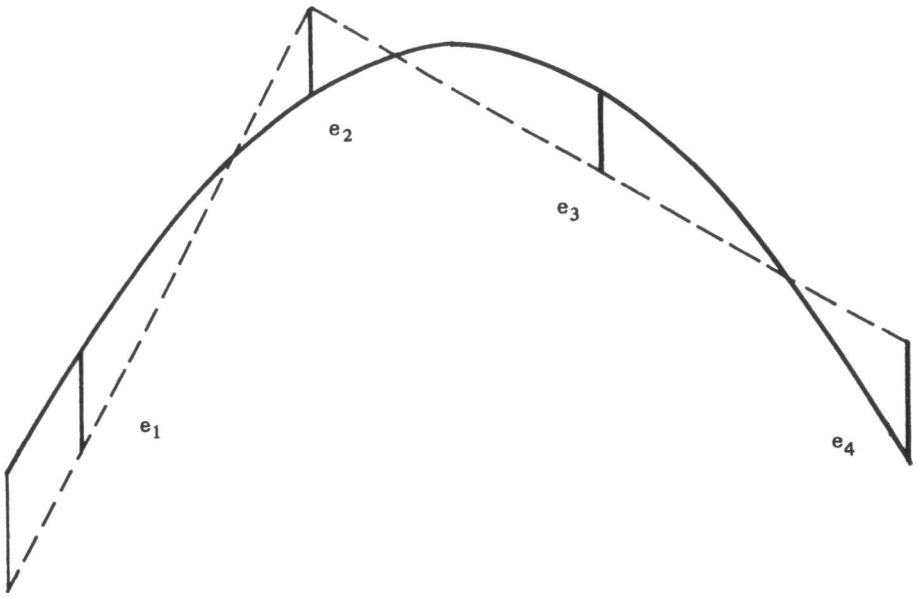

Fig. 5.21

6

Iron arches

Cast iron is a material which, like stone, is strong in compression but weak in tension. If a particular type of stone structure has been proved by experience to be satisfactory, there would seem to be no reason why a structure of the same shape should not be equally satisfactory in cast iron. Indeed, for bridge construction the iron arch might well show advantages, not least in a reduction in overall dead weight and consequent reduction in the abutment thrust.

Certainly bridges of cast iron, and later of wrought iron, were much in fashion from the early years of the nineteenth century onwards, and many of these were constructed in imitation of the masonry arch. There were, however, differences. In the first place, the continuous masonry barrel made up of the voussoir arch rings could be replaced either by cast-iron 'voussoirs', which were really box-section frames, or by individual parallel iron ribs, braced together to give lateral stability to the whole structure. Secondly, the conventional construction of a masonry bridge usually (but not always) involves the provision of spandrel walls to contain non-structural fill to carry the roadway. In the iron bridge there is the possibility of connecting the roadway to the arch by means of an open iron framework.

The profiles and dimensions of these new iron arches were worked out by using the theory established for the masonry arch. In particular, the shape of the arch could be checked against the thrust line resulting from given loading. However, a technical difference is at once apparent between the design of masonry and of iron arches. The massive continuous barrel of the masonry arch is subject to low stresses, and, apart from final checks on the actual stress levels, a 'geometrical' approach to design, as has been indicated throughout this book, is valid. By contrast the iron arch bridge, whether in the form of hollow 'voussoirs' or of individual ribs, has a barrel consisting largely of voids, and the stress levels in the main members will be a significant fraction of the fracture strength of the material. It can no longer be assumed that the ratio of fracture stress to working stress is so large that the material can be considered to be infinitely strong; on the contrary, it is essential for the designer to make some estimate of the strength of his bridge by reference to the known fracture strength of his material.

It is no surprise, therefore, to find an early interest (for example, that of Tredgold in the 1820s) in the calculation of the strength of iron members. What was needed, for the analysis of an iron arch rib, was an understanding of the way that rib would respond to an eccentric thrust. Elastic methods were being developed which could be used to deal with this kind of problem, and Navier in 1826 is usually credited with giving the first correct analysis of the behaviour of the cross-section in bending. (He had in fact not quite grasped the role of principal axes in the bending of asymmetrical sections, and Tredgold made a similar mistake.)

Elastic theory was, then, advancing at a time when civil engineering construction could make use of its findings, and the whole science of 'strength of materials', dealing with local behaviour of members in response to known loading, was developed. It was inevitable that elastic methods should also come to be used to study the overall behaviour of the structure; that is, the position of the thrust line in a redundant arch could be determined by the new elastic principles – for example, by the use of Castigliano's theorems. It was seen in Chapter 4 that Pippard relied on this same elastic theory in his twentieth-century studies of the arch.

There is no need, however, to use the same types of theory for two very different types of analysis. On the one hand the overall state of equilibrium must be determined, and this is a problem in 'theory of structures'. This analysis will lead to an estimate of the internal structural forces, and it is a second step to design local cross-sections to resist those forces; this is a problem in 'strength of materials'.

The designer must determine the overall state of his structure as best he can; elastic theory will give only one of the infinite number of possible equilibrium states. The use of the 'middle-third' rule, or, what is exactly equivalent, of a geometrical factor of safety, is an alternative way, not involving elastic concepts, of deriving a set of primary structural forces. For the masonry bridge, the idea of an arch of minimum thickness just containing the thrust line leads in some sense to the derivation of the most favourable equilibrium state; the procedure is, however, 'safe', as is demonstrated by the plastic theorems.

The determination of an overall state is usually all that is necessary for the design of the masonry arch, although a small excursion must be made into the field of strength of materials to ensure that stresses are indeed low, as has been assumed. For the cast iron arch, however, the thrust and bending moment acting at any cross-section, whose values have been found by the use of a theory of structures, must be used in the second stage of the calculations; the resulting values of the stresses at the cross-section must be determined. These second-stage calculations may well be elastic, although there is no need for them to be so. If the arch material were a ductile steel, then the calculations might well refer to full plastic moments. Similarly, for wrought iron, the material has sufficient ductility to prompt the use of plastic theory. However, in the two examples which follow which will illustrate the process of analysis of iron arches, elastic stresses are quoted.

MAGDALENE BRIDGE, CAMBRIDGE

As was implied in the previous section of this chapter, conclusions about the strength of cast-iron arches must be reached with some care. The brittle nature of the material may preclude that essentially ductile structural behaviour that is at the heart of the plastic theorems. In specific terms, it may not be possible to rely on the development of any assumed value of tensile stress; if a particular section has at some time been overloaded, then the material may have fractured, and no tensile stress can be developed at all. It turns out that there is no problem on this score with the masonry arch; the hinging behaviour between voussoirs generates the necessary structural ductility, and the safe theorem remains valid.

No such absolute assurance can be given in the same terms for brittle material. This note of warning is not sounded at the use of the plastic theorems; rather, it is the structure made of brittle material that is suspect, and not the methods used to analyse the structure. It is merely that the inability to provide a proper base for the plastic theorems brings into sharp focus the importance of choice of material for structural design, whether the analysis be elastic or plastic. The consequences of this view of a brittle structure may be illustrated with reference to an actual bridge.

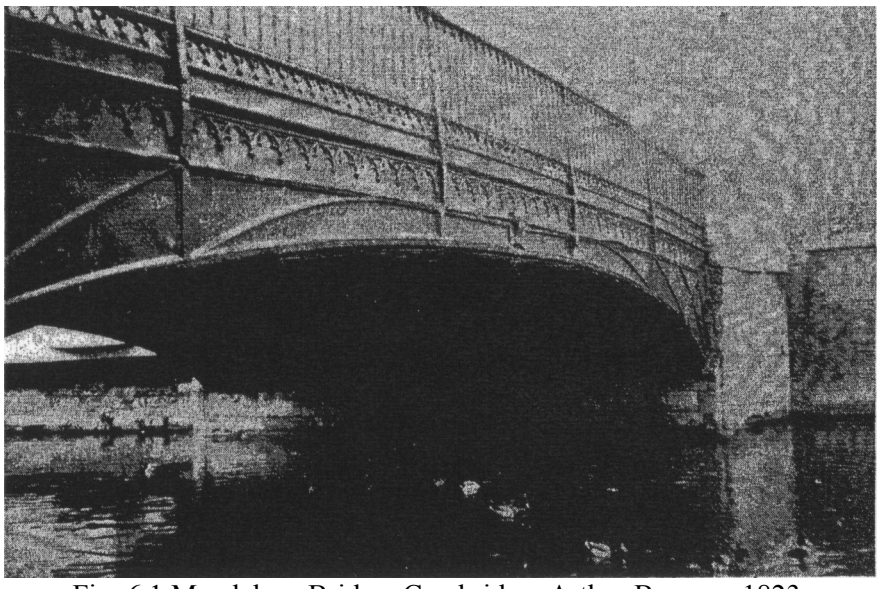

Fig. 6.1 Magdalene Bridge, Cambridge; Arthur Browne, 1823.

Magdalene Bridge, built in 1823, has eight elliptical cast-iron ribs of 45 ft span, Fig. 6.1. Each of the ribs has the idealized cross-section of Fig. 6.2, in which the leading dimensions (in millimetres) are the same as those of the actual rib, but where a slightly more complex outline has been replaced by rectangular blocks for ease of computation. The ribs are spaced at about 4 ft centres, and cast-iron plates span between the ledges at the bottom of the ribs, so that the bridge has an elliptical iron intrados. Earth and rubble (some now replaced by concrete) are placed on these iron plates to form a fill of the conventional kind supporting the roadway. There has been further rehabilitation work in 1981-82.

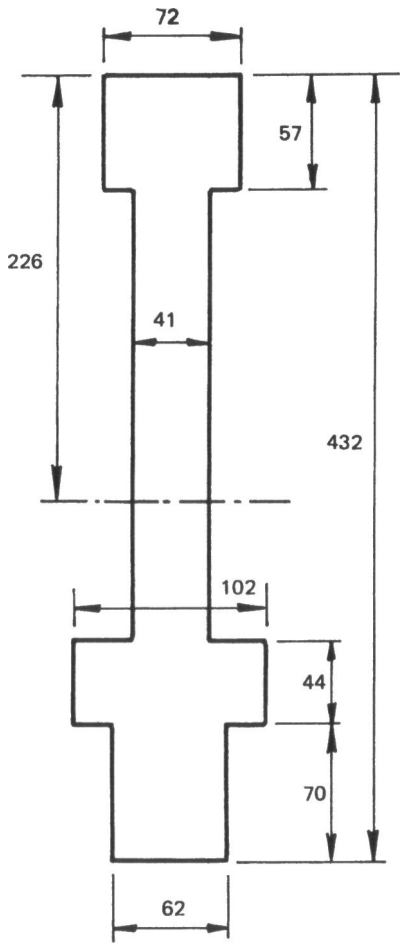

Fig. 6.2 Cross-section of rib of Magdalene Bridge, Cambridge.

For the assessment of the bridge before these recent works, the breaking stress in compression of the cast iron was taken as about 40 ton/in^2, and that in tension as about 10 ton/in^2; correspondingly, permissible working stresses were set at 10 ton/in^2 and 3 ton/in^2 respectively, or about 155 N/mm^2 and 46 N/mm^2. Figure 6.3(a) shows the outline of an arch rib, and also a thrust line for the dead load together with the worst case of live loading that was considered. It will be seen that at the marked "critical section" (which is the section most highly stressed in the rib under the given loading) the thrust line falls below the intrados of the arch; this is of course permissible for a material able to carry tension. However, the stresses at the critical section were calculated as 115 N/mm^2 in compression and 69 N/mm^2 in tension, and this last figure is 50% higher than the permissible value of 46 N/mm^2.

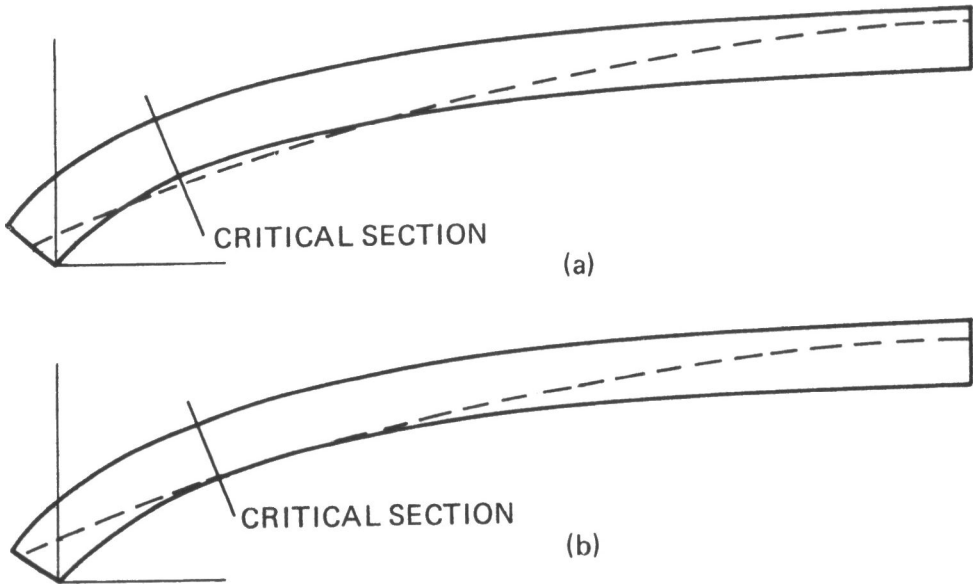

Fig. 6.3

Now the Position of the thrust line in Fig. 6.3(a) was determined by treating the arch as a statically-determinate three-pinned structure. The 'pin' at mid span is a reasonable concept; the connection there is made with a system of yokes and wedges, and the position in the cross-section at which the thrust is transmitted between the two halves is fairly well defined. At the springings, however, the ribs are carried by a thrust plate running the full width of the bridge, and the exact nature of the connection is not known. If there is continuous contact over the full depth of the rib between the rib and thrust plate, and between the thrust plate and the abutment then the thrust line could lie anywhere within the depth of the rib. For the 'statically-determinate' analysis which leads to Fig. 6.3(a), the 'pin' at the abutment was taken arbitrarily at the centroid of the cross-section, so that a uniform compressive stress acts over the full depth of the rib at the springing.

Figure 63(b) shows the results of a second analysis for the same loads in which the abutment 'pin' has been placed some 150 mm above the centroidal axis. Both the compressive stress and the tensile stress at the critical section are reduced, to 97 and 45 N/mm^2 respectively, and in fact the tensile stress has been reduced to just below the nominal permissible value.

Thus if the thrust line of Fig. 6.3(b), representing a first stage of a structural assessment of the bridge, were the correct thrust line, then the corresponding elastic stresses arising at the most highly stressed section would appear to be satisfactory. Now the actual conditions at the abutments are not known, so that it is not possible to decide that the thrust line of Fig. 6.3(b) is more 'correct' than that of Fig. 6.3(a), or vice versa. The matter is not one of mere ignorance; as was pointed out in Chapter 2, even if information were available as to the precise connection of the arch rib to its springing, the passage of time, involving shifts and settlements of the structure, would render that information meaningless. If the safe theorem were valid, then it would not be necessary to choose between the alternative states shown in Figs. 6.3(a) and (b). The stresses corresponding to the thrust line of Fig. 6.3(b) are satisfactory, and there should be an end to the matter; the arch cannot collapse under the given loading.

However, the thrust line could in fact drop to the position shown in Fig. 6.3(a), or lower. In practice, any spread in the abutments of a bridge will lead to a fall in value of the abutment thrust, and a corresponding lowering of the thrust line at the springings of the arches. As was mentioned in Chapter 5, Castigliano noted this drooping tendency of the thrust line, and indeed he advocated the provision of rounded ends to the ribs, to provide a pinned bearing at a definite point in the cross-section. The arches of Magdalene Bridge could apparently be forced to be in an unequivocally satisfactory state if they were jacked off their abutments, and pins inserted to correspond with the position of the thrust line of Fig. 6.3(b).

Such a procedure might be thought to conflict with common sense; the conversion of a redundant into a statically-determinate structure cannot improve its strength. Such a common-sense view can certainly be sustained for any ductile structure, to which the safe theorem will apply. Once again, however, what is suspect is the structure made of brittle material. What might happen in practice is that the thrust line for the redundant arch could in fact drop to a position where iron cracks in the extrados; the line would then rise at once to a position corresponding more closely to that of Fig. 6.3(b). However, the arch rib in its newly cracked state might not be able to accommodate within its depth the new position of the thrust line, and, until this has been checked (and levels of compressive stress verified) no assurance can be given about the state of the rib.

Absolute assurance of the safety of redundant cast-iron arches can be obtained if they are imagined to be cracked throughout. That is, the arch rib of Fig. 6.3 could be thought of as being made up of 'voussoirs' imitating the masonry arch, and unable to accept tensile stresses at any section. If such an arch were analysed by the methods of earlier chapters in this book, and found to be satisfactory, and if in addition compressive stress levels were also checked, then the required assurance would be obtained.

Alternatively, the provision of abutment pins (and a crown pin, if necessary) would make the cast-iron arch statically determinate, with no possibility of ambiguity in the position of the thrust line. The arch rib would no longer be subject to any vagaries of the environment, and the analyst could have some reasonable assurance that his calculated stresses would not in practice be exceeded.

All these difficulties arise from the brittle nature of cast iron (which may in practice have a greater reserve of ductility, even though small, than is assumed). The difficulties disappear with the use of wrought iron, which certainly has enough tensile ductility for there to be no question of fracture.

A WROUGT-IRON BRIDGE

Figure 6.4 shows schematically (but based upon an actual bridge) the central span (of 27.4 m) of a wrought-iron road bridge. The top girders supporting the roadway and the girders forming the arches are built up with riveted construction from solid web plates and angle and plate flanges; the roadway girders and arch girders merge together near mid span. The 'decorative' open spandrel ironwork serves to transmit the loads from the roadway girders to the arches. If the bridge is viewed in this straightforward way, then loads on the roadway will be transmitted to the curved arch members, and these may be analysed by thrust-line techniques. For this particular bridge, all combinations of dead and live loading produced stresses within permissible limits; the bridge was shown, in fact, to be satisfactory.

Fig. 6.4 Schematic diagram of wrought-iron bridge.

However, a conventional elastic analysis did not give this straightforward view. It was easy to adapt an elastic computer program for the analysis; the arch was idealised as an assemblage of elements having locally the section properties of the appropriate point in the arch. A large number of loading cases could then be investigated, and worst values of compressive and tensile stresses tabulated in the usual way.

In addition to various combinations of dead and live loads, two further 'loading' cases were considered. The first of these was a study of the effects of variation of temperature. The second

results from an observed defect in the bridge; one of the river piers has tilted at some time, and the main span of 27.4 m has increased at road level by about 13 mm.

When these different loading cases were taken into account, it was found that the worst tensile stress at any section in the bridge was 309 N/mm^2. Of this total, 57 N/mm^2 was due to the most unfavourable combination of dead and live loading, 114N/mm^2 was due to contraction on change of temperature, and 138 N/mm^2 was due to rotation of the river pier. The accepted permissible tensile stress was 120 N/mm^2, so that the total of 309 N/mm^2 is considerably in excess of this value.

The relative magnitudes of some of these quantities can be checked by simple calculations. An increase of 13 mm in a span of 27.4 m represents a strain of about 0.5×10^{-3}; if this strain is absorbed elastically in the iron then the corresponding tensile stress is about 100 N/mm^2. Similarly, a temperature variation of ± 30°C would lead to a strain of about $\pm 0.4 \times 10^{-3}$, and the corresponding elastic stress would also be of the order ± 100 N/mm^2.

Now both the temperature strain and the strains due to the increase in span lead to self-equilibrating stresses. A qualitative test on the nature of the stresses is very easy; neither temperature variation nor a mismatch in span will give rise to stresses in a statically-determinate structure (for example, a three-pin arch of the same geometry as the one being considered). A redundant structure, however, is capable of sustaining stresses in the absence of external load; indeed, it will inevitably be in such a state. The members of the riveted bridge of Fig. 6.4 will have been forced together to some extent during construction, and it is of note that such unknown erection stresses will be ignored in any elastic calculation.

It is in fact safe, by the plastic theorems, to ignore such stresses; they can have no effect on the final carrying capacity of a ductile structure. Similarly, the temperature stress of 114 N/mm^2, and the stress of 138 N/mm^2 due to rotation of the river pier, arise only because the arch is statically indeterminate; they cannot affect the final strength of the bridge. Of the total worst tensile stress of 309 N/mm^2, only 57 N/mm^2 is due to the loading; the other contributions arise from a 'lack-of-fit' exactly on a par with erection defects.

It is the arguments about small imperfections that are vital, as was seen in Chapter 2, and not the calculations of the magnitudes of the resulting self-equilibrating stresses. Such imperfections (as a tilting of a river pier) may well be very evident on close inspection of the structure, and they may lead to visible overstraining of wrought iron, or to separation of voussoirs in a masonry arch. These overstrains and these cracks will not, however, be visible if the engineer takes a more distant view of his structure; the geometry of the bridge is virtually unchanged. The shift of an abutment will lead to the cracking of a masonry arch. It is the natural state of masonry to be cracked, but its final strength is unaffected by such natural and unavoidable defects.

Bibliographie

GENERAL

Hopkins, H. J., (1970), *A span of bridges*, Newton Abbot (David and Charles).
Ruddock, Ted, (1979), *Arch bridges and their builders 1735-1835*, Cambridge University Press.

CHAPITRE I

Fuller, G., (1875), Curve of equilibrium for a rigid arch under vertical forces, *Min. Proc. Instn civ. Engrs,* **40**, p. 143.
Inglis, C., (1951), *Applied mechanics for engineers*, Cambridge University Press.

CHAPITRE 2

Heyman, J., (1971), *Plastic design of frames; volume 2, Applications*, Cambridge University Press.
Heyman, J., (1969), *The safety of masonry arches, Int. J. mech. Sci.*, **11**, p. 363.
Heyman, J., (1966), The stone skeleton, *Int. J. Solids Structures*, **2**, p. 249.
Kooharian, A., (1953), Limit analysis of voussoir (segmental) and concrete arches, *Proc. Am. Concr. Inst.*, **49**, p. 317.

CHAPITRE 3

Barlow, W. H., (1846), On the existence (practically) of the line of equal horizontal thrust in arches, and the mode of determining it by geometrical construction, *Min. Proc. Instn civ. Engrs,* **5**, p. 162.

Bélidor, B. F. de, (1729), *La science des ingé'nieurs dans la conduite des travaux de fortification et d'architecture civile*, Paris.
Boistard, L. C., *Expériences sur la stabilité des voûtes*, in Lesage, vol 2, p. 171.
Castigliano, C. A. P., (1879), *Théorie de l'équilibre des systèmes élastiques et ses applications*, Turin, Augusto Federico Negro. Translated by Ewart S. Andrews, (1919), *Elastic stresses in structures*, London, Scott, Greenwood and Son. Republished with an introduction by G. AE. Oravas, (1966*). The theory of equilibrium of elastic systems and its applications*, New York, Dover.
Coulomb, C. A., (1773) Essai sur une application des règles *de maximis & minimis* à quelques problèmes de statique, relatifs à l'architecture, *Mémoires de Mathématique & de Physique, présentés à l'Académie Royale des Sciences par divers Savants*, **7**, p. 343.
Couplet, P., (1729, 1730), De la poussée des voûtes, *Histoire de l'Académie Royale des Sciences*, p. 79 and p. 117. '
Danyzy, A. A. H., 1732, (Lyon 1778), Méthode générale pour déterminer la résistance qu'il faut opposer à la poussée des voûtes, *Histoire de la Société Royale des Sciences établie à Montpellier*, **2**, p. 40.
Derand, François, (1643), *L'architecture des voûtes...*, Paris. (Nouvelle édition, revue et corrigée, Paris, 1743).
Frézier, A. F., (1737-39), *La théorie et la pratique de la coupe des pierres...*, 3 vols, Strasbourg and Paris.
Gauthey, E. M., (1809, 1813), *Traité de la construction des ponts*, ed. C. L. M. H. Navier, 2 vols., Paris.
Gautier, H., (1717), *Dissertation sur l'épaisseur des culées des ponts...*, Paris.

Gil de Hontañon, Rodrigo (c. 1500-1577). Insertion in *Compendio de Arquitectura...* (Simon Garcia 1681) edited and published in El arte in España, **7**, Madrid, 1868.
Gregory, D., (1697), Catenaria, *Phil. Trans.* no. 231, p. 367.
Heyman, J., (1972), *Coulomb's memoir on statics*, Cambridge University Press.
Heyman, J., (1976), Couplet's engineering memoirs, 1726-33, *History of Technology 1976*, ed. A Rupert Hall and Norman Smith, Mansell.
Hooke, R., (1676 (*sic*, actually 1675)), *A description of helioscopes, and some other instruments*, London.
Jenkin, H. C. F., (1876), Article "Bridges", *Encyclopaedia Britannica*, 9th edition, Edinburgh.
La Hire, P. de, (1695), *Traité de Mécanique*, Paris.
La Hire, P. de, (1712), Sur la construction des voûtes dans les édifices, *Mémoires de l'Académie Royale des Sciences*, p. 69.
Lamé, M. G. and Clapeyron, E., (1823), Mémoire sur la stabilité des voûtes, *Annales des Mines*, **8**, p. 789.
Lesage, P. C., (1810), *Recueil de divers mémoires extraits de la Bibliothèque Impériale des Ponts et Chaussées à l'usage de MM. les ingénieurs*, 2 vols, Paris.
Moseley, H., (1843), *The mechanical principles of engineering and architecture*, London.
Navier, C. L. M. H., (1833), *Resumé des leçons données à l'Ecole des Ponts et Chaussées, sur l'application de la mécanique à l'établissement des constructions et des machines*, 2nd edition, Paris.
Pippard, A. J. S., Tranter, E. and Chitty, L., (1936), The mechanics of the voussoir arch, *J. Instn civ. Engrs.*, **4**, p. 28 1.
Pippard, A. J. S. and Ashby, R. J., (1938), An experimental study of the voussoir arch, *J. Instn civ. Engrs.*, **10**, p. 383.
Pitot, H., (1726), Examen de la force qu'il faut donner aux cintres dont on se sert dans la construction des grandes voûtes des arches des ponts, &c., *Mémoires de l'Académie Royale des Sciences*, p. 216.
Poleni, G., (1748), *Memorie istoriche della gran cupola del Tempio Vaticano*, Padova.
Prony, R. de, (1802), *Recherches sur la poussée des terres, et sur la forme et les dimensions à donner aux murs de revêtement*, Paris, *An* X.
Séjourné, P., (1913-16), *Grandes voûtes*, 6 vols, Bourges.
Stirling, J., (1717), *Lineae Tortii Ordinis Neutonianae*, Oxford.
Timoshenko, S. P., (1953), *History of strength of materials*, McGraw-Hill.
Truesdell, C., (1960), *The rational mechanics of flexible or elastic bodies* 1638-1788, Introduction to Leonhardi Euleri Opera Omnia, 2nd series, vol 11(2), Zürich.
Ware, S., (1809), *A treatise of the properties of arches, and their abutment piers*, London.
Yvon Villarceau, A., (1854), L'établissement des arches de pont, *Institut de France, Académie des Sciences, Mémoires présentés par divers savants*, **12**, p. 503.

CHAPITRE 4

Heyman, J., (1980), The estimation of the strength of masonry arches, *Proc. Instn civ. Engrs*, **69**, p. 921.
Military Engineering Experimental Establishment, (1952), *Classification of masonry arch bridges*, Christchurch (MEXE).
Ministry of Transport, (1967), *The assessment of highway bridges for construction and use vehicles*, Tech. Memo. (Bridges) BE4, London, Ministry of Transport, and *ibid*. Tech. Memo. (Bridges) BE3/73, 1973.
Pippard, A. J. S., and Baker, J. F., (1943), *The analysis of engineering structures*, 2nd edition, London, Edward Arnold.
Pippard, A. J. S., (1948), The approximate estimation of safe loads on masonry bridges, *Civil engineer in war*, **1**, p. 365, London, The Institution of Civil Engineers.

CHAPITRE 5

Heyman, J., Hobbs, N. B. and Jenny, B. S., (1980), The rehabilitation of Teston bridge, *Proc. Instn civ. Engrs*, **68**, p. 489.

Nicholson, W. A., (1842), Report on the construction of a stone arch between the west towers of Lincoln Cathedral, *Trans. RIBA*, **1** Part 11, p. 180.

Papworth, J. B., (1842), A suggestion referring to the stone arch at Lincoln Cathedral, *Trans. RIBA*, **1** Part II, p. 184.

CHAPITRE 6

Morgan, S. K. and Heathorn, T. J., (1981), A study of the design and construction and a structural analysis of Magdalene Bridge, Cambridge, *The Structural Engineer*, **59** A; p. 255.

Tredgoid, T., (1824), *Practical essay on the strength of cast iron...* second edition, London.

ELLIS HORWOOD SERIES IN ENGINEERING SCIENCE

STRENGTH OF MATERIALS
J. M. ALEXANDER, University College of Swansea.
TECHNOLOGY OF ENGINEERING MANUFACTURE
J. M. ALEXANDER, R. C. BREWER, Imperial College of Science and Technology, University of London, J. R. CROOKALL, Cranfield Institute of Technology.
VIBRATION ANALYSIS AND CONTROL SYSTEM DYNAMICS
CHRISTOPHER BEARDS, Imperial College of Science and Technology, University of London.
COMPUTER AIDED DESIGN AND MANUFACTURE
C. B. BESANT, Imperial College of Science and Technology, University of London.
STRUCTURAL DESIGN AND SAFETY
D. I. BLOCKLEY, University of Bristol.
BASIC LUBRICATION THEORY 3rd Edition
ALASTAIR CAMERON, Imperial College of Science and Technology, University of London.
STRUCTURAL MODELLING AND OPTIMIZATION
D. G. CARMICHAEL, University of Western Australia
ADVANCED MECHANICS OF MATERIALS 2nd Edition
Sir HUGH FORD, F.R.S., Imperial College of Science and Technology, University of London and J. M. ALEXANDER, University College of Swansea.
ELASTICITY AND PLASTICITY IN ENGINEERING
Sir HUGH FORD, F.R.S. and R. T. FENNER, Imperial College of Science and Technology, University of London.
INTRODUCTION TO LOADBEARING BRICKWORK
A. W. HENDRY, B. A. SINHA and S. R. DAVIES, University of Edinburgh
ANALYSIS AND DESIGN OF CONNECTIONS BETWEEN STRUCTURAL JOINTS.
M. HOLMES and L. H. MARTIN, University of Aston in Birmingham
TECHNIQUES OF FINITE ELEMENTS
BRUCE M. IRONS, University of Calgary, and S. AHMAD, Bangladesh University of Engineering and Technology, Dacca.
FINITE ELEMENT PRIMER
BRUCE IRONS and N. SHRIVE, University of Calgary
PROBABILITY FOR ENGINEERING DECISIONS: A Bayesian Approach
1. J. JORDAAN, University of Calgary
STRUCTURAL DESIGN OF CABLE-SUSPENDED ROOFS
L. KOLLAR, City Planning Office, Budapest and K. SZABO, Budapest Technical University.
CONTROL OF FLUID POWER, 2nd Edition
D. McCLOY, The Northern Ireland Polytechnic and H. R. MARTIN, University of Waterloo, Ontario, Canada.
TUNNELS: Planning, Design, Construction
T. M. MEGAW and JOHN BARTLETT, Mott, Hay and Anderson, International Consulting Engineers
UNSTEADY FLUID FLOW
R. PARKER, University College, Swansea
DYNAMICS OF MECHANICAL SYSTEMS 2nd Edition
J. M. PRENTIS, University of Cambridge. -
ENERGY METHODS IN VIBRATION ANALYSIS
T. H. RICHARDS, University of Aston, Birmingham.
ENERGY METHODS IN STRESS ANALYSIS: With an Introduction to Finite Element Techniques
T. H. RICHARDS, University of Aston, Birmingham.
ROBOTICS AND TELECHIRICS

M. W. THRING, Queen Mary College, University of London
STRESS ANALYSIS OF POLYMERS 2nd Edition
J. G. WILLIAMS, Imperial College of Science and Technology, University of London.

First published in 1982 by ELLIS HORWOOD LIMITED
Market Cross House, Cooper Street, Chichester, West Sussex, PO 19 1 EB, England

The publisher's colophon is reproduced from James Gillison's drawing of the ancient Market Cross, Chichester.

Distributors:

Australia, New Zealand, South-east Asia:
Jacaranda-Wiley Ltd., Jacaranda Press,
JOHN WILEY & SONS INC.,
G.P.O. Box 859, Brisbane, Queensland 40001, Australia

Canada: JOHN WILEY & SONS CANADA LIMITED 22 Worcester Road, Rexdale, Ontario, Canada.

Europe, Africa: JOHN WILEY & SONS LIMITED Baffins Lane, Chichester, West Sussex, England.

North and South America and the rest of the world: Halsted Press: a division of JOHN WILEY & SONS 605 Third Avenue, New York, N.Y. 10016, U.S.A.

British Library Cataloguing in Publication Data
Heyman, Jacques
The masonry arch. - (Ellis Horwood series in civil engineering)
1. Arches
I - Title
624.1'775 TA660-A7

Library of Congress Card No. 82-11809

ISBN 0-8S 312-5 00-7 (Ellis Horwood Ltd. - Library EdnJ
ISBN 0-85312-501-5 (Ellis Horwood Ltd. - Student Edn.)
ISBN 0-470-27544-8 (Halsted Press)

Typeset in Press Roman by Ellis Horwood Ltd. Printed in Great Britain by Butler & Tanner, Frome, Somerset.

Building Science, University of Edinburgh

"Much-needed book sets out the latest theory and design practice for loadbearing brickwork ... gives the background to the code and shows its applications to practical design problems ... well presented and illustrated ... should be essential reading, The principal author is a leading authority in the field of structur brickwork research and a member of the new masonry -ode drafting -committee. The other authors have also been closely associated in this area" - T~ J. MacGin1,2,/ in British Book N,.-vv5.

J_ M. ALEX AND ER, Professor and Head of Mech an ical Engineering, University College, Skrvanse a

The text, divided into two logical volumes, achieves a comprehensive coverage of the complete and self-contained undergraduate courses in this subject. Combines the erudite mathematicai approach with the more direct engineering approach, begins at an elementary level, and builds up gradually to embrace the , more sophisticated notions and difficult problems. VVorked examples test the student's learning of the techniques,

D. 1. BLOCKLEY, Department of Civil Engineering, University of Bristol

"a book that should be read by all intending and practising structural engineers ... should also be compulsory reading for all academics concerned ... will help them to devise programmes of learning ... a rare feast of engineering philosophy and new ideas which should stimulate wider discussion and better understanding in the future" - John Armitage in The Structural Engineer,

"both the practising and the academic engineer will find a great deal to enrich their understanding of basic design process . . . well illustrated" -- J_ Heyman, Professor of Engineering, Universitv of Cambridge, in Numerical Methods in Engineering,

M. HOLMES, Professor and Head of Civil Engineering, and L. H. MARTIN, Department of Civil Engineering, University of Aston in Birmingham

This book, written at undergraduate and postgraduate level, deals systematically and comprehensively with the analysis and clesign,of connections between structural elements such as beams and columns, and commonly used materials, such as steel and reinforced concrete. References are kept.to codes of practice, in the main body of each chapter, concentrating on the principles involved.

SIR HUGH FORD, Emeritus Professor, Imperial College of Science and Technology, and R. T. FENNER, Department of Mechanical Engineering, Imperial College of Science and Technology, University of London

Comprehensive coverage divided into three logical parts to aid understanding. Part 1 deals with analysis of stress and strain; Part 2 with engineering applications of elasticity theory; Part 3 with numerical solution methods. Presents principles and outlines rather than precise details of computing algorithms. For advanced undergraduate and graduate study, and professional engineers and designers.

published by ELLIS HORWOOD LIMITED

Publishers Chichester
distributed by HALSTED PRESS i division of JOHN WILEY & SONS